Practical Considerations for Ageing of Drinking Water Membranes

by
Shona Jacquelyn Robinson

M.Sc., University of Toronto, 2011
B.Sc.H., Queen's University (Kingston), 2009

A dissertation submitted in partial fulfillment
of the requirements for the degree of

Doctor of Philosophy
in
The Faculty of Graduate and Postdoctoral Studies
(Civil Engineering)

The University of British Columbia
(Vancouver)

June 2018

Committee Page

The following individuals certify that they have read, and recommend to the Faculty of Graduate and Postdoctoral Studies for acceptance, the dissertation entitled:

Practical Considerations for Ageing of Drinking Water Membranes

submitted by Shona Robinson

in partial fulfillment of the requirements for the degree of Doctor of Philosophy

in Civil Engineering.

Examining Committee:

Pierre Bérubé, Department of Civil Engineering
Supervisor

Eric Hall, Department of Civil Engineering
Supervisory Committee Member

Scott Dunbar, Department of Mining Engineering
University Examiner

Frank Ko, Department of Materials Engineering
University Examiner

Additional Supervisory Committee Members:

Jayachandran Kizhakkedathu, Department of Pathology and Laboratory Medicine, Department of Chemistry
Supervisory Committee Member

Pierre Le-Clech, Department of Chemical Engineering, University of New South Wales
Supervisory Committee Member

Abstract

This dissertation advances our understanding of practical considerations for ageing of membranes used in drinking water treatment. Fouling and cleaning of membranes are well understood, but knowledge of long-term changes (i.e. ageing) have not been fully explored. To date, changes in physical and chemical characteristics, and changes in membrane performance, have been attributed to ageing. The three major sections in this dissertation were structured around membrane performance.

Firstly, the existing literature was comprehensively reviewed. Important membrane performance factors were identified via this review: resistance, fouling rate, cleaning rate, and susceptibility to breach. How chemical and physical characteristics impact these performance factors was also systematically assessed. Almost all of the reviewed research involved bench-scale ageing of membranes, with scant attention to full-scale ageing, and even less on how bench-scale ageing can be useful in understanding full-scale ageing. This recognition led to the two further research projects.

Secondly, we investigated changes in performance factors and chemical characteristics for PVDF membranes aged in 8 full-scale water treatment plants (14 treatment trains ranging from new to 10 years of age). Membranes were harvested by plant operators regularly and analyzed in a standardized laboratory setting. Membranes exhibited stable behaviour until about 5 years of operation; after this time, performance factors and chemical characteristics began to change significantly. Clean membrane resistance and fouling rate increased for aged membranes. The mechanical properties of aged membranes

deteriorated, suggesting that their susceptibility to breach was heightened. These performance changes correlated with the removal of hydrophilic additives from the membranes.

The final research project sought to link performance changes observed at bench-scale with performance changes observed in the full-scale study. Two bench-scale ageing techniques were used to probe changes in performance and characteristics: soaking membranes in NaOCl cleaning agent, and cycling them with foulant and cleaning agent. The changes in membrane chemistry were similar for bench-scale and full-scale ageing, but performance differed. By comparing the two bench-scale techniques with the full-scale ageing findings, it was established that irreversible foulants are critical components of full-scale ageing, and the involvement of these can be approximated to some extent by cycling membranes.

Lay Summary

Several technologies are used to create safe drinking water for communities. One popular option is using membranes to filter natural water. Water treatment membranes are microscopic sieves, removing contaminants and microorganisms. Membranes' advantages include a small treatment plant footprint, and high quality drinking water.

Unfortunately, membranes also have a disadvantage; as they filter natural water, the removed material accumulates, causing membrane fouling. Sometimes fouling is so severe that membranes are cleaned with harsh chemicals (e.g. bleach). This causes long-term membrane degradation, termed "membrane ageing".

Most studies of membrane ageing involve soaking membranes in concentrated bleach and measuring their performance and properties. However, we found that membranes from full-scale water treatment plants age differently from those simply soaked in concentrated bleach. We also carried out bench-scale experiments which indicated why full-scale ageing differs from our expectations. This furthered our understanding of ageing, while also providing tools for improved study design.

Preface

This confirms that Shona Robinson is primarily responsible for the research presented in this dissertation. Several manuscripts and conference presentations resulted from this work. These contributions are listed as follows:

Journal Publications:

Robinson, S.; Bérubé, P. Seeking Realistic Membrane Ageing at Bench Scale, In Preparation, 2018.

Robinson, S.; Bérubé, P. Membrane Ageing in 8 Drinking Water Treatment Plants, In Preparation, 2018.

Robinson, S.; Bérubé, P. Considerations for Storage & Transport of Biopolymer-Containing Water Samples, In Preparation, 2018.

Robinson, S.; Abdullah, S. Z.; Le-Clech, P.; Bérubé, P. Ageing of Membranes for Water Treatment: Linking Changes to Performance, Journal of Membrane Science, 503, 177-187 2016.

Conference Presentations:

Robinson, S.; Bérubé, P. Seeking More Realistic Membrane Ageing at Bench Scale. Water Quality Technology Conference, Toronto ON, November 2018. (oral - abstract submitted)

Robinson, S.; Bérubé, P. Seeking More Realistic Membrane Ageing at Bench Scale. Euromembrane, Valencia Spain, July 2018. (oral - abstract accepted)

Robinson, S.; Bérubé, P. Membrane Ageing: Understanding Changing Performance in Water Treatment Plants. IWA Membrane Technology Conference, Singapore, September 2017. (oral)

Robinson, S.; Bérubé, P. Ageing Membranes in the Wild: Putting Lab Research in Context. Water & Environment Student Talks, Vancouver BC, June 2017. (oral)

Robinson, S.; Bérubé, P. Ageing Membranes in the Wild: Putting Lab Research in Context. BC Water & Waste Association Annual Conference, Victoria BC, May 2017. (oral)

Robinson, S.; Bérubé, P. Membrane Ageing: Understanding Changing Performance in Water Treatment Plants. AMTA Membrane Technology Conference, Long Beach USA, February 2017. (oral, presented by second author)

Robinson, S. A Practical Approach to Membrane Ageing: A Canada-Wide Collaboration with Water Treatment Plants. BC Water & Waste Association Annual Conference, Kelowna BC, May 2015. (oral)

Robinson, S. Membrane Ageing: From a Practical Perspective. Applied Science Research Day, Vancouver BC, October 2014. (oral, invited)

Robinson, S. Membrane Ageing: Studying a 15-Year Process While Graduating in 3. Water & Environment Student Talks, Vancouver BC, June 2014. (oral)

TABLE OF CONTENTS

List of Tables

List of Figures

List of Abbreviations

AFM	Atomic Force Microscopy
ATR-FTIR	Attenuated Total Reflectance - Fourier Transform Infrared [Spectroscopy]
BSA	Bovine Serum Albumin
CA	Cellulose Acetate
CEB	Chemical-Enhanced Backwash
DSC	Differential Scanning Calorimetry
FTIR	Fourier Transform Infrared [Spectroscopy]
GPC	Gel Permeation Chromatography
HA	Hydrophilic Additive
HF	Hollow Fibre
MALDI	Matrix-Assisted Laser Desorption Ionization
MF	Microfiltration
MS	Mass Spectrometry
NF	Nanofiltration
NMR	Nuclear Magnetic Resonance [Spectroscopy]
PES	Polyethersulfone
PVDF	Polyvinylidene Difluoride
PVP	Polyvinyl Pyrrolidone
SEM	Scanning Electron Microscopy
SDS	Sodium Dodecyl Sulfate
TGA	Thermogravimetric Analysis
ToF-SIMS	Time of Flight - Selected Ion Monitoring Spectroscopy

UF	Ultrafiltration
XPS	X-Ray Photoelectron Spectroscopy
XRD	X-Ray Diffraction

Acknowledgements

The research in this dissertation was made possible thanks to collaborations with partner facilities, and with several UBC departments. Dozens of obliging staff at our partner plants were involved in establishing the project and coordinating membrane harvesting. Four external UBC departments allowed my use of analytical instruments, with the help of Fred Rosell, Safwat Rabae, Sonia Lin, HeeJae Yang, Frank Ko, and Jacob Kabel. Within Civil Engineering, Scott Jackson, Paula Parkinson and Tim Ma provided essential support in building the bench-scale experimental setups.

Thank you to Pierre Bérubé for providing thoughtful criticism throughout the research and writing process, as well as wonderful mentorship over the years. Thanks also to my other committee members, Eric Hall, Jayachandran Kizhakkedathu, and Pierre Le-Clech, for their support and insight.

Beyond this dissertation, I am grateful that the Civil Engineering Department enabled me to teach courses during my PhD, a true highlight. I was also fortunate to have abundant support from my family, lab-mates, and friends.

Chapter 1 - Introduction

1.1 Membranes for Water Treatment[1]

Natural water must be treated before it is safe for consumption. The most important aspect of drinking water treatment, from a public health perspective, is deactivation or removal of pathogens. Filtration is often used in conjunction with disinfection processes, helping to remove particulates and pathogens. Several filtration processes are employed in water treatment, all exhibiting different removal mechanisms and advantages. Slow sand, granular media, and membrane filtration are the most prevalent. Of these technologies, membrane filtration is the most recent innovation and it presents a popular and growing technology for water treatment. Membrane drinking water systems have many advantages including a small footprint, ease of automation, reduction of required disinfection, and high product water quality.

Low-pressure membranes for water treatment act as microscopic sieves, with pores that allow water and small molecules to pass, but which retain pathogens and particles. The raw water is referred to as the 'feed', the retained material as the 'retentate', and the treated water as the 'permeate'. The driving force for separating the retentate from the permeate is the application of pressure, either via pressurizing the feed side of the membrane or applying a vacuum to the permeate side. This pressure difference is referred to as the

[1] Background introductory material on water treatment and membrane system operation is based on information from a widely used and extensively referenced textbook in the field (Crittenden et al., 2005).

trans-membrane pressure (TMP), described below by the pressure difference between the feed (P_{feed}), and permeate ($P_{permeate}$) sides.

$$TMP = \Delta P = P_{feed} - P_{permeate} \qquad \text{Equation 1}$$

Low-pressure processes are classified by various descriptors, the first of which is the pore size or molecular weight cut-off. Microfiltration (MF, ~0.1 μm pore size) and ultrafiltration (UF, ~0.01 μm pore size) membranes are common for water and wastewater applications because their pore sizes are appropriate for excluding most microorganisms of concern.

By considering the pore size and other geometric features of a membrane, the trans-membrane pressure can be estimated. This is then normalized to flux and viscosity to provide a metric called membrane resistance, as described below:

$$R_m = \frac{\Delta P}{\mu \cdot J} \qquad \text{Equation 2}$$

$$R_m = \frac{8\tau LA}{nr^4\pi} \qquad \text{Equation 3}$$

The resistance of a clean membrane (R_m), depends on the trans-membrane pressure (ΔP), flux (J), and dynamic viscosity (μ). These variables, in turn, are related to the membrane area (A), pore length (L), number of pores (n), pore radius (r), and pore shape (τ), if pores are simplified to uniform tubes with friction factor equal to Re/64.

Membrane properties can be tailored to a specific application based on the membrane material, which can be either polymeric or inorganic. In the present research, polyvinylidene difluoride (PVDF) based membranes were studied, as these are common in

drinking water treatment. Because PVDF is a hydrophobic polymer, the membranes studied incorporate hydrophilic additives (HA), to mitigate membrane fouling.

Membranes foul due to accumulation of retained material, both inside the pores and on the surface of the membrane. Foulants cause the total membrane resistance to rise, adding to the intrinsic membrane resistance as follows:

$$R_{tot} = R_m + R_f \qquad \text{Equation 4}$$

The total (R_{tot}) changes over time as material accumulates and the fouling resistance (R_f), increases. If membranes foul more rapidly, R_{tot} will increase quickly requiring higher pressure to achieve a given flow rate.

Various hydraulic cleaning strategies are employed to control or reverse membrane fouling. A common strategy employed to periodically remove fouling is backwashing of membranes with clean water by reversing the pressure gradient. This allows particulate material within membrane pores and on the membrane surface to be lifted away. Shear may be introduced via air sparging or cross-flow to remove material from the membrane surface. However, after repeated filtration and backwash cycles, chemical cleaning is required to remove material which has adsorbed onto the membrane and which cannot be removed hydraulically.

Long-term foulant and cleaning agent exposure results in irreversible changes to membrane performance and characteristics; these irreversible changes define a phenomenon termed membrane ageing. Despite considerable research on membrane

fouling and cleaning, ageing of membranes has received less attention, as illustrated in Figure 1:

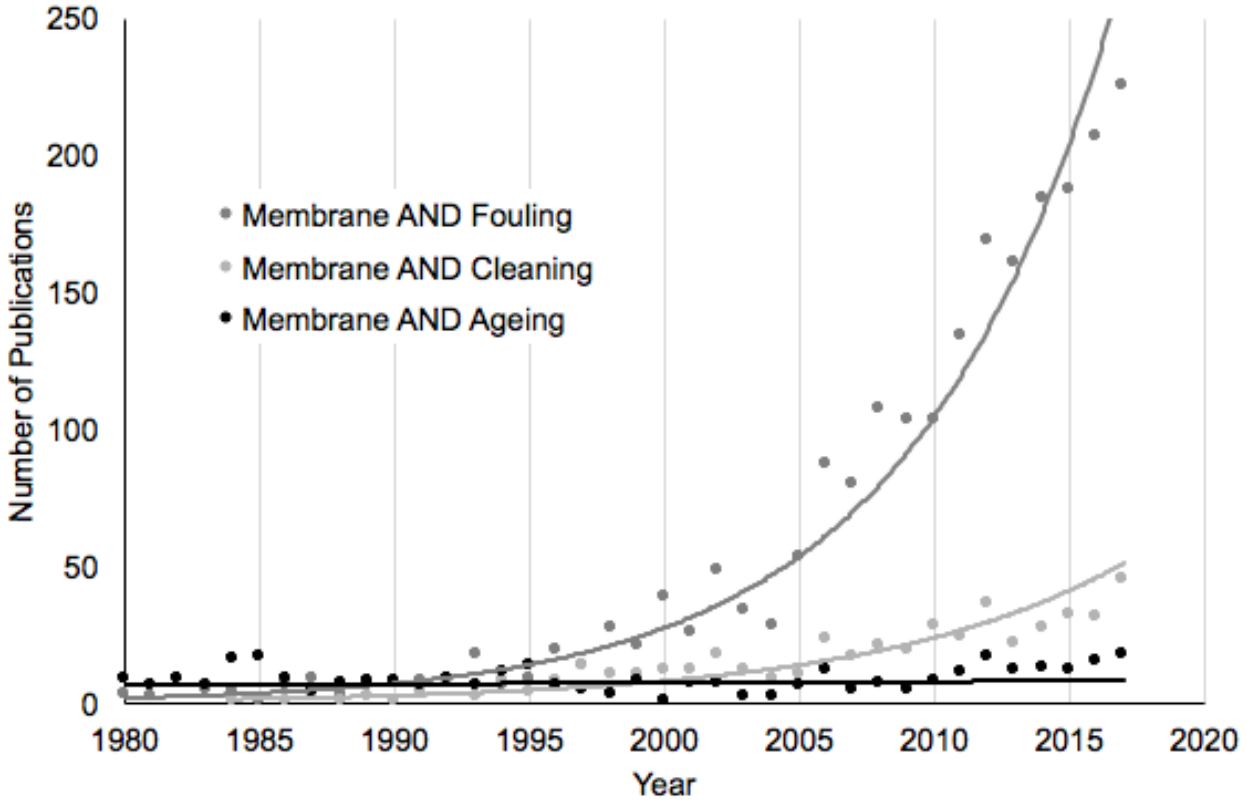

Figure 1. Annual membrane research publications since 1980. Y-ordinate corresponds to number of journal articles with the words listed in the legend present in the article title. The search database was the ScienceDirect web database.

The cursory search presented in Figure 1 indicates that membrane fouling and cleaning dominate the published literature. At the last major conference on membranes (i.e. the 2017 Membrane Technology Conference, Singapore), work from this dissertation constituted the only presentation (out of 230) with 'ageing' in the title. The first objective of the present work was to assess the existing knowledge in membrane ageing through a comprehensive literature review. In our review, the work to-date was organized by performance implications.

1.2 Components of the Research

This dissertation is comprised of three main sections. The impetus for each of these sections, and the corresponding objectives, are presented in the following discussion.

1.2.1 Defining Membrane Performance Factors

In the literature review of membrane ageing, operational performance factors were identified which may deteriorate in membranes as they age, and techniques to assess each factor in a controlled experimental setting were explored (Chapter 2). These performance factors were: clean membrane resistance, fouling rate, cleaning rate, susceptibility to breach, and infrastructure reliability. Throughout our dialogue with collaborator WTPs (water treatment plants) in the present work, these factors were recognized as relevant concerns by plant personnel. The performance factors are described briefly below, with more detail in the remainder of the dissertation.

In benchtop ageing studies, a decrease in clean membrane resistance is generally observed for PVDF membranes aged via an extended single-soak in NaOCl (Abdullah and Bérubé, 2013; Hajibabania et al., 2012; Le-Clech, 2014). However, an increase in resistance has also been observed when membranes were cycled (fouled and cleaned repeatedly) during ageing (Hajibabania et al., 2012; He et al., 2014; Wang et al., 2010). Resistance likely decreases due to pore expansion from membrane degradation, or increases due to irreversible fouling (Chapter 2).

Most ageing experiments indicated an increase in fouling rate with membrane age (Abdullah and Bérubé, 2013; Arkhangelsky et al., 2008; Gaudichet-Maurin and Thominette, 2006; Levitsky et al., 2012, 2011, Qin et al., 2004, 2003). It has been hypothesized that aged membranes become more hydrophobic as hydrophilic additives are removed, causing them to foul more readily (Abdullah and Bérubé, 2013; Gaudichet-Maurin and Thominette, 2006; Qin et al., 2004, 2003).

Membrane cleaning rate, reflecting how easily permeability can be recovered by membrane cleaning, is a potentially important performance factor for two reasons. Severe cleaning of membranes uses additional resources (chemicals and down-time), as well as potentially causing the membranes to age more quickly than necessary. In one study (Abdullah and Bérubé, 2013) chemical cleaning was observed to be less effective for older membranes.

The membrane susceptibility to breach cannot be assessed directly as a performance factor; however, mechanical properties are often used as surrogates. In general, PVDF membranes become weaker as they age (Hajibabania et al., 2012; Wang et al., 2010).

The performance of the surrounding module infrastructure is technology-specific and independent of the membrane material, so it was not addressed in the present study.

1.2.2 Objectives & Scope of Full-Scale Ageing Component

Benchtop accelerated ageing studies (bench-scale ageing) indicate that chemical cleaning, by sodium hypochlorite (NaOCl) in particular, negatively impacts long-term membrane

performance (Chapter 2). However, bench-scale ageing cannot replicate the nuances or timescales of membranes that undergo field operation (full-scale ageing). The complexity that can be considered at bench-scale is limited; water quality, suites of cleaning procedures, and hydraulic conditions add variability that experiments usually strive to minimize. Most research studies age membranes used for drinking water treatment via a single soak of the membranes in an NaOCl (single-soak ageing). Repeated cycles of fouling and cleaning to achieve bench-scale ageing (cycled ageing) may better simulate full-scale operation. However, cycled ageing has only been applied in a few studies (Arkhangelsky et al., 2008, 2007b; Causserand et al., 2008; Hajibabania et al., 2012).

Furthermore, the concentration of NaOCl used in bench-scale ageing is typically 10 to 1000 times higher than that used in full-scale ageing (Abdullah and Bérubé, 2013). Abdullah and Bérubé examined the applicability of the widely-used concept of C*t (concentration * exposure duration) for characterizing membrane NaOCl exposure (Abdullah and Bérubé, 2013). They reported that ageing is more sensitive to duration than concentration, so accelerated bench-scale ageing trials may be underestimating long-term negative impacts. For example, changes in membrane permeability and chemistry were more responsive to a given C*t when membranes were exposed at a lower concentration.

A limited number of studies have also investigated field-ageing in treatment plants. Keucken *et al.* observed polyetherssulfone (PES) membranes for 1 year in an operational WTP; unfortunately, the time period considered was too short to observe changes in membrane performance (Keucken et al., 2016). He *et al.* observed decreasing permeability

over a 3-year period for polyvinylidene difluoride-based (PVDF-based) membranes operated in a drinking water application (He et al., 2014). Fenu *et al.* observed permeability decline in PVDF-based membranes over 10 years in an MBR (Fenu et al., 2012). Most studies to date have focused on PVDF-based membranes, as PVDF is currently the dominant membrane chemistry utilized in drinking water treatment applications (Pearce, 2017). Although these studies provide insight into field ageing, they (a) measured only limited performance factors, (b) included only a short timeframe during which other parameters were measured, and (c) only considered one water treatment plant. To build on this existing work the field of membrane field-ageing would benefit from:

- Performance factor data (beyond permeability) for multi-year timescales,
- Analysis of membrane characteristics to explain performance changes, and
- Data from a variety of WTPs, to control for plant-specific variation in water quality, operation, etc.

The primary objective of the full-scale ageing component of the present work was to determine which performance factors change over many years of field-ageing. We hypothesized that performance outcomes similar to those observed in cycled bench-scale ageing would be reflected in field-aged membranes: an increase in fouling rate and clean membrane resistance, and a decrease in cleaning rate and a deterioration of membrane mechanical properties.

We also hypothesized that the chemical characteristics of field-aged membranes would provide a basis for explaining the observed changes in performance. For example, hydrophilic additives have been observed to decline in lab-aged membranes, resulting in

greater fouling (Abdullah and Bérubé, 2013). We anticipate that the same causal relationships would hold for field-aged membranes.

Finally, although C*t is not measured accurately in most water treatment plants, it is the most common ageing metric used in laboratory studies. We anticipated that membrane ageing at full-scale would be accelerated for membranes exposed to higher doses of NaOCl. Therefore, a secondary objective of the study was to compare bench-scale ageing and full-scale ageing.

1.2.3 Objectives & Scope of Bench-Scale Ageing Component

For membranes used in water treatment, long-term exposure to NaOCl, along with other facets of operation, causes membranes to age irreversibly. Membrane ageing is reflected in declining membrane performance.

Bench-scale experiments are popular tools to probe membrane ageing. Most involve soaking membranes in NaOCl solution at a high concentration for an extended period (single-soak). Few bench-scale experiments incorporate cycled fouling and cleaning (cycled operation), with the aim of better mimicking full-scale membrane operation.

In the full-scale experimental project (Chapter 4), stark differences in performance were observed between full-scale aged membranes and reports from the literature for similar bench-scale aged membranes. Notably, membrane resistance increased in full-scale aged membranes and decreased in bench-scale aged membranes. Unfortunately, full-scale

ageing studies have drawbacks: an ageing experiment within a full-scale water treatment plant would require many years of observation, cannot be rigorously controlled (e.g. for feed quality), and would be expensive and labour-intensive to run. Therefore, appropriate bench-scale tools are required. Overall, the three main approaches to membrane ageing are full-scale operation, and bench-scale cycling or soaking, as illustrated in Figure 2. The links among these three approaches are key to understanding membrane ageing. The bench-scale component of the present dissertation aimed to develop and better-understand bench-scale tools for membrane ageing. There were two major objectives.

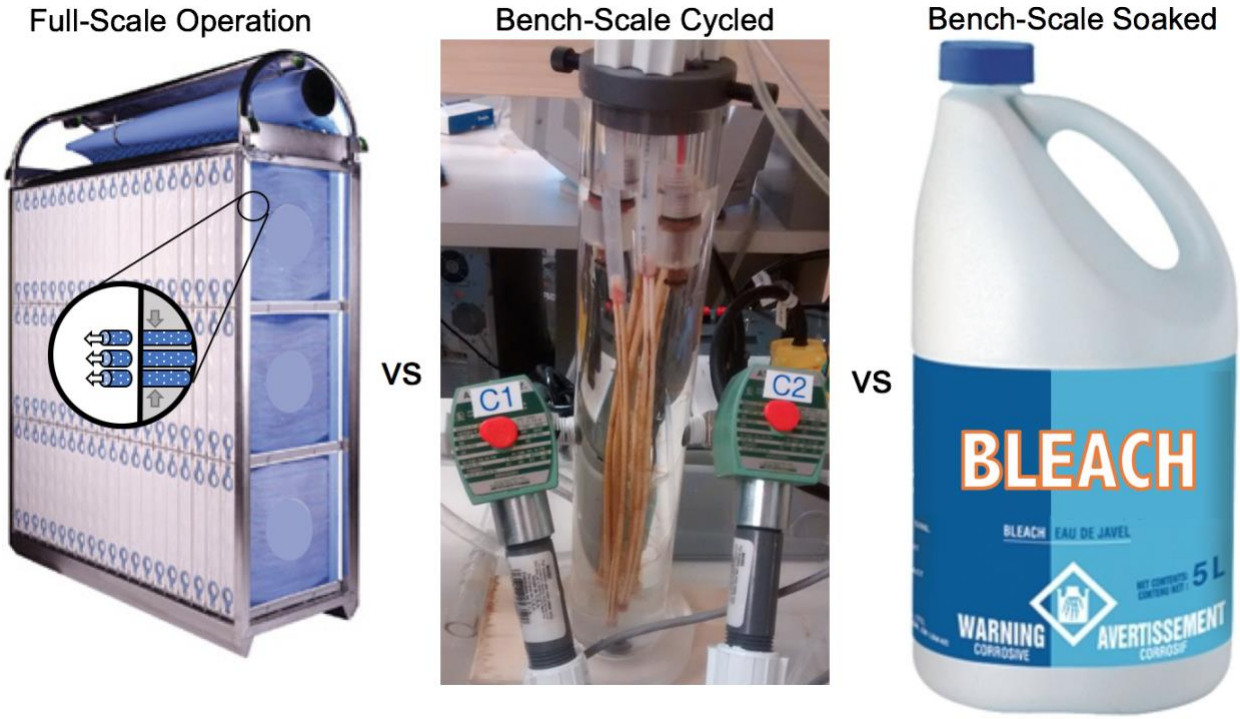

Figure 2. Illustration of the three different ageing concepts considered in this dissertation.

First, we aimed to understand the discrepancies between results from bench-scale ageing (i.e. single-soak and cycled operation) and full-scale ageing. We hypothesized that the effects of permeation and fouling are important factors in membrane ageing, in addition to the NaOCl exposure dose.

Second, we sought to use bench-scale ageing to understand how physical and chemical characteristics change and impact membrane performance. We hypothesized that by comparing single-soak to cycled membranes at bench-scale, we could extrapolate observed ageing behaviours to those observed or expected in full-scale operation.

1.3 Organization of the Dissertation

Chapter 1 - Introduction

This chapter provides background on membranes for water treatment and the relevance of membrane ageing. Objectives for the dissertation are identified.

Chapter 2 - Literature Review

This chapter is based on our 2016 publication in the Journal of Membrane Science. It has since been updated with recent publications, up to the beginning of 2018, as it was initially published in 2016.

Chapter 3 - Methods & Materials

This provides a general explanation of the materials and methods used in the experimental aspects of the present work. For more detailed explanations, please refer to Appendix 2.

Chapter 4 - Membrane Ageing in Full-Scale Water Treatment Plants

This chapter follows a similar roadmap to the eponymous publication, but provides more detailed discussion than was possible in the publications.

Chapter 5 - Seeking Realistic Membrane Ageing at Bench-Scale

This chapter follows a similar roadmap to the eponymous publication, but provides more detailed discussion than was possible in the publications.

Chapter 6 - Conclusions & Recommendations

This chapter summarizes the major conclusions from all parts of the dissertation. The implications of the present work for operation of water treatment plants, and for the future of membrane ageing research are discussed. Remaining knowledge gaps and future recommendations for research are also included in this section.

Appendices

There are 6 appendices, as follows:

1. Appendix from the literature review, including a comprehensive list of which connections are considered in each publication.
2. Storage considerations for natural water. This section presents a publication that was prepared as part of the preliminary work in this research project. Based on these findings, "raw" water in the present dissertation was not stored for long periods at room temperature.
3. Detailed description of the methods employed in this work.
4. Appendix that includes additional figures and details on statistical analysis relating to the full-scale ageing research project.
5. Data collected on a third membrane type (ZW500) which was excluded from the full-scale ageing study due to the limited number of samples available.
6. Appendix that includes additional figures and details on statistical analysis relating to the bench-scale ageing research project.

Chapter 2 - Literature Review

2.1 Introduction

In low-pressure membrane research, performance deterioration is a ubiquitous topic. In the 1980's and 1990's, research focused on understanding fouling and designing cleaning procedures to combat fouling. Since 1980, thousands of journal publications have been published which focus on membrane fouling, and hundreds on membrane cleaning. Recently, the study of the long-term changes in membranes during use, dubbed 'ageing' has grown as well. Of these, roughly 50 journal articles address ageing of low-pressure membranes for water treatment. This literature analysis was first performed using the ScienceDirect database by Regula *et al*. but updated using identical search terms (Regula et al., 2014).

Most low-pressure membrane ageing research relates to water treatment, which is widespread in application for high-volume use. In drinking water treatment, membrane systems are easily automated, and reliably produce a high quality effluent, despite variable raw water characteristics. For wastewater treatment, membranes are generally incorporated into membrane bioreactors (MBRs) to minimize plant footprint and provide high effluent quality. These advantages have enabled membranes to become one of the fastest-growing water treatment technologies.

Fouling in low-pressure membranes is caused by the accumulation of feed solution constituents at or in the membrane, usually causing an increase in resistance to permeate flow. Fouling control methods include both physical or hydraulic cleaning, and chemical

cleaning techniques. It is common to use multiple cleaning methods in any particular application. For example, hydraulic cleaning is often carried out using air scouring, cross-flow, and backwashing. Cleaning with various chemical reagents is common in routine operation (i.e. chemically-enhanced backwash), as well as periodically, when more extensive cleaning is required (recovery or clean-in-place) (Le-Clech, 2014). Chemical cleaning agents include oxidants, acids, bases, surfactants, and chelating agents, each targeting particular foulants. Sodium hypochlorite, an oxidant and disinfectant, is the most common cleaning agent used in water treatment applications, (Porcelli and Judd, 2010) so it is featured in this review.

Despite the importance of fouling control for maintenance of long-term membrane performance, cleaning agents can have unintended impacts on the membrane materials (Gaudichet-Maurin and Thominette, 2006). The combination of long-term exposure to cleaning agents, accumulation of irreversible foulants, and other rigours of membrane use combine to result in membrane ageing. In this review, membrane ageing is defined as the change observed in membrane properties over long-term use (i.e. irreversible changes). These properties can be expressed either as membrane physical and chemical characteristics (e.g. chemical composition, pore size), or be measurable performance factors (e.g. fouling rate, membrane resistance). Though membrane characteristics cause changes in performance, the relationship between the two types of parameters is not thoroughly understood.

The present discussion focuses on low-pressure polymeric membranes. These types of membranes are prone to organic reactions with cleaning agents and components of the feed water and, therefore, are susceptible to ageing. Although ceramic or inorganic membranes are also applied in water treatment, their very low reactivity and high resilience mean that ageing effects can be easily reversed, without compromising membrane chemical or physical properties (Van Der Bruggen et al., 2003). Also, polymeric membranes account for 80-90% of the global treatment capacity (Regula et al., 2014).

To date, three major studies have focused on membrane ageing (Fenu et al., 2012; Le-Clech, 2014; Regula et al., 2014). In addition to these, approximately 50 journal publications have reported on ageing of specific types of membranes in specific applications. Most publications consider performance factors or membrane characteristics without emphasizing the link between these. Also, no work to date has considered an overview of all performance factors and characteristics. The present chapter focuses on three objectives to begin to bridge this knowledge gap.

The first objective was to identify changes in membrane performance factors as membranes age, and determine the characteristics that cause these changes. Because the mechanism leading to the ageing process itself was not considered as part of this objective, multiple types of membrane chemistries were considered in parallel. However, only ageing resulting from exposure to NaOCl was considered, as this is the most common cleaning agent. The second objective was to understand changes in chemical and physical characteristics associated with membrane ageing. To do this, data from analytical methods

used in ageing experiments were interpreted. Because changes are generally chemical-specific, membranes with polyvinyledene difluoride (PVDF)-based chemistry were considered. PVDF-based membranes are among the most commonly used in water treatment applications (Regula et al., 2014), but the approach developed in the present discussion can be used to investigate ageing of other membrane chemistries. The third objective was to use the compiled knowledge to identify research directions that are necessary to understand and strategically minimize membrane ageing.

2.2 Approach to Literature Review Analysis

To visualize the objectives, a three-category framework (Figure 3) was developed. The first category contains performance factors: features of membrane performance during use, which change as membranes age. The second category contains chemical and physical characteristics of the membrane material itself, which cause changing performance. The third category contains analytical methods that are employed to investigate membrane characteristics. Recalling the objectives identified in Section 2.1, objective 1 links the first and second categories of the framework, objective 2 links the second and third categories, while objective 3 identifies what can be learned from the existing and missing links between the categories. Others have explored membrane failure during commissioning and due to improper operation (Antony and Leslie, 2011; Tng et al., 2015), so the focus here is on ageing during normal operation.

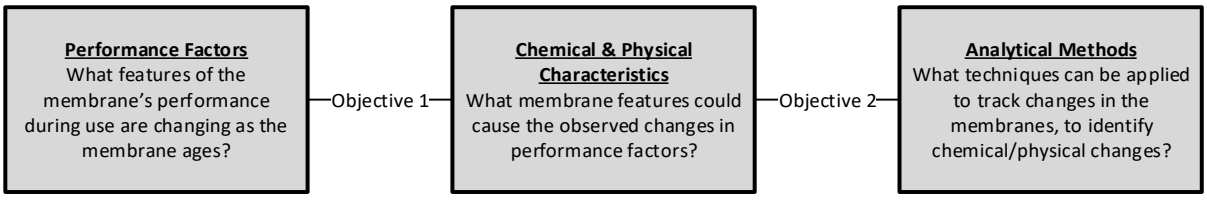

Figure 3. Three-category framework for understanding membrane ageing.

Five membrane performance factors were identified for consideration in the present chapter; these are:

- Resistance,
- Fouling rate,
- Breach frequency,
- Cleaning rate, and
- Deterioration of infrastructure

Approximately 50 journal publications discussing ageing of membranes for water treatment were reviewed (Appendix 1). These publications were identified using a ScienceDirect search, supplemented by Google Scholar and SciFinder, with both of the terms “membrane” and “ageing” in the title or abstract. They were narrowed down by selecting the papers which address low-pressure membrane ageing in water treatment applications. Studies investigating short-term changes are encompassed in existing reviews handling cleaning and fouling; thus, the ageing papers in this review discussed long-term effects exclusively. For each publication, reported performance factors, membrane physical and chemical characteristics, and links between these were identified. Analytical methods used, in the various studies, to characterize membrane physical or chemical characteristics were also identified. In Sections 2.3 and 2.4, these observed and postulated links are discussed. The findings are compiled and summarized graphically in Section 2.5.

2.3 The Influence of Membrane Characteristics on Performance Factors

2.3.1 Resistance

Resistance describes membrane impedance to fluid flow. Both the membrane itself and material retained by the membrane can affect the total resistance; however most ageing studies have been performed using 'clean' water filtration tests, and therefore only focus on the intrinsic clean membrane resistance. As introduced in Equation 2 (Section 1.1), the intrinsic resistance can be determined based on the operating trans-membrane pressure (ΔP), the fluid viscosity (μ), and the permeate flux (J) when filtering clean water (Crittenden et al., 2005). Insight into the parameters affecting the intrinsic resistance can also be obtained by considering the physical features of a membrane (Equation 3), namely the pore length (L), pore radius (r), number of pores (n), and membrane area (A), as well as a tortuosity correction factor (τ).

Resistance is measured in 63% of the membrane ageing publications reviewed. Most experiments involve measuring clean water flux or pressure through a bench-scale membrane module, which has been artificially aged by soaking in a cleaning solution. The results of the clean water filtration tests are a common surrogate for the performance factor in full-scale membrane applications.

Most studies performed with clean water and artificially aged membranes report an increase in pore size and porosity, resulting in decreasing resistance as membranes age (Abdullah and Bérubé, 2013; Arkhangelsky et al., 2007a; Do et al., 2012a; Hajibabania et al., 2012; Jung et al., 2004; Liang et al., 2013; Pellegrin et al., 2015a, 2013; Puspitasari et al.,

2010; Qin et al., 2005a, 2005b, 2004, 2003; Qin and Wong, 2002; Wolff and Zydney, 2004; Yadav and Morison, 2010). Several researchers have suggested that the increase in pore size resulted from the removal of additives from the membrane matrix (Arkhangelsky et al., 2007a; Jung et al., 2004; Qin et al., 2005a, 2005b, 2004, 2003; Qin and Wong, 2002). It was suggested that additive removal occurs in tandem with primary polymer chain scission (Arkhangelsky et al., 2007a; Jung et al., 2004; Pellegrin et al., 2013), and that polymer chain scission 'opens' the pore structure with ageing (Do et al., 2012a). A few lab-based studies have seen the opposite effect - decreasing permeability. Da Costa (da Costa et al., 2015) observed decreasing permeability for membranes artificially aged by soaking in NaOCl as well as with oxalic acid or citric acid. They attributed these changes to pore collapse resulting from degradation in membrane chemistry. A similar argument was made by Arkhangelsky *et al.* (Arkhangelsky et al., 2008), Liang (Liang et al., 2013), and Do (Do et al., 2012b), attributing decreasing permeability to disintegration of the membrane surface.

Several authors have attributed observed changes in resistance to changes in membrane surface chemistry (Arkhangelsky et al., 2008, 2007a, Do et al., 2012a, 2012c; Hajibabania et al., 2012; Levitsky et al., 2011; Puspitasari et al., 2010; Wolff and Zydney, 2004). However, based on Equation 2, it is unclear that there is a basis for the effect when filtering clean water: the functional groups present on the membrane surface would be expected to have little impact on pore dimensions (thus, resistance) of microfiltration and ultrafiltration (MF and UF) membranes.

In contrast to most lab-scale results, operational data from full-scale membrane systems generally indicate an increase in resistance as membranes age (He et al., 2014). The increase in resistance likely results from interactions between material in raw water, the membrane, and chemical cleaning agents, leading to irreversible fouling (Causserand et al., 2008; Hajibabania et al., 2012; Wang et al., 2010). The levels of fouling and cleaning agent exposure seen in operational systems need more consideration in research: although cleaning agent concentration can be increased considerably to accelerate ageing, concentrating foulants on operational membranes introduces fouling challenges.

As illustrated in Figure 4, it is very common to associate changes in resistance with changing physical and chemical characteristics of the membrane, with only 1 of the 28 publications that measured resistance lacking connections to characteristics.

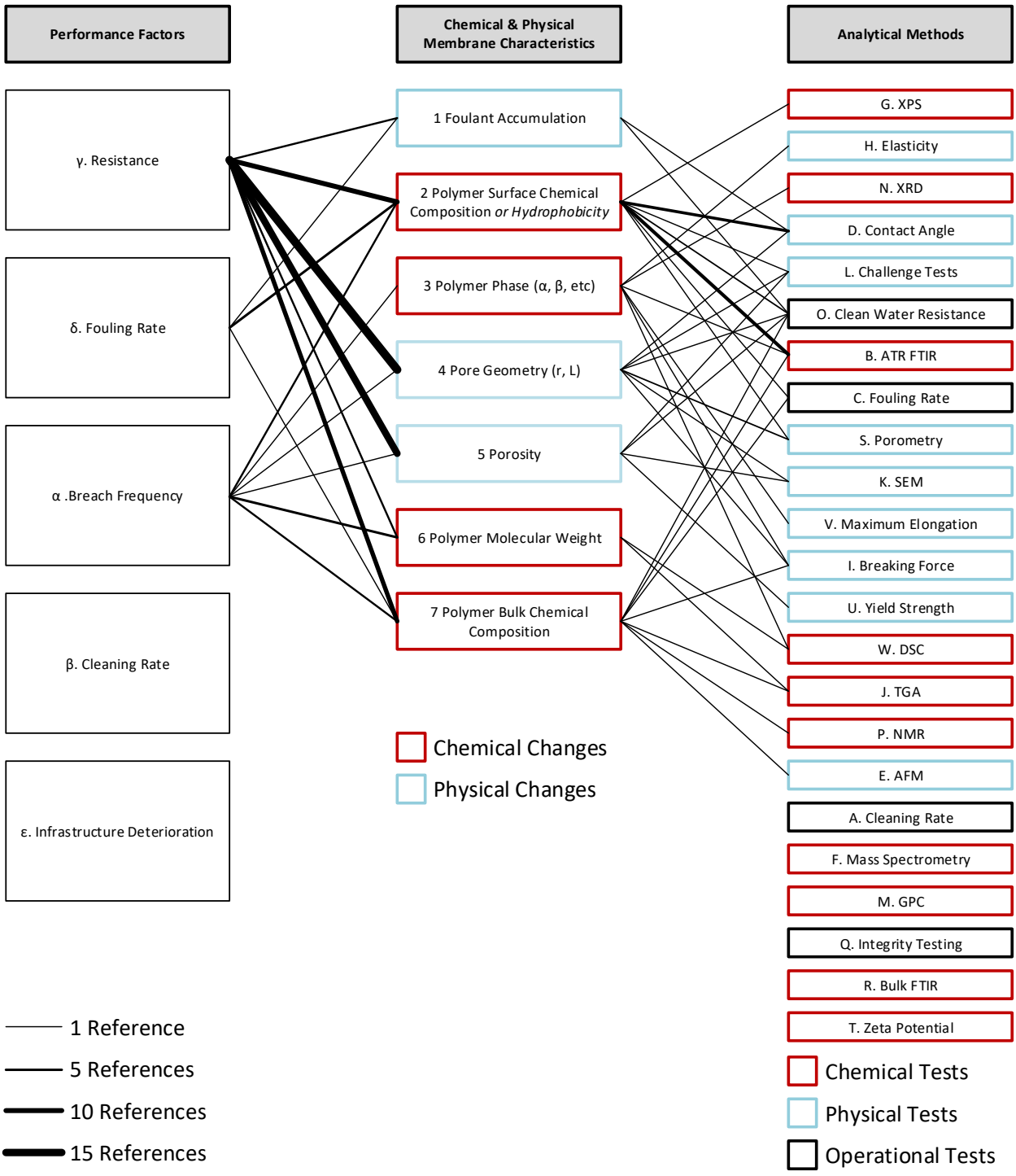

Figure 4. Relationships, as established in the membrane literature, between performance factors, membrane characteristics, and experimental techniques. The line thickness corresponds to the number of references that suggest a particular relationship.

2.3.2 Fouling Rate

Fouling generally results from the accumulation of retained material on (cake fouling and blocking) or in (adsorption) a membrane, and causes an increase in the resistance to the permeate flow . Chemical reaction with the membrane and bacterial growth can also lead to membrane fouling (Pabby, 2009). The fouling rate is usually expressed as a change in membrane resistance over time during one cycle of operation. This contrasts with resistance itself, which is defined based on permeability of clean membranes.

Fouling rate was measured in 20% of membrane ageing publications reviewed. Most studies were performed using artificially aged membranes that were then exposed to various matrices, either synthetic (e.g. bovine serum albumin, BSA) or real (e.g. activated sludge). Resistance change over the course of fouling was measured to determine the fouling rate.

Most reports indicated that the fouling rate increases with age, and attribute the change to an increase in the hydrophobicity of the membrane surface (Abdullah, 2013; Arkhangelsky et al., 2008; Hajibabania et al., 2012; Qin et al., 2005a, 2004, 2003). Some studies have suggested that the change in the rate of fouling over time results from an increase in the surface charge or hydrophilicity of the membrane surface over time (Arkhangelsky et al., 2007a; Levitsky et al., 2012, 2011). The contradictory results in the literature indicate that understanding is not resolved on this fundamental aspect of ageing. Only two studies have considered accelerated ageing using cycled fouling and cleaning (Hajibabania et al., 2012; Wang et al., 2010). These consider the interplay of foulant and cleaning agent, which may

become important after prolonged use (i.e. cycling). As observed when considering membranes aged by soaking in cleaning agent, an increased fouling rate for aged membranes is also observed in the cycled experiments.

As illustrated in Figure 4, it is very common to link fouling rate with changing physical and chemical characteristics of the membrane, with only 3 of the 9 publications that measured resistance lacking connections to these characteristics.

2.3.3 Membrane Breaches

Most membrane breaches in UF and MF systems result due to fibre breakage, with pore enlargement contributing very little to failure (Gijsbertsen-Abrahamse et al., 2006). Due to the very low frequency at which broken fibres are observed, the actual breach frequency cannot be measured via surrogate experiments in a lab setting in the same way that resistance and fouling rate have been investigated. Gijsberten-Abrahamse discusses the true importance of breach frequency in membrane systems (Gijsbertsen-Abrahamse et al., 2006). In addition to the work by Gijsberten-Abrahamse, an AWWA Research Foundation report proposed a correlation between increased TMP and increased fibre breakage (Pressdee et al., 2006). Because higher TMPs tend to occur later in membrane life, this work suggests a correlation between membrane age and membrane breaches. Unfortunately, according to the AWWA report, statistics on actual breach frequency are very limited because, due to warranty implications, this is a relatively sensitive topic for water treatment operations (Pressdee et al., 2006).

Change in susceptibility to membrane breach is generally assessed based on changes in mechanical properties, such as elasticity and tensile strength (Arkhangelsky et al., 2007b). Decline in these properties has been attributed to changes in the chemistry of membranes (Arkhangelsky et al., 2008; Gaudichet-Maurin and Thominette, 2006; Rouaix et al., 2006), and related changes in crystallinity and molecular weight (Causserand et al., 2006; Hashim et al., 2011). The decline also been linked to increasing porosity and pore size (Arkhangelsky et al., 2007a; Hanafi et al., 2014; He et al., 2014; Yadav et al., 2009). However, as observed by Gijsberten-Abrahamse (Gijsbertsen-Abrahamse et al., 2006), based on a survey of full-scale systems, membrane breaching is not a common trigger leading to membrane replacement (Gijsbertsen-Abrahamse et al., 2006). In particular, supported membranes - featuring a robust backing for the membranes - would be less susceptible to this mode of failure.

As illustrated in Figure 4, it is very common to link susceptibility to mechanical failure with changing physical and chemical characteristics of the membrane, as all 10 publications that discussed this factor related susceptibility to these characteristics.

2.3.4 Cleaning Rate

The cleaning rate is defined as the rate at which permeability is recovered for membranes during chemical cleaning. Compared with the other performance factors, the cleaning rate has received limited attention, and was only measured in one of the reviewed publications (Abdullah, 2013). Cleaning rate can be estimated in a lab setting by monitoring permeability during cleaning, or relative clean water flux before and after cleaning.

Abdullah (Abdullah, 2013) investigated the rate at which the permeability of artificially aged membranes was recovered after fouling with activated sludge. The rate of recovery was observed to decrease as membranes aged. The extent to which the resistance could be recovered also decreased with age. Some other studies mention cleaning efficiency (Levitsky et al., 2012; Puspitasari et al., 2010), but these only consider change in recoverable resistance as membranes age. Such results were grouped with the resistance performance factor (Section 2.3.1). Abdullah did not link the cleaning rate to any membrane characteristics. In membrane-based treatment plants, it has indeed been reported that more rigorous cleaning protocols are required as membranes age, though there is no published literature on this topic. This observation was made based on discussion with partner water treatment plants; however, these plants have not authorized us to share specific information, so such results are anecdotal.

Cleaning rate may be of particular interest for two reasons. First, longer and more intensive cleans require more system down-time and more chemical consumption, which are costs to a water supplier. Second, if older membranes require more rigorous cleaning, this could contribute to faster ageing with respect to other performance factors.

2.3.5 Infrastructure Deterioration

The membrane infrastructure deterioration (i.e. potting material or the membrane module structure) can also lead to membrane replacement, regardless of the condition of the membrane fibres. Anecdotal discussion with membrane treatment plant operators has identified potting degradation as a major performance factor of concern. Unfortunately,

these facilities prefer not to be identified in this work. This effect has not been studied in lab-based ageing trials, where the focus is on the membranes themselves. Although infrastructure decline is a potentially important performance factor, it is very system-specific and could theoretically be optimized independent of the membranes. It is included here for completeness, but not addressed further. Several researchers have noted the importance of supporting infrastructure on membrane life (Gijsbertsen-Abrahamse et al., 2006; Regula et al., 2014).

2.4 Analysis of Physical & Chemical Characteristics for PVDF Membranes

Chemical, physical and operational methods that can be used to characterize membrane ageing need to be considered. Because changes are generally specific to a given membrane chemistry, the discussion which follows focuses on PVDF-based membranes. As previously discussed, PVDF is one of the most prevalent base chemistries for low-pressure polymeric membranes used in drinking water applications. It should be noted that most PVDF-based membranes also contain various additives and copolymers. Polyvinylpyrrolidone (PVP) is mentioned frequently in the literature (Delattre et al., 2012; Hajibabania et al., 2012; Puspitasari et al., 2010), though often the additives in commercial products are not mentioned as they are proprietary (Abdullah and Bérubé, 2013). Although this discussion only considers PVDF-based membranes, the approach used to assess links between performance factors and physical/chemical changes can also be applied to other membrane chemistries.

2.4.1 Chemical Analytical Methods for Ageing in PVDF Membranes

2.4.1.a Fourier Transform Infrared Spectroscopy (FTIR)

FTIR reveals the infrared vibrational spectrum of functional groups within a sample. Based on the vibrational frequency, the identity of the functional groups and, in cases, the sample's chemical composition can be determined. Though less quantitative than other techniques (e.g. X-Ray Photoelectron Spectroscopy), FTIR is fast and inexpensive. ATR-FTIR (attenuated total reflectance FTIR) involves reflectance of IR radiation by the sample, so it is a surface technique. All of the work that has been published involving FTIR and PVDF membrane ageing uses ATR-FTIR.

There is no known reaction of PVDF with NaOCl (Hashim et al., 2011; Wang et al., 2010), despite one report attributing FTIR observations to NaOCl-induced PVDF cross-linking (Le-Clech, 2014). However, many have concluded from FTIR spectra that additives in PVDF membranes are degraded during NaOCl soaking (Abdullah and Bérubé, 2013; Le-Clech, 2014; Puspitasari et al., 2010). In particular, additives exhibiting a carbonyl group are removed or transformed by NaOCl. Similar carbonyl removal was observed in studies that considered cycled NaOCl cleaning and fouling (Hajibabania et al., 2012; He et al., 2014). In one publication, a carbonyl group was reported to form (rather than disappear) on the membrane surface during ageing (Le-Clech, 2014), but this result is an exception. Overall weakening of FTIR signal has been attributed to foulant layer (Wang et al., 2010), but FTIR has not been used to characterize foulant.

In contrast to NaOCl, hydroxide causes PVDF degradation, via the dehydrofluorination mechanism presented by Ross *et al.* (Ross et al., 2000). The appearance of a carbonyl peak, an outcome of dehydrofluorination, in FTIR spectra after NaOH ageing was observed for one membrane; however, it was attributed to crosslinking of PVDF, rather than dehydrofluorination (Le-Clech, 2014).

Hydrochloric acid and sodium dodecyl sulfate (SDS) effects on the FTIR spectra of PVDF membranes have received little attention. The results differ depending on the specific membrane, and are attributed to changes of the additives, rather than PVDF itself (Le-Clech, 2014).

The majority of the reviewed publications used changes in ATR-FTIR spectra to infer changes in surface chemistry, as illustrated in Figure 4 with a thick line. As described in Section 2.3.2, surface chemistry has an expected impact on the 'fouling rate' performance factor.

In the literature on PVDF membrane ageing, there are no studies that implement bulk FTIR analysis. This technique would give a better understanding of bulk chemistry than the prevalent ATR method. As described in Section 2.3.3, changing bulk composition impacts membrane strength and thus the 'susceptibility to breach' performance factor.

2.4.1.b Nuclear Magnetic Resonance (NMR) Spectroscopy

Nuclear magnetic resonance (NMR) spectroscopy is an analytical technique for substance identification. NMR involves the application of a strong magnetic field to the material of interest, which interacts with atomic nuclei. By observing their specific spin decay, the abundance of various atoms in a sample can be quantified. NMR analysis allows identification and quantification of chemicals present in the bulk membrane. There is relatively little precedent for this technique in the membrane ageing literature.

Only one study has used NMR to understand the changing chemistry of PVDF membranes with age. Abdullah and Bérubé (2013) used NMR to reveal the removal of hydrophilic additive (HA) from PVDF membranes during ageing. They found a strong correlation with an FTIR peak, and therefore deemed ATR-FTIR a workable substitute for NMR. However, NMR is more quantitative than FTIR and is more capable of identifying unknown materials.

2.4.1.c Mass Spectrometry

Mass spectrometry (MS) allows for determination of the molecular masses of substances present in a sample. In the techniques discussed so far, a short oligomer has a similar response to a very high molecular weight polymer. However, MS has the potential to give a range of polymer(s) mass present. Because polymers can have very high molecular weights, the aggressive ionization of typical mass spectrometric techniques would cause excessive fragmentation.

Fortunately, relatively recent techniques are allowing MS to make the foray into polymer science. The most widespread such method is called MALDI-ToF (matrix-assisted laser desorption, time-of-flight spectroscopy). There is little precedent for MALDI-ToF in membrane characterization, though it is used widely for polymeric analysis (Montaudo et al., 2006). For example Ameduri *et al.* used MALDI-ToF to characterize PVDF; the high degree of fluorination made the technique difficult to optimize, due to poor ionization (Ameduri et al., 2004). In principle, the same technique could be used to study PVDF membranes. As membranes age, an increase or decrease in polymeric molecular weight, due to either polymer cross-linking or degradation, could impact its macroscopic physical properties.

ToF-SIMS (time of flight secondary ion mass spectroscopy) has been used in PVDF membrane analysis to observe surface molecular fragments (Ross et al., 2000). This technique samples only the surface of the sample, causing sputtered ionized molecular fragments. The surface specificity is only one or two monolayers thick, so this technique holds potential for characterising surface foulants. However, due to the fragmentation it causes, ToF-SIMS does not reveal polymeric molecular mass. No links have been made between this MS technique and membrane characteristics.

2.4.1.d Gel Permeation Chromatography

Gel permeation chromatography (GPC), also called size exclusion chromatography, provides a means of determining the molecular mass distribution of large molecules and polymers. Species of interest are dissolved and passed through a column which allows

larger molecules to exit more quickly than smaller ones. This technique is less specific and expensive than mass spectrometry, but can take tens of minutes to hours per sample. When basing molecular weight distribution on GPC separation alone, appropriate standards of known molecular mass and similar behaviour to components of the sample must be used. Finally, the solvents used to dissolve sample and the mobile phase must be carefully selected, to properly dissolve the sample and not interfere with the chosen column or detector. This technique has not been applied in the PVDF membrane ageing literature, but holds potential for understanding polymer degradation via the assessment of molecular mass. The implications of changing molecular mass for performance factors were discussed in Section 2.4.1.c.

2.4.1.e Thermogravimetric Analysis

Thermogravimetric analysis (TGA) is a technique by which material is weighed while being gradually heated (Lobo and Bonilla, 2003). As the temperature increases, volatile components are removed, oxidation occurs, and thermal degradation proceeds. Based on the TGA profile of a polymer membrane, the properties of small-molecule additives, preservatives, and the polymer itself can be probed. When the degradation temperature of a polymer is reached, it breaks down into shorter-chain components that are volatile. Larger or more cross-linked polymers volatilize at higher temperatures.

Hajibabania *et al.* used TGA to study the effects of NaOCl ageing in PVDF membranes. The researchers observed an increase in degradation temperature, which they attributed to cross-linking of the polymer network upon ageing (Hajibabania et al., 2012). Le-Clech used

TGA to study membranes aged in various cleaning solutions (Le-Clech, 2014). Depending on the membrane type, both increases and decreases in decomposition temperature were observed for NaOCl ageing. In addition to the degradation temperature, the relative abundance of PVDF and additives was studied via TGA, manifested as two different peaks. In general, when an additive was present in a virgin membrane, NaOCl removed the additive with advancing membrane age.

Le-Clech (2014) also studied other cleaning agents, including HCl, NaOH and SDS, for several PVDF membranes. Results on TGA profiles were very membrane-specific, so general conclusions could not be made.

Although TGA can suggest information about polymer molecular weight, interferences from additives can cause changes in the degradation profile of a polymer. Also, the relationship between polymer molecular weight (scission/crosslinking) and degradation temperature is not necessarily direct; chemical or conformational changes to polymers can also influence the degradation temperature (Lobo and Bonilla, 2003). If used as a surrogate for molecular weight, the implications of TGA results with respect to performance factors are similar to those of mass spectrometry and GPC; that is, polymer degradation could cause decline in mechanical properties, resulting in an increase in breach frequency. This is the most common connection reported for TGA.

2.4.1.f Differential Scanning Calorimetry

Differential scanning calorimetry (DSC) is used to measure melting temperature and melting enthalphy of polymers. The melting enthalpy of a polymer is related to the crystallinity, as more 'bonded' crystal structures require more energy to be broken. Hashim *et al.* (2011) reported that membranes had higher melting temperature and higher melting enthalpy than raw polymers used to make the membranes, suggesting that membrane manufacture increases the crystallinity of the polymer. The degree of crystallinity was measured, and was found to be significantly higher for the membrane than the raw material (Hashim et al., 2011), particularly for low-molecular weight PVDF. NaOH ageing caused melting temperature to decrease, particularly for NaOH ageing at high temperatures. The melting enthalpies also decreased with membrane age. Several different membranes were considered, and the membranes that aged more slowly, with respect to other measured parameters, also exhibited less change in melting enthalpy.

2.4.1.g X-Ray Diffraction (XRD)

There is limited information in the literature on the polymeric structure of membrane materials. Two materials may be identical in their atoms and bonding patterns but, depending on the orientation of these bonds and the resultant intramolecular configurations, may show distinct behaviour. The crystal structure of polymers has an important impact on their physical properties including tensile strength, melting point, brittleness, and even hydrophobicity. One means of examining crystal structure or crystallinity of polymers and structural changes is via x-ray diffraction (XRD).

In the membrane literature, Hashim *et al.* studied crystal structures of PVDF after ageing with NaOH (Hashim et al., 2011). Each observed crystal structure was referred to as a polymer "phase," denoting different arrangements of polymer molecules relative to each other, affecting bulk polymer properties (Gregorio, 2006). Hashim *et al.* reported that XRD spectra of virgin membranes had high prevalence of an isomer called β-phase, whereas the raw PVDF was dominated by α-phase. This suggests that during hollow fibre spinning, the β-phase forms preferentially; however, because the α-phase of PVDF is more stable at ambient conditions, it is conceivable that a phase transition between isomers could affect membrane ageing.

In their artificial ageing experiment, Hashim *et al.* observed that the pure PVDF NaOH-aged membranes had the same crystal structure as virgin membranes. However, as this was not a blended membrane, the effect of additive removal may be important to changing crystal structure. Work with blended non-PVDF membranes by others has suggested that configuration may change due to additive removal (see Section 2.3).

2.4.1.h Contact Angle

Contact angle measurements are widely used to quantify membrane wettability. A high contact angle indicates low wetting and high membrane hydrophobicity, whereas a low contact angle indicates better wetting and a more hydrophilic membrane. In general, more hydrophobic membranes tend to have higher foulant affinity, as many foulants are also hydrophobic in nature.

Most researchers attribute changing contact angle to changing surface chemistry, particularly hydrophobicity, of the membrane. In many cases this involves removal of a hydrophilic additive (Abdullah and Bérubé, 2013; Hajibabania et al., 2012; Levitsky et al., 2012; Puspitasari et al., 2010; Wang et al., 2010). In others it is attributed to increasing charge and hydrophilicity of the membrane surface (Levitsky et al., 2012, 2011). Some researchers mention that it may be due to irreversible foulant accumulation on the membranes (Hajibabania et al., 2012; Wang et al., 2010).

Most of the membrane ageing studies used sessile drop technique based methods for contact angle measurement. However, many membrane surface properties including surface roughness, presence of pores, surface curvature, as well as other factors (e.g., evaporation rate) can affect the result of a contact angle test, but are not widely discussed. Hajibabania *et al.* discussed the limitations of using contact angle measurements to probe the surface chemistry, due to surface roughness, and pore characteristics (Hajibabania et al., 2012). Other authors have noted the difficulty of controlling hysteresis in a reproducible way for contact angle measurements (Abdullah, 2013). The captive bubble method addresses some of the limitations of the sessile drop technique; however this method has seldom been considered.

2.4.1.i X-ray Photoelectron Spectroscopy

X-ray photoelectron spectroscopy (XPS) is used to investigate the elemental composition on a material surface. Although this technique cannot detect hydrogen atoms, it can be used to observe others (C, F, O, N, S), which are common in polymeric membrane materials. In

cases where polymeric membranes contain additives or copolymers, such a technique could be used to study the surface prevalence of these additives with age. XPS has been used to probe organic foulants on non-PVDF membrane surfaces, suggesting additive removal (Arkhangelsky et al., 2007a), as well as to study the membranes themselves (Ross et al., 2000). Although XPS in conjunction with a bulk elemental analysis technique has not been reported, this approach would be useful in attributing membrane ageing to components of the membrane bulk and surface. Puspitasari *et al.* (Puspitasari et al., 2010) made an observation of oxygen removal correlating with hydrophilic additive removal in aged PVDF membranes (Puspitasari et al., 2010). Because changing elemental character of surface layers is caused by alteration of functional groups, this has the potential to affect performance factors such as fouling rate and, potentially, cleaning efficiency.

2.4.1.j Streaming Potential and Zeta Potential

The surface charge of a membrane would be expected to impact fouling behavior. Surface charge can be quantified by streaming potential measurements. In these tests, the potential difference between two electrodes is measured, as a fluid is passed over the membrane at various pressures. Streaming potential can be converted to zeta potential, based on a linear relationship (Teella et al., 2014). The outcome is a measure of the charge density of the membrane surface, which has been associated with characteristics of membrane surface chemistry (Teella et al., 2014). To our knowledge, there are no papers which quantify changing surface charge in aged PVDF membranes. However, this technique has been used observe chlorine effects on polyamide membranes (Kwon and Leckie, 2006), polysulfone membranes (Teella et al., 2014), and PES membranes (Arkhangelsky et al., 2007a). These

observations support the idea that surface charge increases with chlorine exposure. If applied to PVDF membrane ageing experiments, streaming potential would be a useful supplement to other surface chemistry characterization techniques.

2.4.2 Physical Analytical Methods for Ageing in PVDF Membranes

2.4.2.a Mechanical Properties

Mechanical properties of a polymeric membrane can be assessed using several metrics. Ultimate elongation, tensile strength, yield strength, and elasticity can all be used to evaluate membrane physical characteristics. Mechanical properties are typically measured by applying controlled tension to a sample of material.

Ultimate/maximum elongation is the most frequently used method of measuring mechanical properties in PVDF membrane ageing. The elongation is the tensile strain at break. For PVDF aged in NaOCl, some studies reported a decrease in elongation (Hajibabania et al., 2012; Le-Clech, 2014). The authors attributed this to a rearrangement of the polymer chains with membrane age (Hajibabania et al., 2012). Whether this is due to loss of crystallinity or a change in crystallinity is not clear. Contrastingly, two studies reported the opposite effect, an increase in elongation with ageing. This was attributed to cross-linking, increasing pore size and porosity (Rabuni et al., 2015; Wang et al., 2010). For PVDF aged in NaOH, elongation was observed to decrease in two studies (Hashim et al., 2011; Le-Clech, 2014). Causes of changing elongation were assigned to polymer bulk chemistry, polymer phase, pore size and porosity, and polymer molecular weight. Elongation effects with ageing in surfactant (SDS) and acid (HCl) were only considered in

one study (Le-Clech, 2014). The results were non-definitive, and no physical basis for the changes was determined.

The ultimate tensile strength is the maximum strain (force per unit cross-sectional area) that can be applied to material under tension prior to ductile fracture. Two studies reported no significant change in strength (Delattre et al., 2012; Le-Clech, 2014), whereas others note a definitive decrease in tensile strength of PVDF membranes aged with NaOCl (Hajibabania et al., 2012; Wang et al., 2010). The decrease in tensile strength was attributed to changing polymer phase (Hajibabania et al., 2012), decreasing molecular weight (Wang et al., 2010), and changing pore size (He et al., 2014). For PVDF membranes aged with NaOH, a decrease in tensile strength was attributed to dehydrofluorination and phase-change of the PVDF (Hashim et al., 2011).

Yield strength is the stress at which irreversible deformation begins to occur. This has only been reported in one study, and was observed to decrease for NaOCl-aged PVDF membranes (Abdullah and Bérubé, 2013). With the support of SEM images, this effect was attributed to increasing porosity, which has the effect of decreasing the effective cross-sectional area.

Young's modulus of elasticity was observed to decrease with age (Wang et al., 2010), demonstrating that the membrane rigidity decreased with NaOCl ageing. Other work has suggested both increasing and decreasing trends for this parameter (Le-Clech, 2014).

Young's modulus was observed to decrease for NaOH-aged PVDF membranes, and attributed to changing crystallinity (Hashim et al., 2011).

In general, ultimate elongation, ultimate tensile strength, yield strength, and Young's modulus for PVDF membranes are negatively impacted by ageing in either NaOCl or NaOH, as explored above. This reveals that membranes are becoming less robust with age, so have the potential to break or breach more frequently. It has been suggested that decline in mechanical properties indicates a propensity for fibre breakage (Hashim et al., 2011). Although this correlation is logical, this particular relationship has not been studied. Such a correlation may have an important impact in membrane configurations where membranes are relatively vulnerable, but less-so in configurations where a membrane support medium is used. Thus, the membrane configuration – flat-sheet, hollow fibre, supported hollow fibre, etc – should be considered in correlating mechanical properties to membrane breaches. Membrane configuration was beyond the scope of this review, but it presents an avenue for research into breach potential.

2.4.2.b Microscopy

SEM (scanning electron microscopy) involves scanning a sample with a beam of electrons to produce an image of the material surface. Depending on the surface topography and composition, electrons will reflect back to a detector, yielding an image of the material of interest. This form of microscopy provides information about topography, as the technique has relatively good depth of field compared with other techniques.

By employing SEM imaging for aged PVDF membranes, an increase in pore size and porosity due to NaOCl ageing has been observed (Abdullah and Bérubé, 2013); if these increase, that can decrease resistance but could also weaken membrane strength, resulting in more breaches. A similar effect on pore size was observed as a result of NaOH aging (Rabuni et al., 2015).

Some studies have used SEM to qualitatively describe membranes where, often, comparison of these qualitative images can be subjective or even misleading, as discussed by Abdullah *et al.* (Abdullah et al., 2014). Yet qualitative information from SEM images can provide useful hints as to the status of the membrane surface, for example in the observation of microbiological foulants (Vanysacker et al., 2014).

AFM (atomic force microscopy), is a related microscopic technique, with less of a precedent than SEM in the membrane ageing literature. Rather than a beam of electrons, AFM uses a mechanical probe to scan the surface of a sample. Levitsky *et al.* used AFM to probe surface roughness of a PVDF membrane aged with NaOCl. They attributed the increasing roughness observed in AFM images to the elimination of preservation residues in the bulk polymer (Levitsky et al., 2011).

Abdullah *et al.* observed that SEM imaging results are extremely sensitive to a number of imaging variables, such as imaging angle and coating material, which are infrequently reported (Abdullah et al., 2014). Thus, comparing new to aged membranes using imaging techniques can be vulnerable to bias if different imaging variables are applied.

Furthermore, SEM and AFM are surface techniques, and cannot be used to reliably differentiate between surface pits and true pores.

2.4.2.c Challenge & Permeate Quality Testing

Challenge tests are designed to probe membrane rejection capabilities and, therefore, pore size. Using a range of molecular weight materials in the feed solution, the fractional rejection of the materials is used to determine pore size (or molecular weight cutoff) for the membranes (Jung et al., 2004). Soluble polymers of various types and sizes are used as probe compounds (Simon et al., 2013; Wolff and Zydney, 2004).

Challenge tests on PVDF membranes aged in NaOCl generally reveal a decrease in retention of either polymeric probe compounds or natural organic matter (NOM) (Abdullah and Bérubé, 2013; Hajibabania et al., 2012). Some publications have reported molecular-weight dependent changes: Levitsky *et al.* observed improved rejection with age for high molecular weight probe compounds, but decreased retention for NOM and lower molecular weight model compounds (Levitsky et al., 2011).

A decrease in rejection is generally attributed to increasing pore size and porosity (Abdullah and Bérubé, 2013; Hajibabania et al., 2012), while a decrease in hydrophilicity has been reported to result in both increasing (Hajibabania et al., 2012) and decreasing (Levitsky et al., 2011) NOM retention. Abdullah and Bérubé reported a negative correlation between clean water permeation and retention of dextran (Abdullah and Bérubé, 2013).

Unfortunately, it can be difficult to differentiate size-based (i.e. sieving) effects from hydrophobic interactions. Though challenge tests can be instructive in a relative sense, they are susceptible to changes in the membrane surface properties. The molecular shape of polymers used as particle models can also skew results; less spherical molecules have the potential to travel through relatively smaller pores, if their orientation allows it.

2.4.2.d Porometry

Porometry is a means of estimating membrane pore size, by monitoring fluid flow through pores of a membrane. Due to capillary forces being higher for narrower pores, a higher pressure for a given flow indicates smaller pore diameters. By applying a "wetting fluid" to one side of the membrane, and a "displacing fluid" to the other, the change in pressure drop with incrementally increasing flow can be used to calculate the pore size distribution. This has been shown to correlate well with membrane retention capabilities (Giglia et al., 2015; Peinador et al., 2011). The bubble point pressure test is a special case of porometry testing, that is used to probe the largest pore size in a membrane. To find the largest pore, a membrane is pressurized with air/gas on one side, and water/liquid on the other, at increasing pressures, until bubble release (Hajibabania et al., 2012; Zondervan et al., 2007). Porometry has been used in the PVDF membrane ageing literature to determine both the bubble point pressure and the mean pore size.

In general, a decrease (Hajibabania et al., 2012; Le-Clech, 2014) or no effect (Le-Clech, 2014) on bubble point pressure has been reported for NaOCl-aged PVDF membranes. A

decrease in bubble point pressure suggests that the pore size of a membrane is increasing when aged with NaOCl, which is consistent with results from challenge testing in these studies. Ageing of PVDF in HCl, alkali (NaOH) and surfactant (SDS) also each resulted in a net decrease in bubble point pressure (Le-Clech, 2014).

Two studies have reported pore size from porometry of NaOCl-aged PVDF membranes. Puspitasari *et al.* observed an initial increase followed by a decrease in pore size (Puspitasari et al., 2010); the authors suggest that the effect may also related to removal of surface modifier. Le-Clech reported no significant change in pore size (Le-Clech, 2014). Measurements made using porometry are relatively variable, making statistically significant comparisons difficult (Le-Clech, 2014). This variability was evident in both of the ageing studies that used this method.

2.4.3 Operational Analytical Methods for Ageing in PVDF Membranes

Operational methods aim to directly probe performance factors; in most cases, these are executed at lab scale using conditions that mimic full-scale conditions. The characteristics that cause changes in membrane resistance were discussed in Section 2.3.1. Clean water flux experiments have been performed in most PVDF ageing studies as part of membrane characterization. Most studies of PVDF revealed a decrease in resistance as membranes were soaked in NaOCl (Abdullah, 2013; Le-Clech, 2014; Levitsky et al., 2012; Puspitasari et al., 2010). A few studies have attributed the change to an increasing pore size and porosity, which was cited most often as the cause of decrease in resistance (Abdullah and Bérubé, 2013; Levitsky et al., 2011). Puspitasari *et al.* observed variable resistance through ageing,

and attributed the effect to variable hydrophobicity during different steps of ageing (Puspitasari et al., 2010), an idea suggested by others (Levitsky et al., 2011). As opposed to studies conducted by soaking membranes in NaOCl, when ageing membranes via multiple filtration and cleaning cycles, an increase in resistance has been reported (Hajibabania et al., 2012; He et al., 2014; Wang et al., 2010), suggesting that the effect of irreversible fouling outweighs that of increase in pore size and porosity. An increase in resistance was also observed when using HCl and SDS in PVDF ageing (Le-Clech, 2014), though the effects of NaOH were mixed (Le-Clech, 2014; Levitsky et al., 2012).

The characteristics that cause changes in fouling rate were discussed in Section 2.3.2. Artificial fouling experiments have been performed in several PVDF ageing studies. Fouling rate is usually measured as the rate at which permeability declines during filtration of a model foulant. Most experiments aged membranes in NaOCl, and reported an increase in PVDF fouling rate with increasing membrane age (Abdullah, 2013). However, Hajibabania *et al.* observed a lower fouling rate for membranes aged in more concentrated solutions of NaOCl, suggesting the opposite trend (Hajibabania et al., 2012). The increasing fouling rate has been attributed to a characteristic cause: the changing surface chemistry of the membrane, caused by removal of the hydrophilic additives as membranes age (Abdullah and Bérubé, 2013).

Breach frequency was discussed in Section 2.3.3. Due to the very low frequency of broken fibres, integrity testing has not been used in the published literature to assess breach

frequency. Changes in susceptibility to membrane breaches is generally assessed based on changes in mechanical properties (Gijsbertsen-Abrahamse et al., 2006).

Cleaning rate was discussed as a performance factor in Section 2.3.4. Only one published study has proposed experiments to track cleaning rate at bench-scale, a surrogate for that performance factor in operational membrane plants (Abdullah and Bérubé, 2018). Both the rate of cleaning, and the time required to recover a set percentage of permeability were presented as ways to express cleaning rate. In that study, PVDF membranes were aged by soaking in a solution of NaOCl. The effect of ageing on the cleaning rate was not attributed to a particular membrane characteristic.

Because infrastructure deterioration is system-related, rather than membrane-specific, this performance factor is not generalizable for PVDF membrane systems.

2.5 Analysis & Discussion of Findings

The results discussed in Sections 2.3 and 2.4 were summarized graphically in Figure 4. Connections correspond to conclusions or suggestions by authors involving different performance factors and membrane physical chemical characteristics, as well as between these characteristics and specific analytical methods. The thicknesses of the lines are proportional to the number of references that discuss a particular link.

In some cases, no line is present, indicating that although a particular performance factor or analytical method was discussed, it was not linked to any physical/chemical

characteristics. These orphan boxes highlight that potential links to membrane physical/chemical characteristics have not been fully considered.

By examining Figure 4, an overall snapshot of membrane ageing research to date emerges. Most research has focused on characterizing changes in chemical/physical characteristics with age; a review of PVDF membranes alone drew many links between columns 2 and 3, yet the implications for performance - linking to column 1 - are incomplete when the NaOCl ageing literature is considered.

For PVDF membranes, the polymer surface chemistry and pore geometry are characteristics that have received the most attention. Polymer surface chemistry has mainly been characterized using ATR-FTIR and contact angle measurements. However, fouling rate, XPS, challenge tests, clean membrane resistance, and porometry have also been linked to changing surface chemistry. Various approaches (challenge tests, SEM, maximum elongation, NMR, porometry) have been implemented to characterize pore geometry.

Publications have only attributed decline in three performance factors to characteristic causes, as mapped in Figure 4. Of the three, the primary focus is on resistance as membranes age. Despite the widespread consideration of membrane resistance, the cause of changes is disputed, as evidenced by strong links to most of the chemical/physical characteristics. Studies that accelerated ageing by simply soaking membranes in concentrated cleaning solutions reported a decrease in resistance with age; however, those

that considered conditions more representative of full-scale systems often reported an increase in resistance with age. This indicates that, beyond interactions between the membrane material and the chemical cleaning agents, interactions with the accumulated foulants must also be considered. In addition to affecting resistance, foulant interactions would also be expected to impact other performance factors, especially the fouling and cleaning rate. Increasing fouling rate is usually attributed to membrane surface chemistry, though it is not commonly measured. Breach frequency was not studied directly, but many publications proposed that breaches would correlate with declining mechanical properties. Almost all chemical/physical changes in Figure 4 were linked to this performance factor, so there is no clear consensus on a single cause of increased breach frequency for aged membranes. The cause of cleaning rate decline has received no mention in the membrane ageing literature. Note that infrastructure deterioration does not relate to membrane characteristics, and therefore it is not linked to the "characteristics" category.

A number of studies have considered performance factors, chemical/physical membrane characteristics and analytical methods independently. Although these can provide insight into changes that occur with ageing, it is difficult to use the outcomes from individual studies to develop operational changes that could be used to minimize the impact of chemical cleaning on membrane life. Additional research is required to fill the knowledge gaps in Figure 4. However, a major outcome from the review is that performance factors are likely each affected by many different changes in characteristics, and that a given characteristic can likely impact membrane performance in multiple ways.

The current literature does not allow the identification of the most important performance factor(s) or physical/chemical membrane characteristic(s) to monitor. An understanding grounded in economic factors could be used to identify these. The consequences of changes in the performance factors on membrane systems are summarized in Table 1. A quantitative assessment of the economic impact of changes in performance factors is beyond the scope of the present discussion. Such an approach could be taken by determining the economic impact of each performance factor with respect to various operational costs. There is a shortage of ageing studies with data from operational membranes, so more data are needed before this model can be constructed. A version of Table 1 would be the basis for such an approach. Ideally, any performance factor contributing egregiously to the overall economic decline of the plant would be targeted by modifying operation. The modifications to be made would stem from the overall understanding of membrane ageing established by Figure 4. Information needed for this analysis is not commonly collected during operation, so would need to be added to existing monitoring of full-scale systems.

Table 1. Overview of economic consequences from decline of five performance factors.

Performance Factor Change	Energy Use	Chemical Use	Personnel	Down-Time	Replacement
Resistance (Increase)	✓	✓			✓
Fouling Rate (Increase)	✓	✓	✓	✓	✓
Breach Frequency (Increase)			✓	✓	✓
Cleaning Rate (Decrease)	✓	✓	✓	✓	✓
Infrastructure Deterioration			✓	✓	✓

2.6 Conclusions & Insights

The review and analysis of published literature emphasize that research into membrane ageing is complex and can only be comprehensively addressed by considering performance factors, chemical/physical membrane characteristics, and analytical methods in parallel, as well as the links between these. A novel framework (Figure 4) was developed as a tool for understanding these complexities; the framework maps proposed relationships between performance factors and characteristics, and of analytical methods used to probe characteristics.

The membrane literature identified changes to all five performance factors as membrane age. It was apparent that the well-studied performance factors (resistance and breach frequency in particular) are affected by many different changes in characteristics, and that a given characteristic can impact performance in multiple ways. However, the cleaning rate was not linked to characteristic changes, and links to fouling rate were relatively few. Chemical and physical changes in PVDF membranes can be understood using classic analytical techniques as well as methods that mimic membrane operation. In most cases, multiple techniques were employed to measure changes to chemical and physical characteristics.

Several research avenues emerged from the literature review. Ageing research must consider foulant effects in addition to interactions between membrane material and chemical cleaning agent. The cause of cleaning rate change has not been identified. From a practical perspective, to optimize membrane lifetime, research should consider the

economic impact of ageing on all performance factors simultaneously. Conditions that optimize one performance factor may not be beneficial for another. Considering that performance factors impact a number of operational aspects of a membrane system (see Table 1), life cycle analysis would be a useful tool future research, for assessing the effect of operational changes on membrane ageing.

Chapter 3 - Methods & Materials

3.1 Ageing of Membranes in Full-Scale

3.1.1 Full-Scale Membrane Harvesting

Membranes were harvested from 14 different trains at 8 water treatment plants (WTPs). These plants were selected because they all utilize similar membranes: ZW1000 from SUEZ Water Technologies & Solutions (Oakville, Canada). The operational age of the membranes in the different trains ranged in age from 0 years to 8.3 years. A train refers to a group of membranes that operate simultaneously, so they experience the same conditions over time. At some plants multiple trains of different ages were harvested. The partner plants from which fibres were harvested for the present study were as listed in Table 2, and their locations are illustrated in Figure 5.

Table 2. List of partner plants which participated in the present full-scale membrane ageing study.

Water Treatment Plant Name	**Location**	**Number of Trains Sampled**
Bare Point Water Treatment Plant	Thunder Bay, ON	2
Burloak Water Purification Plant	Oakville, ON	1
David Street Water Treatment Plant	Sudbury, ON	3
Eagle Lake Membrane Filtration Facility	West Vancouver, BC	2
Lakeview Water Treatment Facility	Region of Peel, ON	2
Lorne Park Water Treatment Facility	Region of Peel, ON	1
South Fork Water Treatment Plant	Nanaimo, BC	1
Surface Water Treatment Plant	Barrie, ON	2

Figure 5. Locations of water treatment plants participating in the full-scale membrane ageing study.

Among the 14 membrane trains, two types of PVDF-based membranes were identified, based on physical and chemical characterization; the specifications of the two membrane types are provided in Table 3. Though both are made primarily from PVDF, they contain slightly different hydrophilic additives (HAs). The two types of PVDF membranes were, therefore, considered independently in the analysis. Because the HAs are proprietary, the two types of membranes are simply identified here as 1000A (current market product) and 1000B (previous market product). Note that initially this project included a third type of membranes; the data from these are presented in Appendix 5. Data from this type of membrane were not presented in the Chapter 4 discussion because an insufficient number of samples of this type were available for analysis.

The target membrane harvesting frequency was twice per year, though some WTPs carried out harvesting events with different frequencies due to operational constraints. Long-term

water quality and membrane operational data were not accessible for most plants, so operated age (i.e. years since installation) was the main quantifier for membrane age.

Membrane fibres were harvested from WTPs immediately after extensive "recovery" cleaning, so that only irreversible foulants were considered to be present. The sampling protocol provided to WTPs is included in Appendix 3.1. The harvested membrane fibres were shipped to the University of British Columbia (UBC) where they were stored in distilled water with approximately 2 ppm NaOCl at 4 °C until analysis.

3.1.2 Assessment of Performance Factors for Full-Scale Aged Membranes

3.1.2.a Test Module Specifications

For each full-scale membrane harvesting event, duplicate test modules were created in order to carry out bench-scale performance testing. Either 5 or 7 membranes fibres were used for each module. The top ends of the fibres were inserted into rigid tubing and sealed in place using epoxy, ensuring that individual fibres were not blocked (Figure 6a). The bottom ends of the fibres were plugged with epoxy (Figure 6b). The modules were pressure-tested at 55 kPa (8 psi) to ensure the integrity of the seal. Compromised modules were repaired with epoxy, whenever possible, or discarded. Test module preparation and membrane specifications are given in Table 3.

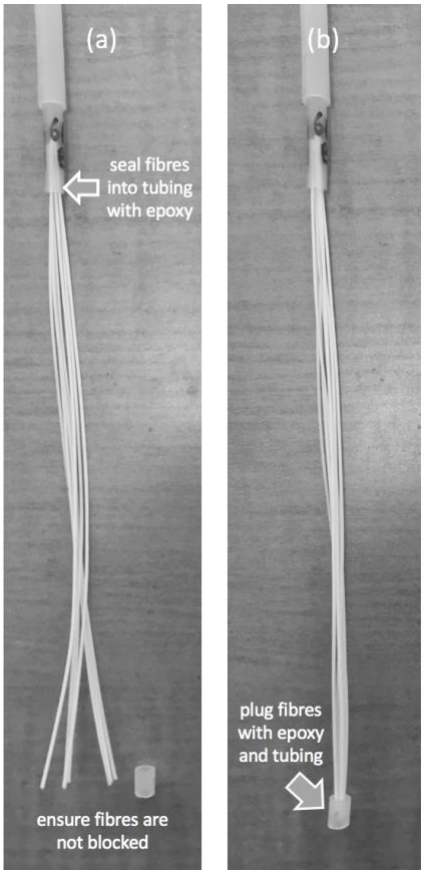

Figure 6. Example 1000B test module, containing full-scale aged membranes. (a) initial step, sealing top fibre ends and testing bottom fibre ends for blockage (b) final module sealed at bottom.

Table 3. Membrane test module dimensions and specifications. Specifications were obtained from membrane manufacturer or measured in lab.

		1000A	**1000B**
test module specifications	number of fibres	5	7
	fibre length	20 cm	18 cm
	total surface area	30 cm^2	30 cm^2
	target testing flux	50 L/(m^2*h)	50 L/(m^2*h)
membrane specifications	nominal pore diameter	0.02 µm	ultrafiltration
	fibre outer diameter	0.95 mm*	0.8 mm*
	flow range	50-100 L/(m^2*h)	15-48 L/(m^2*h)
	pressure range	0-90 kPa	7-66 kPa (max 83)

3.1.2.b Experimental Setup

Three bench-scale experimental setups (Figure 7) were built to execute performance tests on full-scale aged test modules.

Figure 7 Three bench-scale experimental setups; inset shows outside-in membrane test module configuration with arrows 1 and 2 indicating feed and permeate flow direction, respectively.

Each experimental setup included 4 membrane modules, as illustrated in Figure 8, allowing for a total of 12 tests modules to be operated simultaneously.

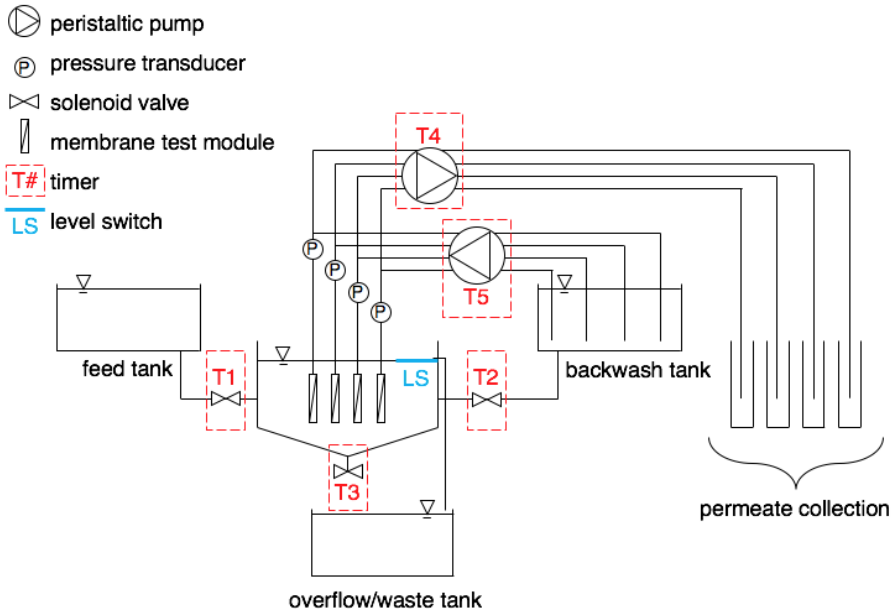

Figure 8. Schematic of bench-top experimental setup used for performance testing of full-scale aged membranes. Timers indicate programmed components.

The feed tank and backwash tanks were located above the filtration tanks, enabling gravity-driven filling of the membrane tanks via solenoid valves controlled by timer 1 (for feed) and timer 2 (for cleaning solution, from backwash tank). Membrane tanks, each 400 mL, drained via gravity using solenoid valves controlled by timer 3. Permeation and backwash were driven by independent pumps (Masterflex, #13 or #14 pump-heads), controlled by timer 4 and timer 5, respectively. Pressure was monitored for all membrane modules using pressure transducers +/-15 psig) logging to LabView SignalExpress software. Flow rate for determining permeate flux was measured gravimetrically.

3.1.2.c Performance Measurements of Full-Scale Aged Membranes

Prior to analysis, membrane test modules were again cleaned by permeating with distilled water and then soaking overnight in an NaOCl solution (pH 10, 500 ppm). After soaking, the clean membrane resistance was determined by filtering distilled water (square in Figure 9) for 30 minutes, and measuring the temperature, flow rate, and trans-membrane pressure.

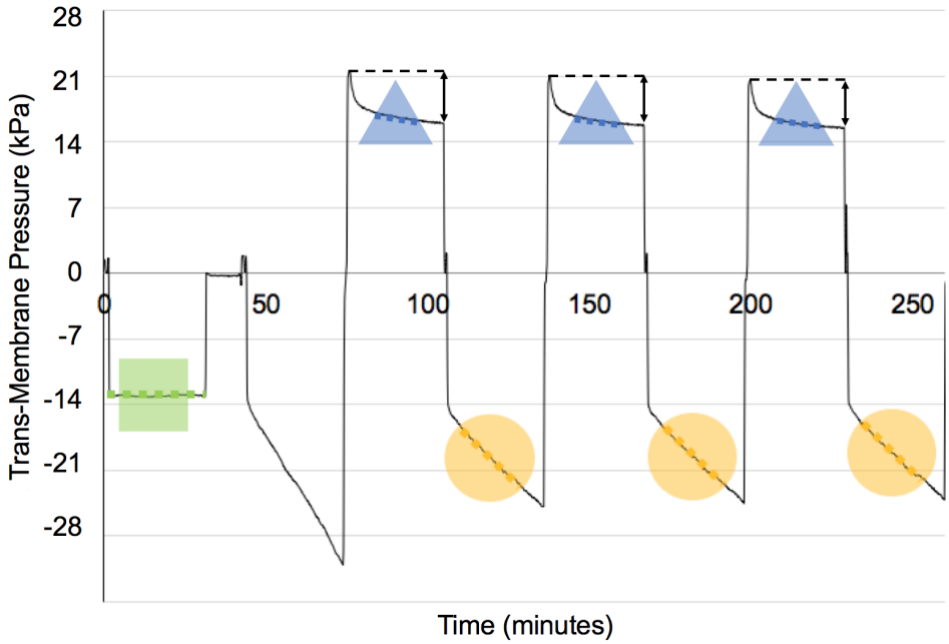

Figure 9 Performance testing protocol for full-scale aged membranes. Clean membrane resistance (square marker), linear fouling rate (circles), cleaning rate (triangles), and extent of cleaning (arrows) data are collected from pressure monitoring. Note that all pressures were ultimately corrected for flow and temperature in determining resistance.

The membrane test modules underwent performance testing, which consisted of a series of 30 minute fouling (circles in Figure 9) and 30 minute chemical-enhanced backwash (CEB) cycles (triangles in Figure 9), both at 50 L/(m^2*h). A model foulant solution was used for filtration and NaOCl solution was used for the CEB.

The model foulant contained humic acid (Sigma-Aldrich), sodium alginate (Sigma-Aldrich) and bovine serum albumin (Sigma-Aldrich), in a 2:1:1 mass ratio. This composition was selected to represent a broad spectrum of natural organic matter (NOM) foulants (Hajibabania et al., 2012). These constituents were dissolved in tap water with characteristics as follows: pH 7.0-7.4, hardness 6.2-9.9 mg/L as $CaCO_3$, alkalinity 4.6-8.9 mg/L as $CaCO_3$, and TOC 0.5-1.0 mg/L (GVWD, 2016). The TOC of the model foulant solution was 10 mg/L for performance testing of 1000A test modules, and 5 mg/L for 1000B test modules. The different TOC concentrations were selected to achieve relatively

similar fouling rates for the 1000A and 1000B test modules (estimated based on preliminary testing). The fouling rates were quantified as the slope of the change in trans-membrane pressure (TMP) during the 2nd, 3rd and 4th fouling cycles. Fouling during the 1st cycle was generally greater than that observed in the other cycles and therefore steady operational conditions were assumed not to have been reached.

The chemical-enhanced backwash (CEB) solution contained 500 ppm NaOCl, adjusted to pH 10 using HCl. This CEB solution is typical of that used in periodic recovery cleans at the partner WTPs from which fibres were harvested for our study.

After 4 repeated fouling and CEB cycles, membranes test modules were again soaked overnight in 500ppm NaOCl, after which the clean membrane resistance was again determined (as previously described). Note that several hydraulic cleans were also performed, though not reported here, as per Appendix 3.4, Figure 35.

Following performance-testing, the membrane test modules were stored (as previously described) until further analysis. Prior to further analysis (Section 3.1.3), the membrane test modules were again rinsed with 500 ppm NaOCl followed by distilled water. Membrane integrity and clean membrane resistance were again confirmed at this time. Example performance data and detailed experimental protocols are presented in Appendix 3.4 and Appendix 3.5.

3.1.3 Chemical & Physical Characterisation of Full-Scale Aged Membranes

Performance-tested membrane modules were rinsed with distilled water. Membrane coupons (8 cm from each hollow fibre) were harvested from the test modules and dried overnight at 50 °C prior to chemical and physical characterisation. The analyses performed are presented here, with specific operational details provided in Appendix 3.

3.1.3.a Attenuated Total Reflectance Fourier-Transform Infrared (ATR-FTIR) Spectroscopy

Attenuated total reflectance Fourier-transform infrared (ATR-FTIR) spectra were collected using a Thermo-Nicolet Nexus 670 FT-IR Raman spectrometer, with a diamond window and resolution of 2 cm^{-1}. Blank and baseline correction were performed within Omnic software across the range of interest: 700 to 2000 cm^{-1}. This window includes characteristic peaks for PVDF (1402 cm^{-1}) and HA (1728 cm^{-1} for 1000A, 1748 cm^{-1} for 1000B), as well as the fingerprint region. Peak integration ranges were determined based on peak shape from composite spectra compiled from all membranes. For all membrane samples, duplicate FTIR spectra were collected for each replicate sample (i.e. 8 per sampling condition) and the HA:PVDF peak area ratios were calculated. The peak ratios do not give a quantitative HA content; however, when normalized against the PVDF peak, which is known to be stable for the conditions investigated, the relative HA content can be assessed (Abdullah and Bérubé, 2013). Example FTIR spectra for 1000A and 1000B membranes and detailed experimental protocols are presented in Appendix 3.6.

3.1.3.b Nuclear Magnetic Resonance (NMR) Spectroscopy

Proton spectra were collected using a 400 MHz Bruker NMR spectrometer, with 128 scans. Dried membrane coupons (0.4 g) were dissolved in d_6-DMSO (0.7 mL), aided by sonication and mild heating (50 °C) for 15 minutes. The triplet peak at 2.9 ppm was integrated as a relative reference for PVDF content. The minor peak at 2.25 ppm corresponds to irregularly polymerized PVDF and was ignored. The peak ratio is not an exact representation of the polymer ratio because the proton fraction in HA versus PVDF differs. Thus, the peak ratio was compared to virgin or newest membranes in the analysis. Example NMR spectra for 1000A and 1000B membranes and detailed experimental protocols are presented in Appendix 3.7.

3.1.3.c Tensile Testing

Tensile testing was performed using a modified version of the ASTM Standard Test Method for Tensile Properties of Single Textile Fibers D3822 (ASTM, 2014). Briefly, a 3.5 cm membrane coupon was held with 2.5 cm exposed between grips on KES-G1 multi-purpose tensile tester, equipped with a 5 kg load cell. Depending on breakpoint elongation, fibres were stretched at a rate of 0.2 mm/s (elongation of <100%, most 1000Bs) or 1 mm/s (elongation of >100%, most 1000As), as per ASTM D3822. Eight replicates were performed per harvesting event (4 from each test module). Voltage was converted into stress-strain curves using a custom MATLAB script. The maximum stress and Young's modulus were plotted as relevant to an individual fibre, rather than per cross-sectional area. Example

stress-strain curves, MATLAB script, and detailed experimental protocols are presented in Appendix 3.8.

3.2 Ageing of Membranes at Bench-Scale

3.2.1 Bench-Scale Membrane Ageing Techniques

3.2.1.a Test Module Specifications

For the bench-scale membrane ageing project, virgin test modules were prepared. New PVDF-based hollow-fibre membranes (ZW500) were obtained from SUEZ Water Technologies & Solutions (Oakville, Canada). These membranes have the same chemistry as the 1000B membranes (Table 3); however, they include an inner support fibre so were a more robust choice for bench-scale use.

Membranes were soaked in distilled water for 3 days prior to potting. Three fibres were used for each test module. The top ends of the fibres were inserted into rigid tubing and sealed in place using epoxy, ensuring that individual fibres were not blocked (Figure 10a). The bottom end of all fibres was plugged with epoxy (Figure 10b). The modules were pressure-tested at 55 kPa (8 psi) to ensure the integrity of the seal. Compromised modules were repaired with epoxy, whenever possible, or discarded. Test module preparation and membrane specifications are given in Table 4.

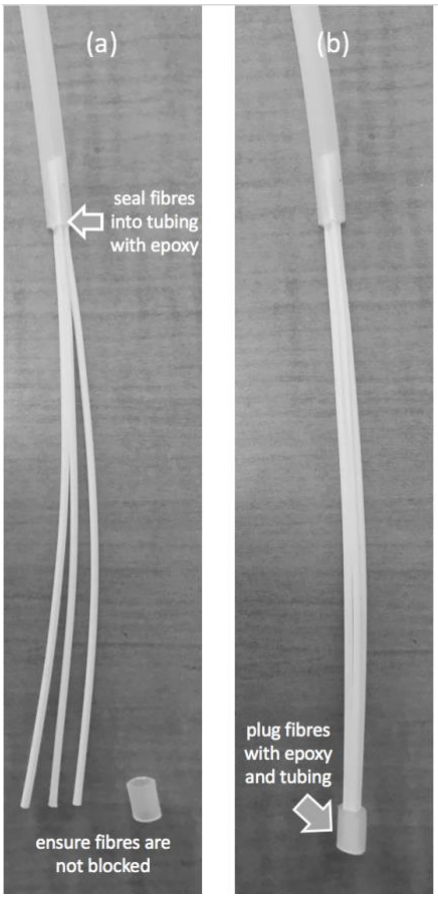

Figure 10. Example ZW500 test module. (a) initial step, sealing top fibre ends and testing bottom fibre ends for blockage (b) final module sealed at bottom.

Table 4. Membrane test module dimensions and specifications. Specifications were obtained from membrane manufacturer or measured in lab.

		ZW500 Membranes
test module specifications	number of fibres	3
	fibre length	17 cm
	total surface area	30 cm^2
	target testing flux	50 $L/(m^2*h)$
membrane specifications	nominal pore diameter	0.04 µm
	fibre outer diameter	1.9 mm
	flow range	19-77 $L/(m^2*h)$
	pressure range	-55 to 55 kPa (-8 to 8 psi)

3.2.1.b Single-Soak Bench-Scale Ageing

Membrane test modules were aged either by a single-soak in NaOCl or by cycled operation.

Single-soak ageing was performed by submerging the membranes in 5000 ppm solution of NaOCl (Javex), adjusted to pH 10 using HCl (Sigma-Aldrich). The soak solution was replaced when the NaOCl concentration decreased to less than 4500 ppm. Four replicate test modules were aged for each NaOCl dose considered. The NaOCl dose is defined by the concentration multiplied by the time of exposure (i.e. C*t), and ranged from 0 to 2 000 000 ppm*h.

The maximum NaOCl dose considered, 2 000 000 ppm*h, is higher than the manufacturer-recommended maximum cumulative lifetime dose of 500 000 ppm*h. However, the impact of NaOCl exposure on ageing of PVDF membranes has been reported to be proportional to $C^n t$ (with $n<1$), rather than C*t (Abdullah and Bérubé, 2013). Thus, when exposure dose was corrected based on $C^n t$, with $n=0.7$, the corrected exposure dose applied at bench scale (i.e. equivalent to 619 000 ppm*h) is comparable to the manufacturer-recommended maximum cumulative lifetime dose of 500 000 ppm*h (Abdullah and Bérubé, 2013). The actual bench-scale NaOCl doses (C*t at 5000 ppm) and the equivalent NaOCl doses at full-scale (assuming $C^n t$ conversion from 100 ppm) considered are presented in Table 5.

Table 5. Summary of membrane ageing conditions applied and tests performed.

	Ageing Conditions			Tests Performed	
membrane description	**approximate # cycles**	**actual NaOCl dose ppm*h[1]**	**equivalent NaOCl dose ppm*h[2]**	**performance**	**characteristics**
Virgin	0	0	0	no	yes
Single-Soaked	2	7000	2000	yes	yes
	2	500 000	… 154 000	yes	yes
	2	2 000 000	… 619 000	yes	yes
Cycled (A, B, & C)	150	500 000	154 000	yes	yes
	300	1 000 000	309 000	yes	yes
	450	1 500 000	464 000	yes	yes
	600	2 000 000	619 000	yes	yes

[1]Actual NaOCl dose applied via accelerated conditions of 5000 ppm.
[2]Corrected for full-scale conditions, assuming $C^n t$ applied with n=0.7 and average C=100 ppm.

3.2.1.c Cycled Bench-Scale Ageing

Cycled operation was performed for 600 filtration cycles, each consisting of a fouling period and a water backwash. Three operational schemes (A, B and C) were considered, as summarized in Figure 11, differing only in cleaning frequency. All cycled test modules received the same foulant exposure, as they performed the same number of 30-minute fouling cycles (i.e. 6 each in Figure 11; 600 total). The membrane tanks were drained between cycles, so concentration factors were the same among the 3 schemes. All test modules received the same NaOCl exposure (C*t, as introduced in 3.2.1.b). Four independent replicate test modules were aged in each cycled operational scheme.

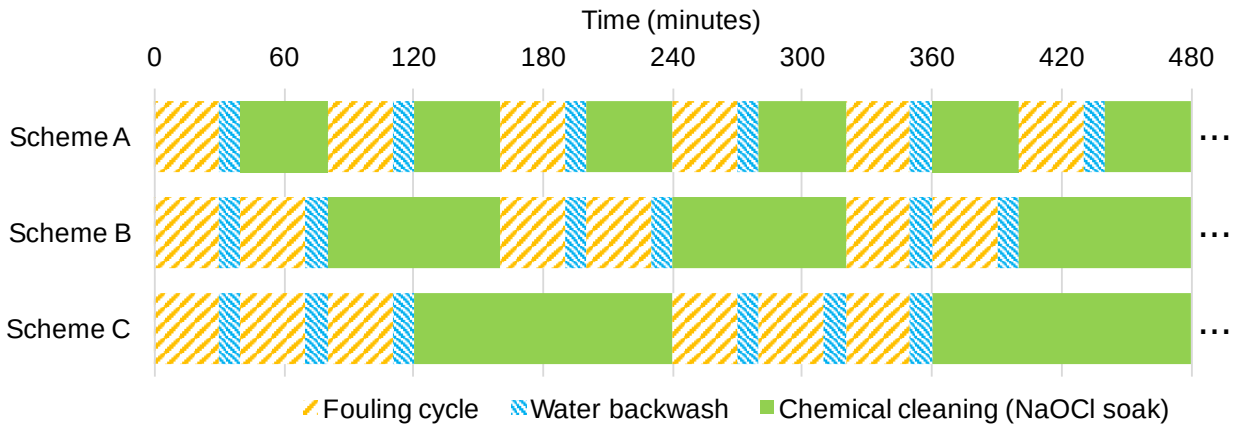

Figure 11. Operational schemes A, B and C. The sequences illustrated were repeated for a total of 600 fouling cycles per scheme, totaling approximately 33 days of operation per scheme.

Three experimental setups, each accommodating 4 test modules as illustrated in Figure 12, were used to age cycled membranes. The experimental setups were similar to those described previously (3.1.2.b), with the exception that backwash was performed with water, while chemical cleaning was performed with NaOCl. The timer programming for the three experimental setups corresponded to operational schemes A, B and C (Figure 11).

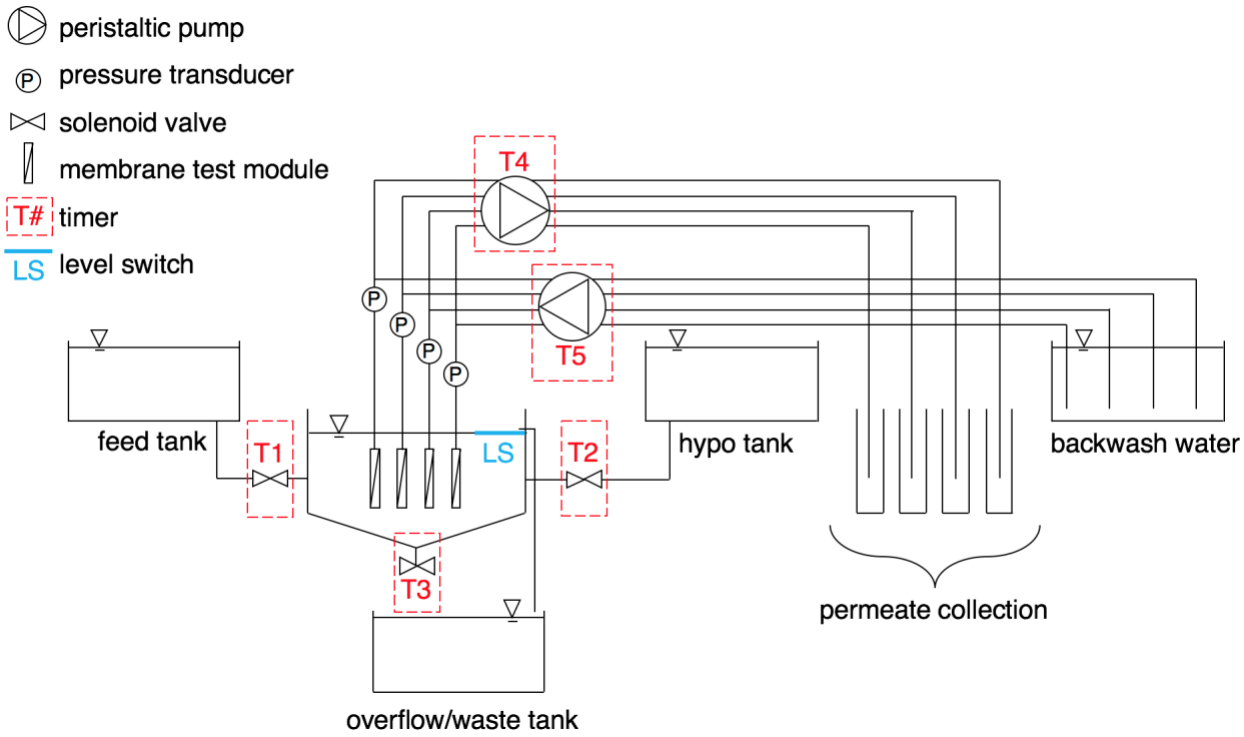

Figure 12. Schematic of bench-top experimental setup used for cycled ageing, as well as performance testing of bench-scale aged membranes. Timers indicate programmed components.

Fouling consisted of 30 minutes of permeation at 50 L/(m^2*h) using a model feed solution. The model feed was prepared as described in Section 3.1.2.c. The target DOC of the model foulant solution was 18.6 mg/L (40 mg/L total constituent mass), to provide a measurable increase in resistance during a fouling cycle.

Water backwash was performed following fouling and consisted of a 10-minute backwash at 50 L/(m^2*h) with distilled water, followed by a rapid tank-drain.

Chemical cleaning was performed following water backwash and consisted of a 40, 80 or 120 minute (recall Figure 11) soak in 5000 ppm NaOCl at pH 10. As suggested by Abdullah and Bérubé a soak for 40 minutes at 5000 ppm is expected to be equivalent to a 3.3 h soak at 500 ppm (Abdullah and Bérubé, 2013). Recovery chemical cleans in full-scale WTPs are

typically performed at concentrations that range from 350 to 500 ppm, over 3-8 hours. Therefore, the chemical cleans at bench-scale were considered to be representative of recovery cleaning at full-scale.

Intensive cleaning was performed only prior to harvesting of cycled membranes. To perform intensive cleans, membrane test modules were again water backwashed into the NaOCl solution following a chemical clean, removed from the filtration system, intensively physically cleaned by wiping the loosened surface fouling away using a lint-free towel, and rinsed with distilled water.

Membrane coupons (2 cm of membrane fibre) were harvested (i.e. cut) from all cycled test modules after 150, 300, 450 and 600 fouling cycles, providing 4 replicate coupons per operational scheme (A, B or C). The harvested coupons were subsequently analyzed for physical and chemical characteristics (refer to 3.2.3). The test modules from which the coupons were harvested were repaired and returned to the experimental setups, with flow rates decreased to maintain a flux of 50 L/(m^2*h) during fouling and backwash cycles. The overall sampling schedule during cycled ageing of test modules was presented in Table 5. Timer programming for cycled operation is presented in Appendix 3.9.

3.2.2 Assessment of Performance Factors for Bench-Scale Aged Membranes

The three experimental setups, each accommodating 4 test modules as illustrated in Figure 12, were used for performance testing of both single-soaked and cycled bench-scale aged membranes.

3.2.2.a Performance Testing of Single-Soaked Membranes

Performance testing of single-soak membranes was performed using the same timing sequence as for operational scheme A. Specifics of fouling, cleaning, flow rates, and data collection are as described in Section 3.2.1.c. The sequence of performance testing is illustrated in Figure 13.

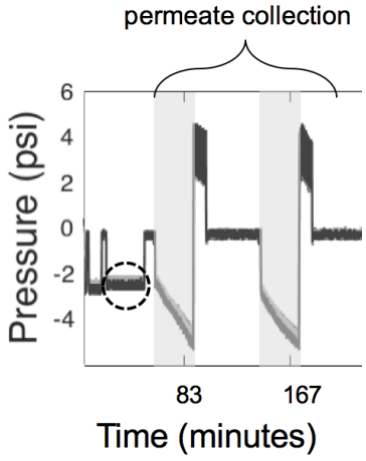

Figure 13. Performance testing for single-soaked aged membranes. Clean membrane resistance (circle), and linear fouling rate (rectangle highlights) data are collected from pressure monitoring. Permeate collection period is indicated with a bracket. Note that all pressures were ultimately corrected for flow and temperature in determining resistance.

After purging, a 30-minute clean membrane resistance test was performed (circle in Figure 13), followed by 2 cycles of fouling/backwash/recovery clean, during which the fouling rate (shaded rectangles in Figure 13) was measured and permeate was collected. Fouling rate was determined during the second of these two fouling cycles using linear regression as the absolute TMP increased linearly. Single-soaked membranes were then intensively cleaned (see Section 3.2.1.c) prior to physical and chemical analyses.

The clean membrane resistance of virgin membranes was measured using clean water filtration; however, fouling and cleaning were not performed to allow for performance testing of never-fouled virgin membranes.

3.2.2.b Performance Testing of Cycled Membranes

Performance testing of cycled membranes was done continuously throughout the ageing experiments, with operational details as specified in Section 3.2.1.c. However, as noted in 3.2.1.c, characteristics were only determined 4 time-points, following intensive cleans corresponding to 150, 300, 450 and 600 cycles. Figure 14 illustrates performance testing pre- and post-intensive cleaning for operational schemes A, B and C. The trans-membrane pressure was monitored continuously via LabView SignalExpress. Mass flow rates and water temperature were recorded before and after sampling events, as well as approximately every 30 cycles between sampling events. The initial resistance in a cycle (stars in Figure 14), immediately following chemical cleans, was measured and defined as "operational resistance". The fouling rate (shaded rectangles in Figure 14) was measured during fouling cycles following chemical cleans, to allow fair comparison among operational schemes A, B and C. Fouling rate was determined using linear regression as the TMP increased linearly during fouling cycles (Figure 14). Clean membrane resistance (circles in Figure 14), was measured using clean water permeation tests with distilled water, immediately following intensive cleans.

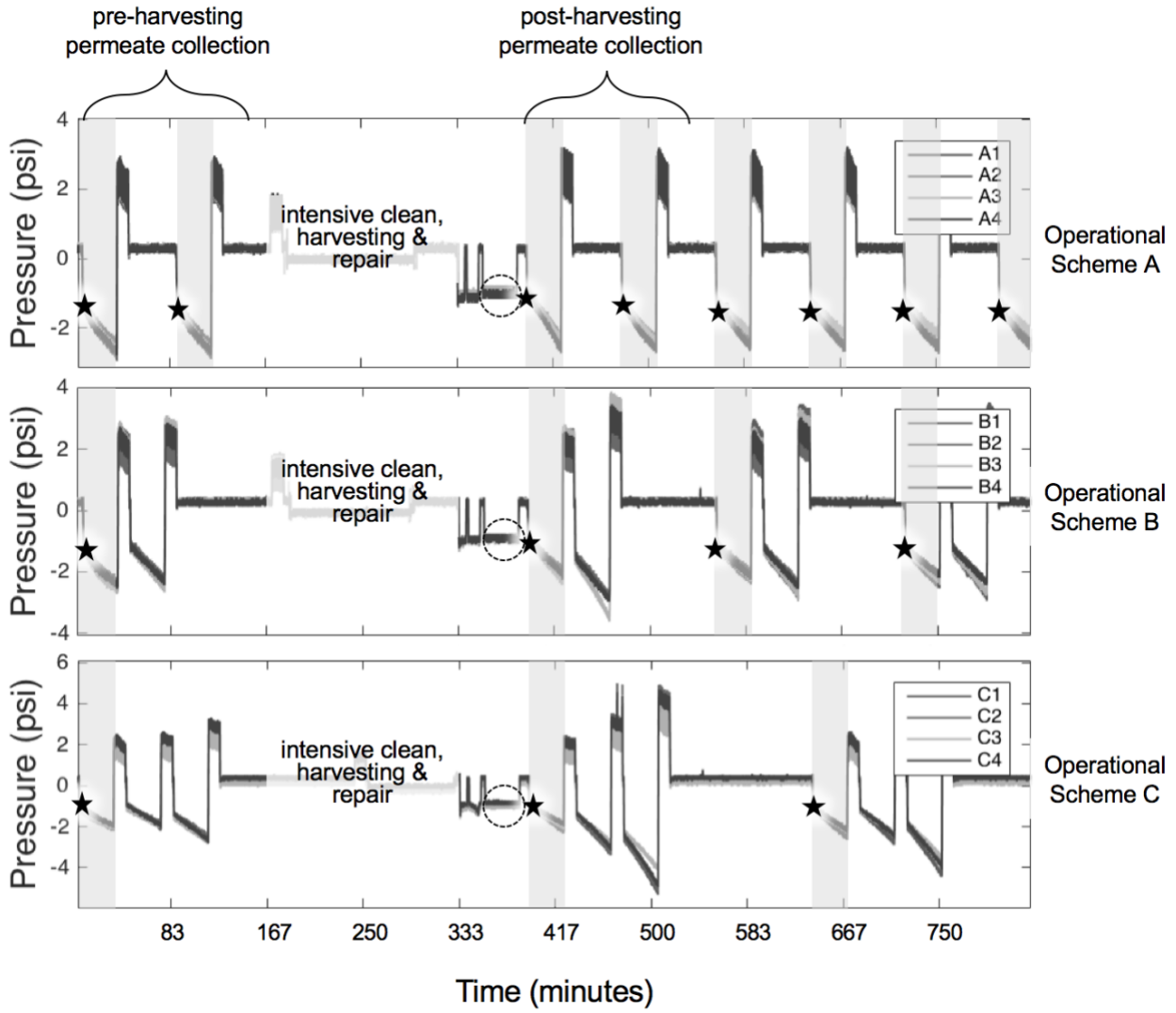

Figure 14. Performance testing for cycled aged membranes, before and after an intensive clean. Operational resistance (stars), clean membrane resistance (circles), and linear fouling rate (rectangle highlights) data are collected from pressure monitoring. Permeate collection period is indicated with brackets. Note that all pressures were ultimately corrected for flow and temperature in determining resistance.

3.2.3 Chemical & Physical Characterisation of Bench-Scale Aged Membranes

Prior to all physical & chemical analyses, intensively cleaned test modules were rinsed with distilled water. Membrane coupons (8 cm from each hollow fibre) were harvested from the test modules and dried overnight at 50 °C prior to chemical and physical characterisation. The analyses performed are presented here, with specific operational details provided in Appendix 3.

3.2.3.a Attenuated Total Reflectance Fourier-Transform Infrared (ATR-FTIR) Spectroscopy

ATR-FTIR spectroscopy for bench-scale aged membranes followed the same protocol as for full-scale aged membranes. Refer to section 3.1.3.a for this protocol.

3.2.3.b Water Contact Angle

Water contact angle was measured by applying a 20 μL drop of distilled water to the top of a dried membrane fibre. Because the fibres are cylindrical, the contact angle was captured by photographing fibres from the side. The initial contact angle was measured, as well as the angle after 2 minutes. Contact angle measurements were performed for each side of the drop for four replicate membrane samples (i.e. 8 angles per sampling condition tested). Example contact angle measurements and detailed experimental protocols are presented in Appendix 3.11.

3.2.3.c Scanning Electron Microscopy

Scanning electron microscopy (SEM) was performed using an FEI Quanta 650 VP/ESEM. Dried membranes were coated in 5 nm of gold, and imaged at 10000x and 50000x. Example SEM images and detailed experimental protocols are presented in Appendix 3.12.

3.2.3.d Dissolved Organic Carbon & UV Analysis

Dissolved organic carbon was measured using a Shimadzu TOC-L analyzer . UV absorbance was measured using a 1 cm quartz cell at 254 nm with a Spectronic Unicam UV-Vis spectrometer.

3.2.3.e Size Exclusion Chromatography

For size-exclusion chromatography (SEC) analysis, the separation method developed by Huber *et al.* was used (Huber et al., 2011). Briefly, an HPLC (PerkinElmer Flexar) with a size exclusion column (TOSCH Bioscience TSKgel HW-50S) with UV/Vis detector at 254 nm were used. SEC injections were 1 mL with a buffer (2.26 g Na2HPO4•7H2O, 2.5 g KH_2PO_4 per L Milli-Q water) flow rate of 1 mL/minute and 100 minutes between injections.

Chapter 4 - Membrane Ageing in Full-Scale Water Treatment Plants

4.1 Project Objectives

The primary objective of the full-scale ageing component of the present work was to determine which performance factors change over many years of operation. We hypothesized that performance outcomes similar to those observed in cycled bench-scale ageing would be reflected in full-scale aged membranes: an increase in fouling rate and clean membrane resistance, and a decrease in cleaning rate and mechanical properties.

We also hypothesized that the chemical characteristics of field-aged membranes would provide a basis for explaining the observed changes in performance. For example, hydrophilic additives have been observed to decline in bench-scale aged membranes resulting in higher fouling (Abdullah and Bérubé, 2013). We anticipate that the same causal relationships would hold for field-aged membranes.

Finally, although C*t is not measured accurately in most water treatment plants, it is the most common ageing metric used in laboratory studies. We anticipated that membrane ageing would be accelerated in full-scale compared with bench-scale laboratory studies, due to the extended cleaning durations at lower concentrations (Abdullah and Bérubé, 2013). Therefore, a secondary objective of the study is to begin to extrapolate bench-scale ageing to full-scale ageing.

4.2 Effect of Ageing on Performance Factors

Four performance factors were investigated: clean membrane resistance, fouling rate, cleaning rate, and susceptibility to breach.

4.2.1 Clean Membrane Resistance

The clean membrane resistance, with respect to membrane age, is presented in Figure 15a (1000A membranes) and Figure 15b (1000B membranes). Linear trends in clean water resistance were modeled, and P-values relate to the null hypothesis that the slope of each trend equals zero.

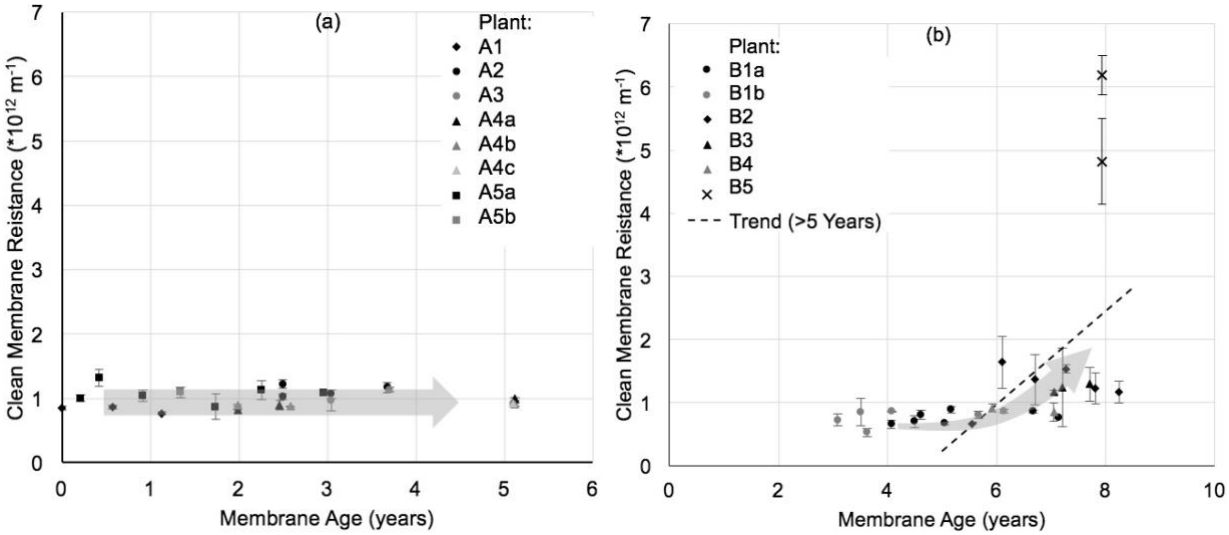

Figure 15. Clean membrane resistance with respect to membrane age for 1000A (a) and 1000B (b) membranes. The large grey arrows are included to illustrate overall trends. Error bars reflect the difference between duplicate performance tests for a given sampling event. The trend-line for 1000B membranes older than 5 years has a slope of 0.738±0.309 (std err), and a slope P-value of 0.029.

For 1000A membranes, ranging from 0 (i.e. new) to 5 years of age, the clean membrane resistance was relatively constant with respect to membrane age (P>0.05), as illustrated in Figure 15a. For 1000B membranes less than 5 years of age, the clean membrane resistance was also relatively constant with respect to membrane age (P>0.05), as illustrated in Figure

15b. For 1000B membranes greater than 5 years of age, the clean membrane resistance was higher than for those less than 5 years of age; the magnitude of the clean membrane resistance increased with membrane age (P=0.029), as illustrated in Figure 15b. Statistical analyses are presented in Appendix 4.4.

Most lab-based single-soak accelerated ageing studies of PVDF membranes have reported a decrease in membrane resistance with age (Abdullah and Bérubé, 2013; Hajibabania et al., 2012; Le-Clech, 2014). These studies attributed the reduction in resistance to an increase in pore size caused by ageing. The general explanation is that prolonged exposure to NaOCl (cleaning agent) causes removal of additives (e.g. HA), resulting in an opening of the membrane pore structure (Abdullah and Bérubé, 2013; Arkhangelsky et al., 2007b; Hajibabania et al., 2012; Jung et al., 2004; Pellegrin et al., 2015b). However, in studies where cycled accelerated ageing was applied (i.e. repeated fouling and cleaning), an increase in resistance was observed (Hajibabania et al., 2012; He et al., 2014; Wang et al., 2010). The increase in resistance was attributed to an accumulation of irreversible foulants, causing the pore radius (r) or number (n) to decrease. The irreversible fouling mechanism would support the increase in resistance observed in the present study for full-scale membranes after 5 years of operation.

Unfortunately no data are available for 1000A membranes that had aged for more than approximately 5 years; therefore, no conclusions can be drawn regarding potential differences, in clean membrane resistance or other performance factors, between membrane types. Note that the magnitudes of clean membrane resistance for the 1000A

and 1000B membranes should not be compared directly as they are slightly different products with slightly different chemical and physical characteristics (see Table 3).

4.2.2 Fouling Rate

The fouling rate, with respect to membrane age, is presented in Figure 16a (1000A membranes) and Figure 16b (1000B membranes). Units reflect the rate of resistance change over time, normalized to the foulant concentration. Linear trends in fouling rate were modeled, and P-values relate to the null hypothesis that the slope of each trend equals zero.

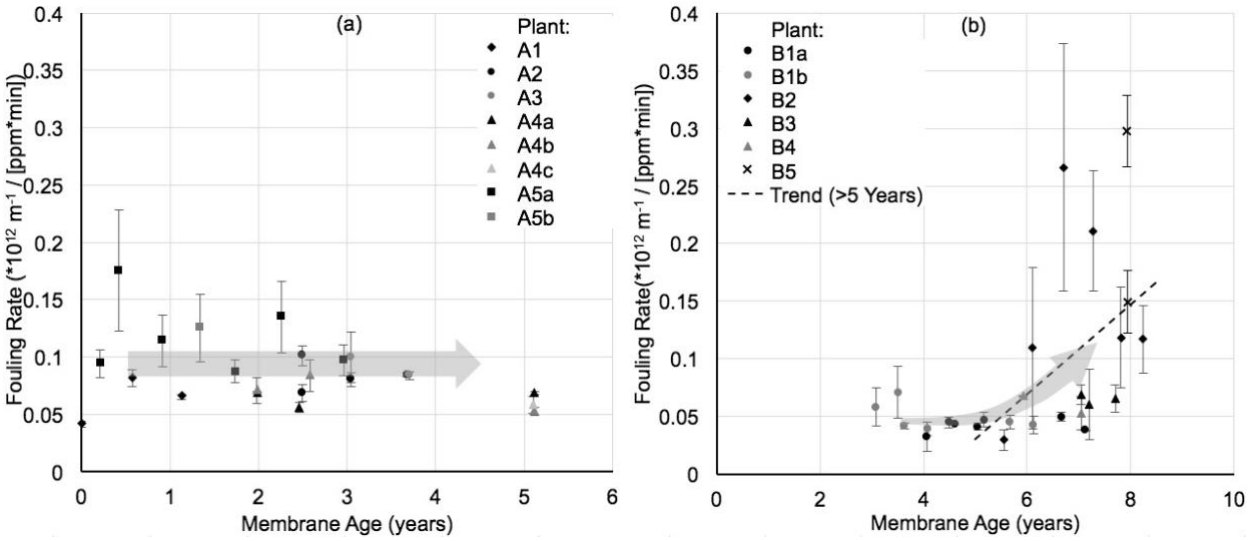

Figure 16. Membrane fouling rate with respect to membrane age for 1000A (a) and 1000B (b) membranes. The large grey arrows are included to illustrate overall trends. Error bars reflect the difference between duplicate performance tests for a given sampling event. The trend-line for 1000B membranes older than 5 years has a slope of 0.039±0.017 (std err), and a slope p-value of 0.036. Note that fouling rates are normalized to foulant concentration.

For 1000A membranes, ranging from 0 (i.e. new) to 5 years of age, the fouling was relatively constant with respect to membrane age (P>0.05), as illustrated in Figure 16a. For 1000B membranes less than 5 years of age, the fouling rate was also relatively constant with respect to membrane age (P>0.05), as illustrated in Figure 16b. For 1000B

membranes greater than 5 years of age, the fouling rate was higher than for those less than 5 years of age; the magnitude of the fouling rate increased with membrane age (P=0.036), as illustrated in Figure 16b. Statistical analyses are presented in Appendix 4.5.

The consensus within the bench-scale membrane ageing literature is that fouling rate increases with membrane age (Abdullah and Bérubé, 2013; Gaudichet-Maurin and Thominette, 2006; Qin et al., 2004, 2003). This is usually attributed to an increasing surface hydrophobicity with age (Abdullah and Bérubé, 2013; Arkhangelsky et al., 2008; Gaudichet-Maurin and Thominette, 2006; Levitsky et al., 2012, 2011, Qin et al., 2004, 2003). The increase in fouling rate after 5 years observed in full-scale 1000B membranes supports the existing consensus.

4.2.3 Membrane Cleaning Rate

Both the extent of cleaning during a given period and the cleaning rate correlated closely with the fouling rate for 1000A and 1000B membranes (see Appendix 4). This was expected because cleaning is greatly impacted by the amount of foulant present on the membrane prior to cleaning. Because the extent and rate of cleaning do not provide additional insight into our understanding of membrane ageing, it is not discussed further. Details of the analysis relating to the extent and rate of cleaning are provided in Appendix 4.3.

4.2.4 Membrane Susceptibility to Breach

Susceptibility to breach, as a performance factor, cannot be assessed directly because breaches are unpredictable and rare events. Gijsbertsen-Abrahamse *et al.* surveyed 20

water treatment plants for frequency of membrane failure, speculating that mechanical properties can provide insight into membrane breaches (Gijsbertsen-Abrahamse et al., 2006). Unfortunately, they did not conclude on which mechanical property would be the best predictor of breaches. Nonetheless, in the present research, changing mechanical properties were used as an indicator of changes in the susceptibility to breach.

The three mechanical properties considered - percent elongation at break, maximum stress, and Young's modulus - with respect to membrane age, are presented in Figure 17a/c/e (1000A membranes) and Figure 17b/d/f (1000B membranes). Linear trends in these three properties were modeled, and P-values relate to the null hypothesis that the slope of each trend equals zero.

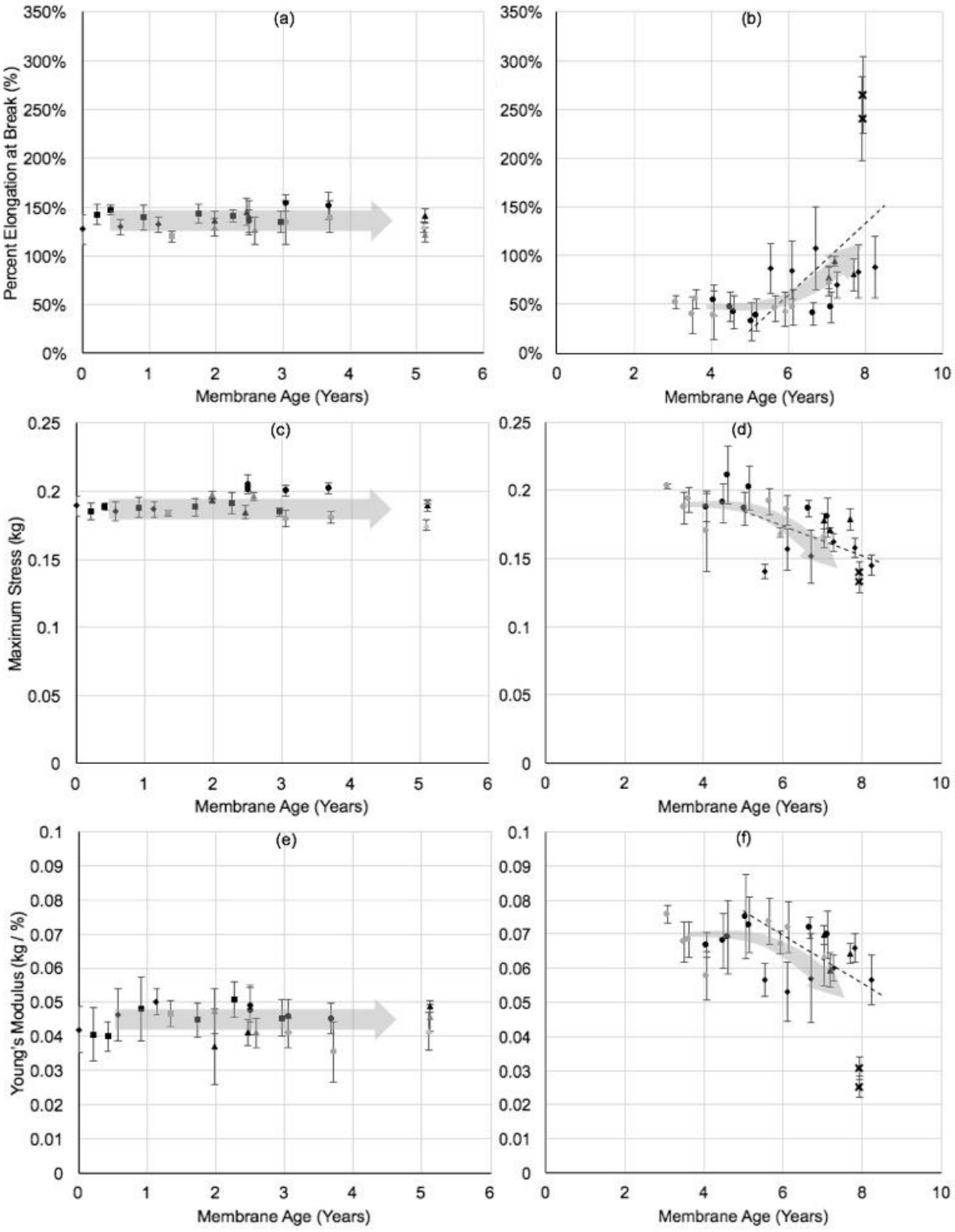

Figure 17. Mechanical properties with respect to membrane age for 1000A (a, c, e) and 1000B (b, d, f) membranes. The large grey arrows are included to illustrate overall trends. Error bars reflect the standard error from eight replicate tests. The trend-lines for 1000B membranes after 5 years have slopes of 0.366±0.127 (% elongation), -0.011±0.004 (maximum stress), and -0.007±0.003 (Young's modulus), and slope p-values of 0.010, 0.017 and 0.017, respectively. The units for Young's modulus and Maximum Stress are with respect to a single fibre (i.e. not normalized to cross-sectional area).

For 1000A membranes, ranging from 0 (i.e. new) to 5 years of age, the percent elongation at break was relatively constant with respect to membrane age ($P>0.05$), as illustrated in Figure 17a. For 1000B membranes less than 5 years of age, the percent elongation at break was also relatively constant with respect to membrane age ($P>0.05$), as illustrated in Figure 17b. For 1000B membranes greater than 5 years of age, the percent elongation at break was higher than for those less than 5 years of age; the magnitude of the percent elongation at break increased with membrane age ($P=0.010$), as illustrated in Figure 17b. Statistical analyses are presented in Appendix 4.6. These results indicate that aged 1000B membranes are more ductile. Similar results have been observed previously (Wang et al., 2010), though others observed decreasing elongation with age (Hajibabania et al., 2012; Le-Clech, 2014).

For 1000A membranes, ranging from 0 (i.e. new) to 5 years of age, the maximum stress was relatively constant with respect to membrane age ($P>0.05$), as illustrated in Figure 17c. For 1000B membranes less than 5 years of age, the maximum stress was also relatively constant with respect to membrane age ($P>0.05$), as illustrated in Figure 17d. For 1000B membranes greater than 5 years of age, the maximum stress was lower than for those less than 5 years of age; the magnitude of the maximum stress decreased with membrane age ($P=0.017$), as illustrated in Figure 17d. Statistical analyses are presented in Appendix 4.6. These results indicate that aged 1000B membranes are weaker. Similar results have been observed for lab-aged membranes in two prior studies (Hajibabania et al., 2012; Wang et al., 2010).

For 1000A membranes ranging from 0 (i.e. new) to 5 years of age, the Young's modulus was relatively constant with respect to membrane age ($P>0.05$), as illustrated in Figure 17e. For 1000B membranes less than 5 years of age, the Young's modulus was also relatively constant with respect to membrane age ($P>0.05$), as illustrated in Figure 17f. For 1000B membranes greater than 5 years of age, the Young's modulus was lower than for those less than 5 years of age; the magnitude of the Young's modulus decreased with membrane age ($P=0.017$), as illustrated in Figure 17f. Statistical analyses are presented in Appendix 4.6. These results indicate that aged 1000B membranes are more readily elastically deformed with age; decreasing Young's modulus has been observed for lab-aged membranes (Wang et al., 2010).

Mechanical deterioration has been attributed to evolution in crystallinity of the PVDF as additives are removed around the PVDF molecules (Hashim et al., 2011). However, the mechanism behind the deterioration of mechanical properties is not well understood, and was beyond the scope of the present research.

4.3 Membranes' Chemical Characteristics

Two analytical techniques, ATR-FTIR spectroscopy and NMR spectroscopy, were used to quantify the amount of hydrophilic additive (HA) present on the membrane surfaces and in the membrane bulk, respectively.

4.3.1 Surface Hydrophilic Additive Content (ATR-FTIR Spectroscopy)

The surface HA content, with respect to membrane age, is presented in Figure 18a (1000A membranes) and Figure 18b (1000B membranes). Linear trends in surface HA content were modeled, and P-values relate to the null hypothesis that the slope of each trend equals zero.

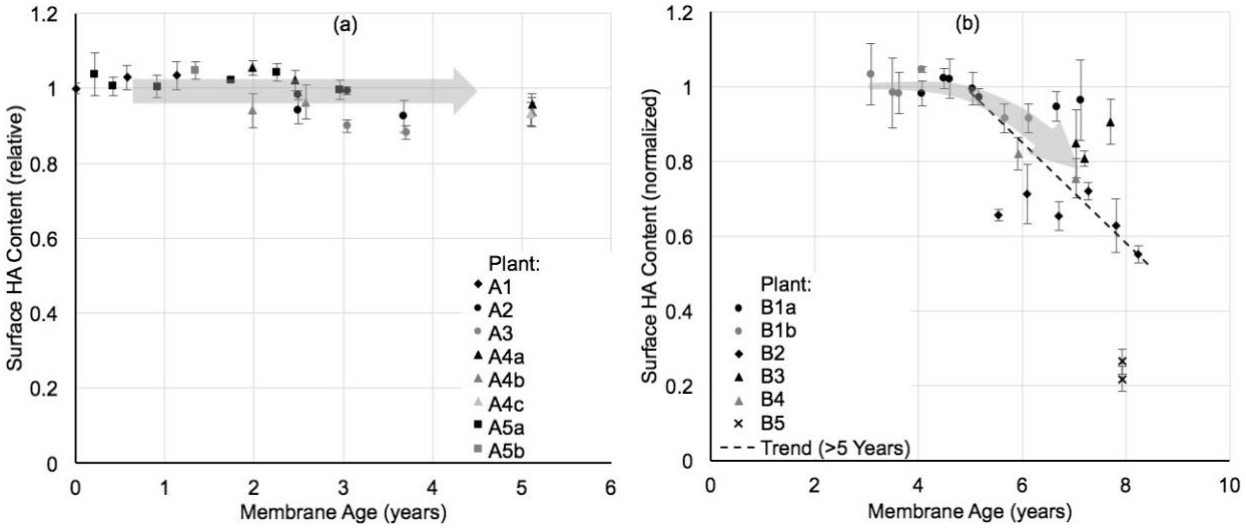

Figure 18. Surface HA content (ATR-FTIR) with respect to membrane age for 1000A (a) and 1000B (b) membranes. The large grey arrows are included to illustrate overall trends. Error bars reflect the standard error from four replicate spectra. The trend-line for 1000B membranes older than 5 years has a slope of -0.135±0.044, (std err), and a slope p-value of 0.007. Plots are normalized to virgin (1000A) or newest (1000B) HA content, and within-sample HA was measured relative to PVDF.

For 1000A membranes, ranging from 0 (i.e. new) to 5 years of age, the surface HA content decreased slightly with respect to membrane age (P=0.0007), as illustrated in Figure 18a; although this decrease was statistically significant, it amounted to less than 10% surface HA removal over 5 years. For 1000B membranes less than 5 years of age, the surface HA content was relatively constant with respect to membrane age (P>0.05), as illustrated in Figure 18b. For 1000B membranes greater than 5 years of age, the surface HA content was lower than for those less than 5 years of age; the magnitude of the surface HA content decreased with membrane age (P=0.007), as illustrated in Figure 18b. Statistical analyses are presented in Appendix 4.7.

4.3.2 Bulk Hydrophilic Additive Content (NMR Spectroscopy)

The bulk HA content with respect to membrane age, is presented in Figure 19a (1000A membranes) and Figure 19b (1000B membranes). Linear trends in bulk HA content were modeled, and P-values relate to the null hypothesis that the slope of each trend equals zero.

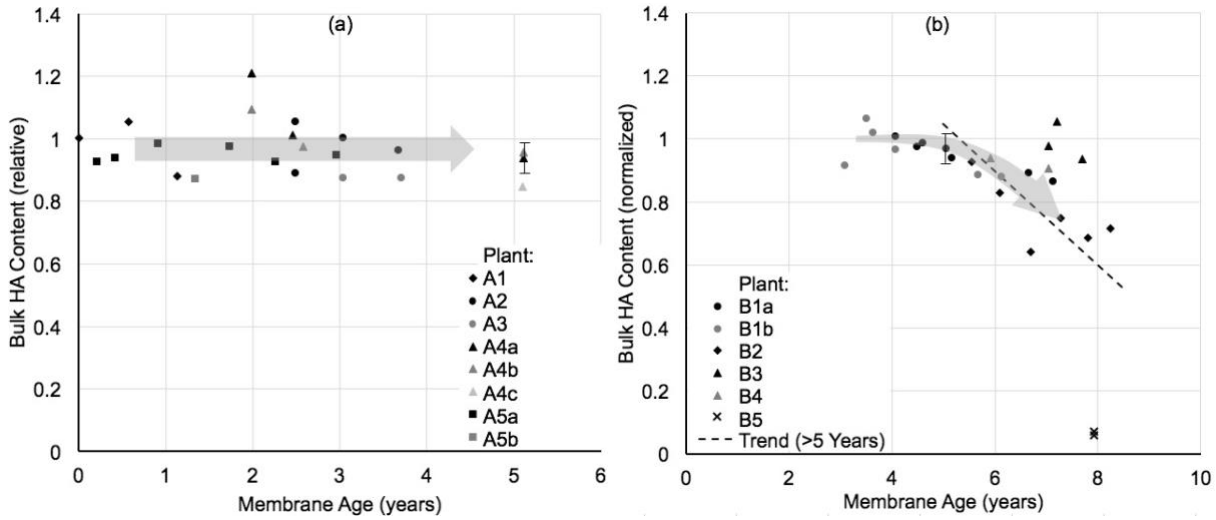

Figure 19. Bulk HA content (^{1}H-NMR) with respect to membrane age for 1000A (a) and 1000B (b) membranes. The large grey arrows are included to illustrate overall trends. Due to limited instrument availability, four replicates were performed for only 2 samples, selected at random. Representative error bars, showing standard error, are illustrated for these two samples. The trend-line after 5 years has a slope of -0.150±0.058, (std err), and a slope p-value of 0.018. Plots are normalized to virgin (1000A) or newest (1000B) HA content, and within-sample HA was measured relative to PVDF.

For 1000A membranes, ranging from 0 (i.e. new) to 5 years of age, the bulk HA content was relatively constant with respect to membrane age (P>0.05), as illustrated in Figure 19a. For 1000B membranes less than 5 years of age, the bulk HA content was also relatively constant with respect to membrane age (P>0.05), as illustrated in Figure 19b. For 1000B membranes greater than 5 years of age, the bulk HA content was lower than for those less than 5 years of age; the magnitude of the bulk HA content decreased with membrane age (P=0.018), as illustrated in Figure 19b. Statistical analyses are presented in Appendix 4.7.

4.3.3 Comparison of Chemical Characteristics

To better understand membrane degradation, bulk and surface HA:PVDF ratios were compared to each other in Figure 20; in this comparison, membrane age correlates with data point size.

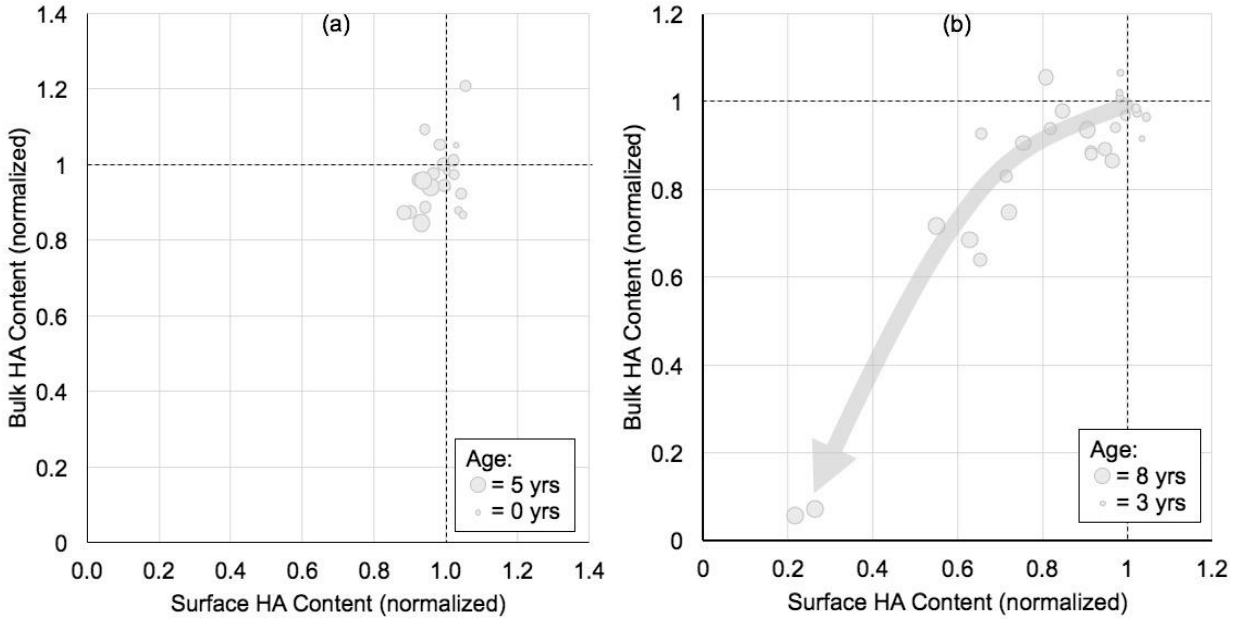

Figure 20 Surface and bulk composition comparison for 1000A (a) and 1000B (b) membranes. The large grey arrow is included to illustrate the apparent overall trend. Data are normalized to virgin (1000A) or newest (1000B) HA content, and within-sample HA was measured relative to PVDF. Symbol size is proportional to membrane age.

For 1000A membranes, bulk and surface HA content remained relatively constant (Figure 18a and Figure 19a, respectively) and, as ilustrated in Figure 20a, the bulk and surface HA content are clustered together, regardless of membrane age. However, the bulk and surface HA content was generally greater for less aged 1000B membranes (Figure 18b and Figure 19b, respectively). For 1000B membranes, a correlation was observed for the bulk to surface HA content, indicating that the removal of HA occurred throughout the membrane matrix and not just at the surface (Figure 20b). Comparison of HA remaining between the surface and bulk over time suggests that the surface HA is initially preferrentially removed, but that bulk HA is removed to a greater extent as membranes age. This trend is illustrated

with a curved arrow (Figure 20b), though it was beyond the scope of the present work to establish a model for this phenomenon.

Although the mechanism of HA removal was not investigated in the present work, others have observed that HA in membranes with 1000B type chemistry is oxidized by NaOCl (Abdullah and Bérubé, 2013). The oxidation products are soluble, and are therefore released from the membrane matrix.

To gain insight into the stability of HA for 1000A membranes, beyond a 5-year period, an *ad hoc* single-soaked accelerated ageing test was performed. New1000A membranes were soaked in a 5000 ppm solution of NaOCl, at pH 10, for 16 days: equivalent to a dose of 2 000 000 ppm*h. Based on this test, 35% of the HA content was removed from 1000A membrane surface (ATR-FTIR analysis) and 22% from the bulk (NMR analysis). These results indicate that the HA content of full-scale 1000A membranes is expected to decrease in a manner similar to that observed for the 1000B membranes. This suggests that the performance factors are also expected to change in a manner similar to those observed for the 1000B membranes. Continued characterization of the performance factors and characteristics of membranes aged at full-scale is recommended for both the 1000A and 1000B membranes.

4.4 Linking Performance to Characteristics

Potential links among the changes in performance factors and chemical characteristics were assessed, in order to better understand ageing phenomena. Because there was no significant change in the 1000A membranes for the range of membrane ages available (i.e.

less than 5 years old), the following analysis is based only on 1000B data from membranes of all ages.

4.4.1 Potential Cause of Increase in Fouling Rate

Figure 21 illustrates the correlation of membrane fouling rate with membrane surface composition.

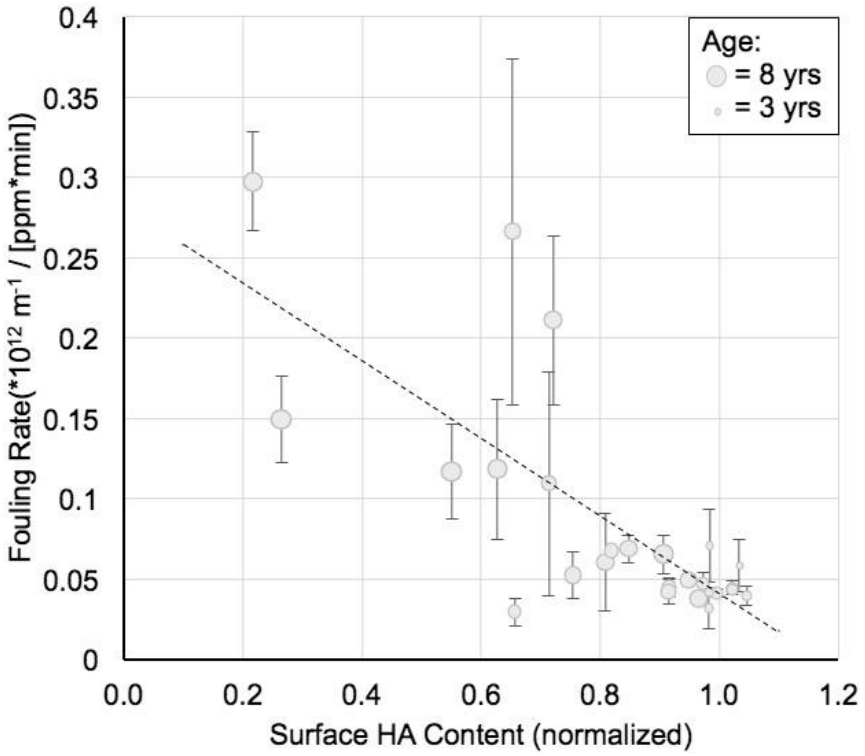

Figure 21. Fouling rate versus HA content (FTIR) for 1000B membranes. The trend-line has a slope of -0.241±0.043, (std err), and a slope p-value of 0.00001. Symbol size is proportional to membrane age.

The fouling rate was the highest for 1000B membranes with lower HA content on the membrane surface. This suggests that more hydrophobic membranes have a higher affinity for organic foulants as the surface HA content decreases. This mechanism is broadly supported in the membrane ageing literature (Section 2.3.2).

4.4.2 Identifying Benchmarks for Operational Water Treatment Plants

To adapt the findings of the present study for use by operational WTPs, we sought to identify a convenient metric as an ageing benchmark for operational membranes. Ageing was observed in all metrics (performance factors and chemical characteristics) after about 5 years for 1000B membranes, but routine measurement of most metrics would be onerous for WTPs. Clean membrane resistance, however, can be routinely measured in WTPs following intensive cleaning, so it was considered as an ageing benchmark.

Clean membrane resistance correlated well with all other metrics as membranes age (Appendix 4.3). Therefore, high clean membrane resistance could be used as an indicator of membrane ageing. The observed change in the various metrics considered with respect to age, and with respect to observed clean membrane resistance, are summarized in Table 6.

Table 6. Change in ageing metrics with membrane age and clean membrane resistance, for 1000B membranes. Correlations with age were discussed in Sections 4.2 and 4.3. Data from correlations with resistance are provided in Appendix 4.

	Correlation with Membrane Age	Correlation with Clean Membrane Resistance
Fouling Rate	↑	↑
Surface HA	↓	↓
Bulk HA	↓	↓
Percent Elongation	↑	↑
Maximum Stress	↓	↓
Young's Modulus	↓	↓

Based on these observations, WTPs with sustained and irreversible increases in clean membrane resistance should be vigilant of membrane ageing. To account for seasonal changes in temperature, absolute resistance values used to assess changes as membranes

age must be normalized to a standard temperature (e.g. 20 °C). As observed by soaking 1000A membranes in NaOCl, HA removal with age is probable in other membrane chemistries. Thus, if membrane manufacturers hope to monitor installed products at full-scale, without harvesting membrane fibres, the clean membrane resistance would also be useful as an ageing benchmark. This could enable manufacturers to optimize full-scale operating conditions, or better-predict the expected product life.

4.5 Implications of C*t as an Ageing Ordinate

At the outset of this project, we hoped to track ageing of membranes base on cumulative exposure to NaOCl, using the C*t relationship. Unfortunately, accurate and complete cumulative C*t exposure records were not available for all of the water treatment plants in the project. For the 5 plants for which C*t data were available, dose estimates were plotted with respect to membrane age (Figure 22). Note that most of the plants assumed the concentration of NaOCl remained constant during storage and use, and therefore the estimated cumulative exposure is likely greater than the actual exposure. A strong correlation (R^2= 0.95) was observed between membrane age and reported NaOCl exposure for most plants (Figure 22). However, one plant used atypical operational protocols, resulting in much higher cumulative NaOCl exposure than expected using typical protocols.

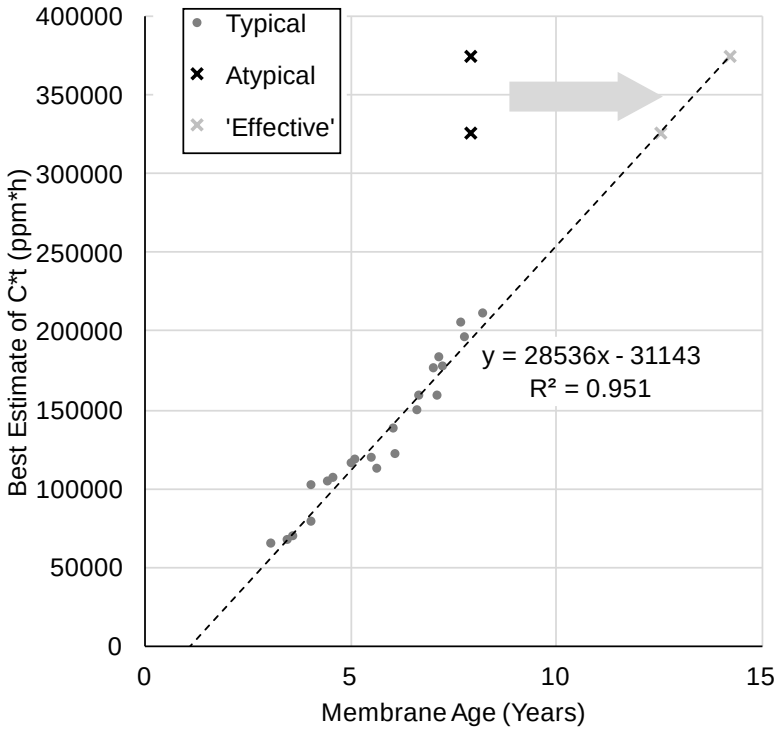

*Figure 22. Best estimates of cumulative lifetime NaOCl C*t for all 1000B membranes in the study. The membranes indicated with "X" are from an atypical plant and were excluded from the regression analysis.*

Using Figure 22, an effective age of approximately 13 years (grey X symbols in Figure 22) can be estimated by extrapolation for the plant with atypical operation. Unfortunately, the membranes in the plant with atypical operation were replaced soon after our study commenced, so further temporal data were unavailable for these membranes. Nonetheless, the proposed effective age of 13 years, for membranes from the atypical plant, is consistent with trends observed in Sections 4.3 and 4.4. The data from the plant with atypical operation were indicated using X symbols in Figure 15 through Figure 19. Recalling Sections 4.3 and 4.4, the clean membrane resistance for membranes from the atypical plant was more than double that of all other plants (Figure 15b), and fouling rates were among the greatest observed (Figure 16b). The mechanical properties of membranes from the atypical plant were poorer than the other 1000B membranes in the study (Figure

17b, d, f), and they also had the lowest HA content (both surface and bulk) in the entire study (Figure 18b and Figure 19b, respectively). The ageing trends in Figure 15 through Figure 19 included the membranes from the atypical plant at their true age (approximately 8 years). However, when the data from these atypically operated membranes are plotted instead with respect to their effective age, the p-values improve for all correlations considered, as presented in Appendix 4.4.

Overall, if extensive and frequent chemical cleaning is required for operation, beyond what is typical, membrane ageing is expected to accelerate; thus, changes in performance and characteristics are expected to occur earlier and to a greater magnitude. In such cases, operational protocols should be reviewed to reduce the extent and frequency of chemical cleaning - for example, by improving or implementing pre-treatment.

4.6 Conclusions on Full-Scale Aged Membranes

The present research investigated changes in performance factors as well as chemical characteristics for full-scale aged membranes. Our work bridges the knowledge gap between results from previous lab-based ageing studies and performance factors and characteristics relevant to operational water treatment plants.

For 1000A membranes, no significant changes in performance or characteristics were observed over the course of the study. Older 1000A membranes would be necessary to determine whether this stable operation persists, but such full-scale aged membranes are not yet available. Results from a single-soaked ageing test of 1000A membranes indicated

that HA content of full-scale aged 1000A membranes is expected to decrease with sufficient NaOCl exposure; thus, we anticipate that performance may also change after long-term full-scale ageing.

We observed that the clean membrane resistance of 1000B membranes increased after about 5 years of operation. This is consistent with some lab-aged membranes that have been cycled with foulant and cleaning agent. However, our results contradict those from others for lab-ageing using a prolonged single-soak in NaOCl. The discrepancy likely stems from the opposing effects of pore enlargement and irreversible fouling on the clean membrane resistance. The membrane fouling rate also increased for older membranes, consistent with the literature on lab-ageing. Though the susceptibility to breach cannot be measured directly, three metrics (elongation at break, maximum stress, and Young's modulus) were all observed to deteriorate with membrane age, also in agreement with lab-based ageing.

Both bulk and surface chemistry of the 1000B membranes changed with age after 5 years of operation. The hydrophilic additives were observed to decrease in the bulk and on the membrane surface. The reduction in HA content likely increases the fouling rate for older membranes, as foulants tend to sorb to more hydrophobic surfaces.

We observed that the clean membrane resistance correlated well with all other performance factors and characteristics studied. If a sustained irreversible increase in clean membrane resistance is observed over time, plant operators should be cognisant that

fouling and achieving sufficient flux may become difficult, and that membrane breaches may occur more frequently. This finding is useful to water treatment plant operators or managers seeking a metric to assess their infrastructure, and for membrane manufacturers in better-understanding their products.

Finally, although C*t was not used as a metric of membrane age, we observed that for one plant that applied an atypically high dose of NaOCl, the effective age of the membranes appeared to be greater than their actual age. Thus, as indicated by the results of lab-studies, avoiding excessive cumulative NaOCl exposure is advised. Furthermore, NaOCl C*t would likely provide a suitable ageing metric for full-scale ageing if dose fluctuates over years of operation.

Chapter 5 - Seeking Realistic Membrane Ageing at Bench-Scale

5.1 Project Objectives

As noted in Chapter 2, bench-scale experiments are popular tools to investigate membrane ageing. Most involve soaking membranes in a NaOCl solution at a high concentration for an extended period (single-soak). Some bench-scale experiments incorporate cycled fouling and cleaning (cycled operation), with the aim of better mimicking full-scale membrane operation.

In the studies reviewed in Chapter 2, stark differences in performance were observed between full-scale aged membranes and similar bench-scale aged membranes. Notably, membrane resistance was observed to increase in full-scale aged membranes, yet was reported to decrease in most bench-scale aged membranes. Unfortunately, carrying out all research at full-scale would not be possible, so appropriate bench-scale tools are required. The present study aimed to develop and better-understand bench-scale tools to probe membrane ageing. The study focused on addressing two major objectives.

First, we aimed to understand the discrepancies between bench-scale ageing (i.e. single-soak and cycled operation) and full-scale ageing. We hypothesized that the effects of permeation and fouling are important factors in membrane ageing, in addition to the NaOCl exposure dose.

Second, we sought to use bench-scale ageing to understand how physical and chemical characteristics change and impact membrane performance. We hypothesized that by comparing single-soak to cycled membranes we could extrapolate observed ageing behaviours to those observed or expected in full-scale operation.

5.2 Performance Factors

Three performance factors were investigated: clean membrane resistance, operational resistance, and fouling rate.

5.2.1 Clean Membrane Resistance

The clean membrane resistance was measured following intensive cleaning (for cycled membranes), or following soaking (for single-soak membranes), as an indicator of the intrinsic membrane resistance. The clean membrane resistance with respect to age, here expressed as cumulative NaOCl dose, is presented in Figure 23.

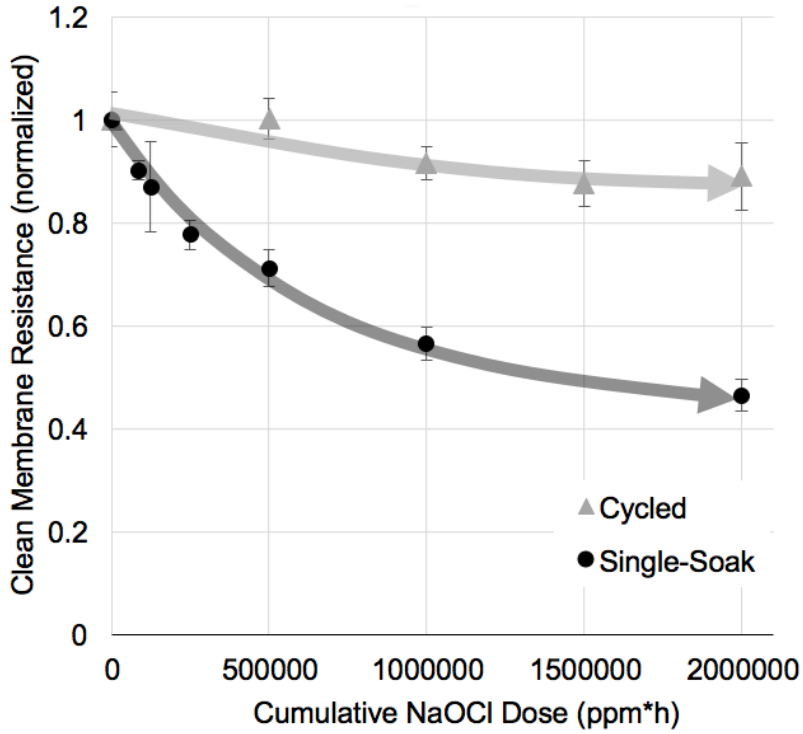

Figure 23. Clean membrane resistance with respect to NaOCl dose for cycled and single-soaked membranes. Error bars correspond to the standard error of 4 replicate test modules. Arrows illustrate overall trends.

For single-soaked membranes, the clean membrane resistance decreased relatively rapidly with age, to approximately 46% of the initial value when dosed with 2 000 000 ppm*h NaOCl (Figure 23). This observation supports the literature consensus for single-soaked PVDF membranes exposed to NaOCl. At least four other studies have reported that NaOCl single-soaking of PVDF caused a decrease in clean membrane resistance (Abdullah and Bérubé, 2013; Le-Clech, 2014; Levitsky et al., 2012; Puspitasari et al., 2010). Abdullah and Bérubé observed a 30% decrease in clean membrane resistance at a cumulative NaOCl dose of 2 000 000 ppm*h for PVDF membranes from the same manufacturer as those used in the present study (Abdullah and Bérubé, 2013). The prevailing understanding is that the change in resistance is due to increasing pore size and porosity, as hydrophilic additives (HAs) are removed from a membrane matrix after solubilizing due to NaOCl exposure (Chapter 2).

The clean membrane resistance from cycled operational schemes A, B, and C were not significantly different from one another, so the results from these three conditions were combined for the discussion that follows. For cycled membranes, the clean membrane resistance decreased less rapidly with age than for single-soaked membranes, to approximately 89% of the initial value when dosed with 2 000 000 ppm*h NaOCl (Figure 23). The observed difference in behaviour, between single-soaked and cycled, supports the literature consensus that cycled membranes are less prone to resistance decrease than single-soaked membranes. Hajibabania *et al.* actually reported an increase in resistance for cycled operation at bench scale (Hajibabania et al., 2012). The discrepancy between the results observed for single-soaked and cycled membranes suggests that mechanisms other than pore size and porosity increase from the removal of HAs are impacting the membrane resistance. Wang *et al.* observed decreasing initial resistance for cycled membranes (Wang et al., 2010). However, they did not suggest possible mechanisms that would explain their results. We initially considered that the discrepancy in change of clean membrane resistance was due to the presence of foulants, which either rapidly consumed NaOCl, decreasing the actual exposure dose, or shielded the cycled membranes from contact with NaOCl. However, the concentration of NaOCl during chemical cleaning remained constant during cycled operation, suggesting that the actual exposure was not impacted by foulants. In addition, the chemical characteristics of the membranes for single-soaked and cycled operation were similar for a given NaOCl dose (Section 5.3.1), suggesting that the foulants did not significantly shield the membrane from exposure to NaOCl. As discussed in Section 5.3.3, the discrepancy in resistance is likely due to the accumulation of irreversible foulants

on the membrane surface. The presence of irreversible foulants would cause a resistance increase offsetting the resistance decrease resulting from pore enlargement. The similar results obtained for operational schemes A, B, and C indicate that clean membrane resistance is not significantly impacted by differences in operational scheme (i.e. cleaning frequency). As discussed in Section 5.2.2 and Section 5.2.3, the similarity of clean membrane resistance among operational schemes is inconsistent with operational resistance and fouling rate.

Clean membrane resistance has also been reported to increase with age at full-scale for PVDF membranes (Fenu et al., 2012; He et al., 2014, Chapter 4). We assume that, for full-scale aged membranes, increasing resistance due to irreversible fouling is more substantial than decreasing resistance due to pore size and porosity increase with age. If this assumption is correct, the results suggest that the impacts of irreversible foulants are more substantial in full-scale ageing than in bench-scale cycled ageing. Based on these results, it cannot be concluded that clean membrane resistance changes caused by ageing at bench-scale are fully representative of ageing in full-scale operation. This is likely due the fact that cumulative foulant mass loading is much lower in bench-scale experiments than for full-scale operated membranes. This practical limitation arises because higher foulant mass loading would cause extreme fouling or necessitate much longer bench-scale experiments. In the present study, over 600 cycles, the cumulative foulant mass loading was approximately 25 times lower than would be expected for membranes operating at full-scale over 10-years (assuming filtration of 2 ppm organic carbon at 50 LMH, 80%

operational time). Despite this limitation, cycled bench-scale ageing appears to be a better surrogate for full-scale ageing than single-soak bench-scale ageing.

5.2.2 Operational Resistance

The resistance at the start of each filtration cycle was measured as an indicator of the operational membrane resistance. The operational resistance (stars in Figure 14) is of interest because it is relevant to full-scale membrane operation as it defines the system throughput. The operational resistance with respect to age, here expressed as cumulative NaOCl dose and number of cycles, is presented in Figure 24.

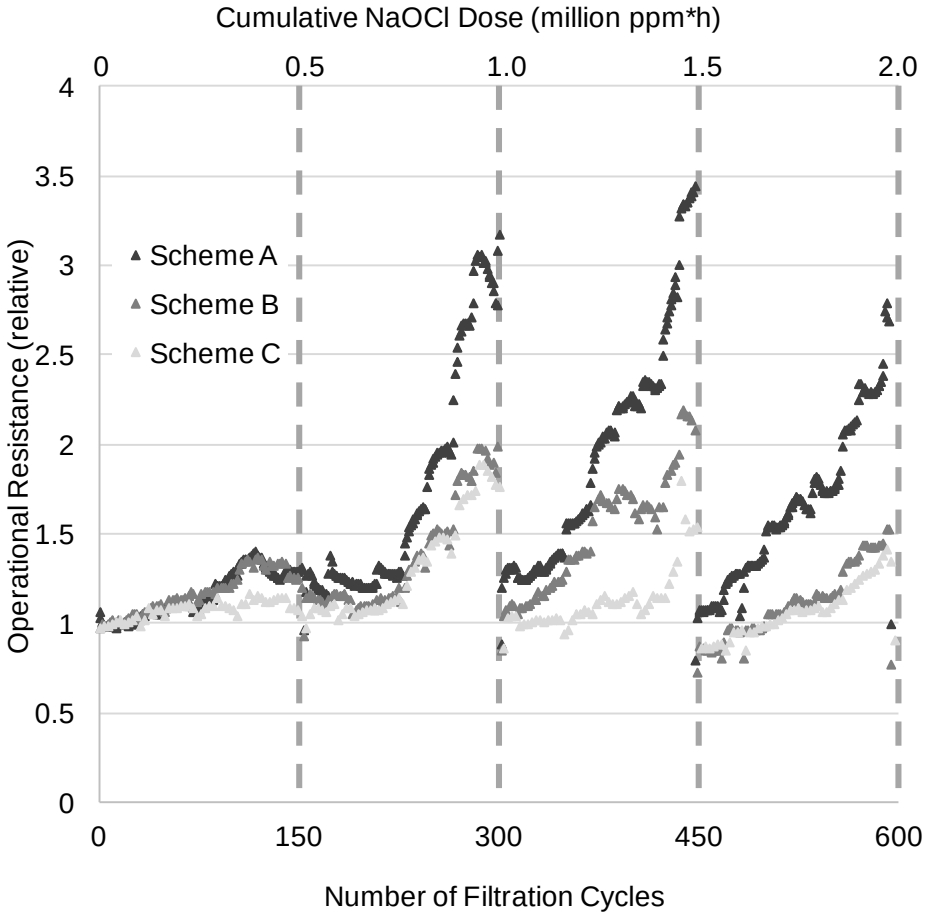

Figure 24. Operational resistance with respect to number of cycles and cumulative NaOCl dose applied. Resistance was normalized to the operational resistance at t=0. Dashed lines correspond to intensive cleaning events.

For single-soaked membranes the operational resistance could not be determined, because these membranes were not cycled repeatedly, (i.e. only 2 filtration cycles were performed).

For all conditions investigated, the operational resistance of cycled membranes generally increased with NaOCl dose (Figure 24). Intensive cleaning performed after 500 000 ppm*h did not significantly decrease the operational resistance. However, subsequent intensive cleanings (after 1 000 000, 1 500 000, 2 000 000 ppm*h) significantly decreased the operational resistance. These results suggest that the efficacy of the chemical cleaning, although initially good, decreased as cumulative NaOCl dose increased.

The decrease in chemical cleaning efficacy was generally most pronounced for scheme A, followed by schemes B and C. To compare the three schemes, the data were divided into four periods, separated by intensive cleaning events, as follows:

- period 1 from 0 to 500 000 ppm*h
- period 2 from 500 000 to 1 000 000 ppm*h
- period 3 from 1 000 000 to 1 500 000 ppm*h
- period 4 from 1 500 000 to 2 000 000 ppm*h

The operational resistance was significantly higher for scheme A than scheme B in periods 2, 3 and 4. The operational resistance was significantly higher for scheme A than scheme C in all four periods. The operational resistance was significantly higher for scheme B than scheme C in periods 1 and 3. The consistently greater operational resistance for scheme A indicates that, in general, more frequent chemical cleaning resulted in higher operational

resistance, particularly for membranes exposed to a high cumulative NaOCl dose. Statistical analysis is provided in Appendix 6.

Similar results have been reported by others for cycled membranes. Hajibabania *et al.* reported an increase in resistance over time for cycled membranes, though their observations might be classified as "clean membrane" resistance rather than operational resistance, depending on their specific cleaning protocols (Hajibabania et al., 2012). Wang *et al.* reported a similar phenomenon following intensive cleaning: a significant decrease in clean membrane resistance following cleaning (recall Section 5.2.1) followed by a faster increase in operational resistance for aged membranes (Wang et al., 2010). However, neither study considered potential changes in cleaning efficacy as membranes age. Abdullah and Bérubé did investigate changes in cleaning efficacy for membranes that had previously been aged using single-soak operation (Abdullah and Bérubé, 2018). Their results indicated that the efficacy of chemical cleaning decreased as membranes age.

Potential changes in operational resistance with age for PVDF membranes have not been investigated at full-scale, so further research is required to determine whether this phenomenon is relevant to WTP operation.

The greater operational resistance likely resulted from an increase in affinity of the membrane for foulants with age. As membranes lose hydrophilic additives with age (Section 5.3.1), they become more hydrophobic (Section 5.3.2), and therefore foul more extensively (Section 5.2.3) and are potentially more difficult to chemically clean (Abdullah

and Bérubé, 2013). Consequently, a portion of the foulants accumulate on the membrane each filtration cycle. As a result, the operational resistance between intensive cleaning events increases with age. Scheme A had the shortest chemical soak, which was possibly not long enough for complete foulant removal, while schemes B and C had longer soaks so their foulant removal was correspondingly greater. Thus, the differences among initial cycle resistance for operational schemes A, B and C are likely due to differences in accumulated foulants (Section 5.2.3).

5.2.3 Fouling Rate

Fouling rate was measured during cycles following chemical cleaning. The fouling rate with respect to age, here expressed as cumulative NaOCl dose and/or number of cycles, is presented in Figure 25 (single-soak membranes) and Figure 26 (cycled membranes).

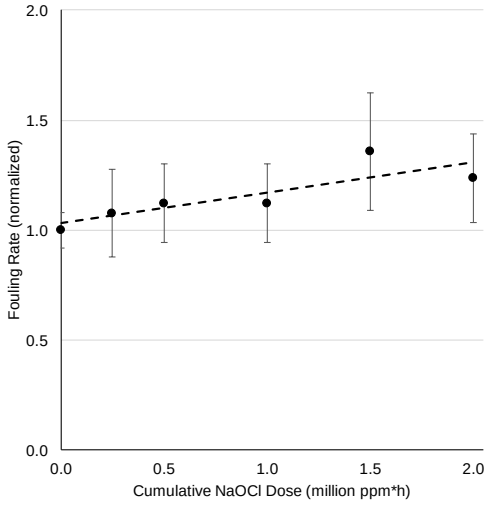

*Figure 25. Fouling rate for single-soaked membranes, normalized to fouling rate observed for new membranes. The error bars represent standard error among four replicates. The dashed line indicates a best-fit, with a slope of 0.14±0.04 per million ppm*h.*

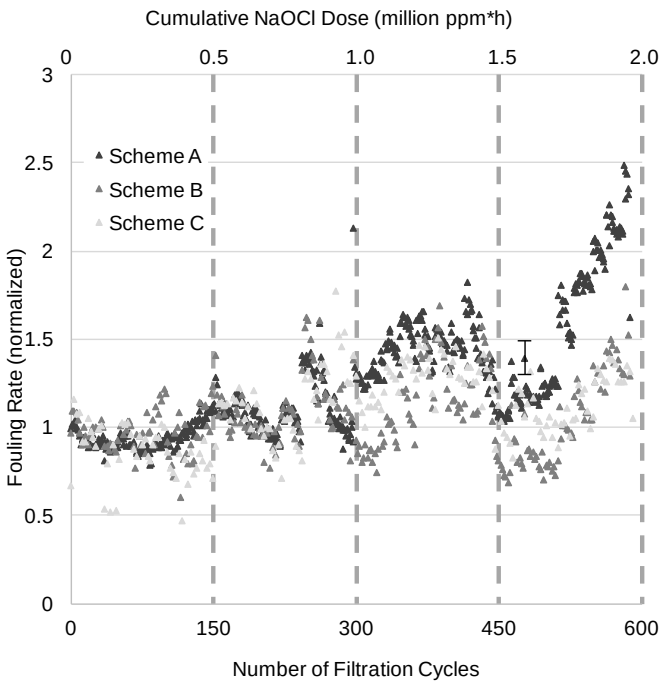

Figure 26. Fouling rate for cycled membranes, normalized to fouling rate observed for new membranes One typical error bar (standard error among four replicates) is presented to maximize plot readability.

A statistically significant increase in the fouling rate was observed for single-soaked membranes with respect to NaOCl exposure dose (Figure 25). Note that the coefficient of variation for clean membrane resistance of single-soaked membranes was less than 10% (Section 5.2.1); however, the coefficient of variation for the fouling rate was greater than 20% (Figure 25), indicating that the inherent variability associated with the fouling rate as a performance factor was relatively high. Others have also reported an increase in fouling rate for single-soaked PVDF membranes exposed to NaOCl, also suggesting that the affinity of the membrane for foulants increased as the cumulative NaOCl dose increased (Abdullah and Bérubé, 2018; Arkhangelsky et al., 2008; Hajibabania et al., 2012; Qin et al., 2005a, 2004, 2003).

For all schemes investigated, the fouling rate of cycled membranes also generally increased with NaOCl dose (Figure 26). Unlike the decrease in operational resistance observed after intensive cleans (Section 5.2.2), the fouling rate did not change significantly when intensive cleans were performed, suggesting that the membranes' affinity for foulants increased as the cumulative NaOCl dose increased, regardless of the presence of residual foulants.

The increase in fouling rate was generally most pronounced for scheme A. To compare the three schemes quantitatively, the data were divided into four periods, as previously considered for the operational resistance.

Differences in fouling rate among schemes were not significant during the first two periods, except that scheme B fouled slightly more than scheme C during period 1. The fouling rate was significantly higher for scheme A than schemes B and C during periods 3 and 4. The fouling rate was significantly higher for scheme C than scheme B during periods 3 and 4. The higher fouling rate for scheme A during periods 3 and 4 suggests that, in general, the most frequent chemical cleaning resulted in a higher fouling rate; however, for less frequent chemical cleaning, the impact on fouling rate was mixed. Statistical analysis is provided in Appendix 6.

Inconsistent results have been reported in the literature by others with respect to fouling rate during cycled ageing. An increase, consistent with the observations of the present study, was observed in one study (Wang et al., 2010), though a decrease in fouling rate with respect to NaOCl dose was observed in another study (Hajibabania et al., 2012).

The study presented in Chapter 4 is the only work to date that has investigated fouling rate of full-scale aged PVDF membranes. As previously discussed, a higher fouling rate was observed for aged membranes (Chapter 4), which is consistent with the present results observed for both single-soaked and cycled membranes.

As previously discussed in section 5.2.2, we expect that the greater fouling rate for aged membranes resulted from an increase in membrane hydrophobicity. As membranes lose hydrophilic additives with age (Section 5.3.1), they become more hydrophobic (Section 5.3.2), which would cause more significant adsorptive fouling (Chapter 2). It is unclear why operational scheme A fouled significantly more than the other schemes during the final two periods. One possible explanation is that the amount of foulants remaining on the membrane surface following a chemical clean was greater for scheme A, because the chemical clean was shorter in duration. Remaining foulants may have caused immediate pore constriction, and providing a 'head start' for additional foulants. Although these foulants may be removed during extensive cleaning, they are quickly re-established after several operational cycles. However, further research, beyond the scope of the present work, is required to confirm this mechanism. In general, these observations indicate that cleaning frequency and/or duration may be manipulated to minimize fouling for aged membranes, and that fouling of aged membranes is more pronounced after either single-soaked or cycled NaOCl exposure than for virgin membranes.

5.3 Membranes' Physical & Chemical Characteristics

5.3.1 Hydrophilic Additive Content (ATR-FTIR)

Because pure PVDF is inherently hydrophobic, hydrophilic additives (HA) are commonly included in PVDF membranes to mitigate fouling, as noted based on the literature review (Chapter 2). To measure HA content, ATR-FTIR spectra were measured for dried membrane coupons, harvested after intensive cleaning. Typical spectra, showing the PVDF (main polymer) and HA peaks for virgin and aged membranes are presented in Figure 27.

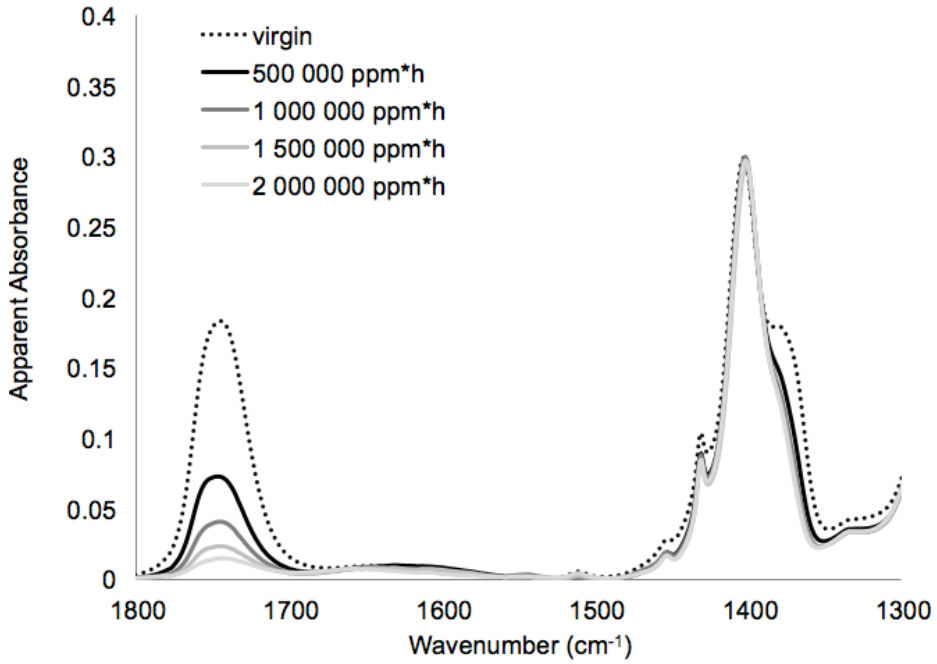

Figure 27. Typical ATR-FTIR spectra (1400 cm^{-1} PVDF; 1750 cm^{-1} HA) for single-soaked membranes.

The HA content with respect to age, here expressed as cumulative NaOCl dose, is presented in Figure 28.

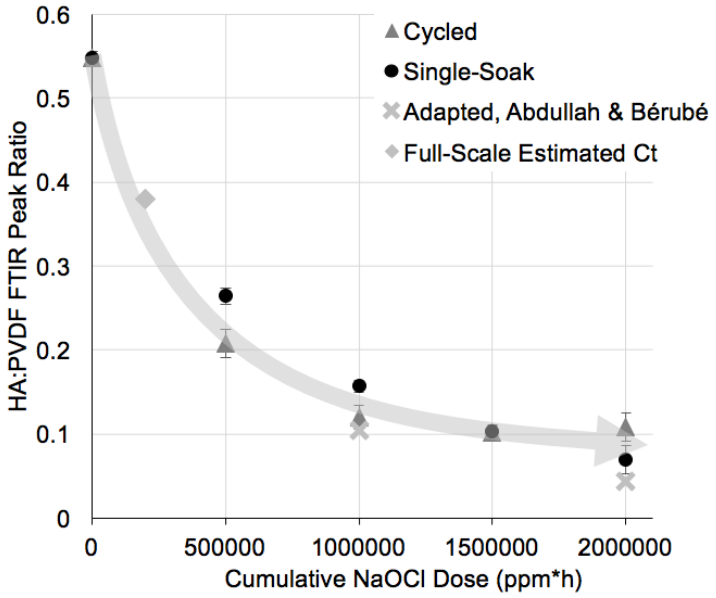

*Figure 28. Impact of NaOCl dose on HA content, as determined by FTIR peak ratio (1750cm^{-1}/1400cm^{-1}). Error bars represent the standard error based on 8 spectra from 4 replicate ageing trials. The diamond is typical field-aged data, based on Chapter 3 (from trend-line of 1000Bs at 8 years + typical C*t data). The X's are estimates of lab-aged data adapted from Abdullah and Bérubé (2013).*

For single-soaked membranes, the surface HA content decreased with age, to approximately 13% of the initial value when dosed with 2 000 000 ppm*h NaOCl (Figure 28). HA removal has been observed in other studies that investigated single-soaked PVDF membranes dosed with NaOCl (Abdullah and Bérubé, 2013; Le-Clech, 2014; Puspitasari et al., 2010). In particular, Abdullah and Bérubé observed that the HA content of PVDF membranes, from the same manufacturer as the membranes used in the present study, decreased with respect to exposure dose (Abdullah and Bérubé, 2013). The findings of Abdullah and Bérubé were plotted in Figure 28.

The HA removal from cycled operational schemes A, B, and C were not significantly different from one another, so the results from these three conditions were combined for

the discussion that follows. For cycled membranes, the surface HA content decreased with age, to approximately 19% of the initial value when dosed with 2 000 000 ppm*h NaOCl (Figure 28). The rate of decrease was not significantly different from that for single-soaked membranes. HA removal has not been reported in other studies that investigated cycled PVDF membranes dosed with NaOCl. Hajibabania *et al.* observed an unidentified HA (carbonyl) peak at 1732 cm^{-1} for virgin membranes but aged membrane data were not reported (Hajibabania et al., 2012). Although HA removal was similar among the three schemes, scheme A membranes generally retained more HA than scheme B, which generally retained more HA than scheme C. These results suggest that the presence of more residual foulants could protect membranes from exposure to NaOCl. However, based on the low significance of these differences, and the similarity of HA removal in all cycled schemes to that with single-soak ageing, the 'protection' of the membrane by residual foulants is not expected to significantly impact membrane ageing.

HA content in full-scale membrane facilities has only been observed in Chapter 4, and was observed to decrease with membrane age. The average HA content in the oldest (i.e. 8-year-old) membranes that were characterized as part of the work presented in Chapter 4 (C*t was estimated to be 20 000 ppm*h, see Section 4.5) was plotted along with results from the present study in Figure 28. Because the removal of hydrophilic additive (HA) from single-soaked, cycled and full-scale aged membranes was similar, it can be concluded that single-soak and cycled ageing are reasonable surrogates to assess the changes in HA content of full-scale membranes as they age.

The decreasing HA content is expected to decrease the hydrophilicity of membranes (Section 5.3.2). As previously discussed, we attributed the greater fouling rate observed with age to a decrease in membrane hydrophilicity (Section 5.2.3).

5.3.2 Contact Angle

Surface hydrophobicity was assessed via contact angle measurements of dried membranes after intensive cleaning. Typical images of water droplets on dried membranes immediately after drop application (0 minutes) and after 2 minutes are illustrated in Figure 29. Note that imaging of droplets was only performed from membranes from cycled operational scheme A and single-soaked.

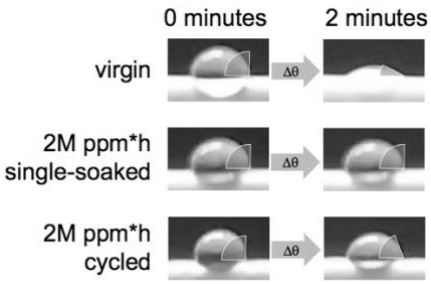

Figure 29. Examples of water droplets, at t=0 min and t=2 min, on the membrane surface, illustrating the impact of cumulative NaOCl dose and ageing method on contact angle.

The contact angle with respect to age, here expressed as cumulative NaOCl dose, is presented in Figure 30.

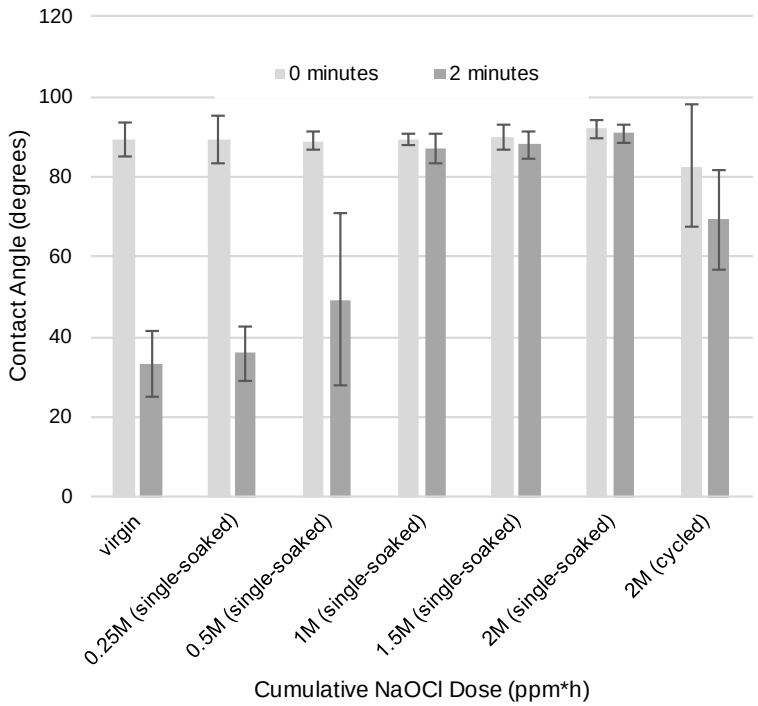

Figure 30. Summary of contact angles measured for single-soaked and cycled (scheme A) membranes; error bars represent standard error from 4 replicate membranes.

For single-soaked membranes the initial (i.e. 0-minute) contact angles remained constant with age, as illustrated in Figure 30. After 2 minutes, virgin membranes had wetted significantly, such that the contact angles decreased to $33^{o}\pm8^{o}$; however, drops applied to the membranes single-soaked to 2 000 000 ppm*h retained their initial contact angle (i.e. $91^{o}\pm3^{o}$). These results suggest that the hydrophobicity is greater for aged membranes. As previously discussed this was likely due to HA removal, as other changes in surface characteristics commonly associated with aged membranes (e.g. higher porosity and surface roughness) would have been expected to improve wettability (Chapter 2). This increase in contact angle is consistent with results from other single-soak studies of PVDF membranes in the literature (Abdullah and Bérubé, 2013; Hajibabania et al., 2012; Levitsky et al., 2012; Puspitasari et al., 2010; Wang et al., 2010).

The contact angle measurements for cycled membranes were more variable than those for single-soaked membranes. In addition, the contact angle was generally lower for cycled membranes than for single-soaked membranes. The higher variability and relatively high hydrophilicity of aged cycled membranes, compared to aged single-soak membranes, was attributed to the presence of a heterogeneous layer of irreversible foulants on the membrane surfaces; irreversible foulants were observed on cycled membranes by SEM imaging (Figure 31). Wang *et al.* observed the opposite effect (decreasing contact angle) in cycled membranes (Wang et al., 2010), attributing the change to surface modifications and foulant accumulation. Based on the FTIR spectra there was no carbonyl-based HA in the membranes of Wang *et al,* so it follows that increasing hydrophobicity due to HA removal would not be expected in that study; however, non-carbonyl-based HA may have been present but not reported.

To date, contact angle has not been quantified for full-scale aged membranes; it was not performed as part of the work presented in Chapter 4 due to the small membrane diameter of full-scale aged membranes considered for the study. However, we expect that contact angle and hydrophobicity would increase in full-scale aged membranes, because the HA content of full-scale aged membranes decreased with age (Chapter 4).

5.3.3 Apparent Surface Features (SEM Imaging)

SEM imaging was used to qualitatively (i.e. visually) assess membrane surface characteristics for selected conditions. SEM images for cycled membranes are for coupons

that were harvested after intensive cleaning, so any residual fouling is considered irreversible. Typical SEM images with respect to age, here expressed as cumulative NaOCl dose, are presented in Figure 31.

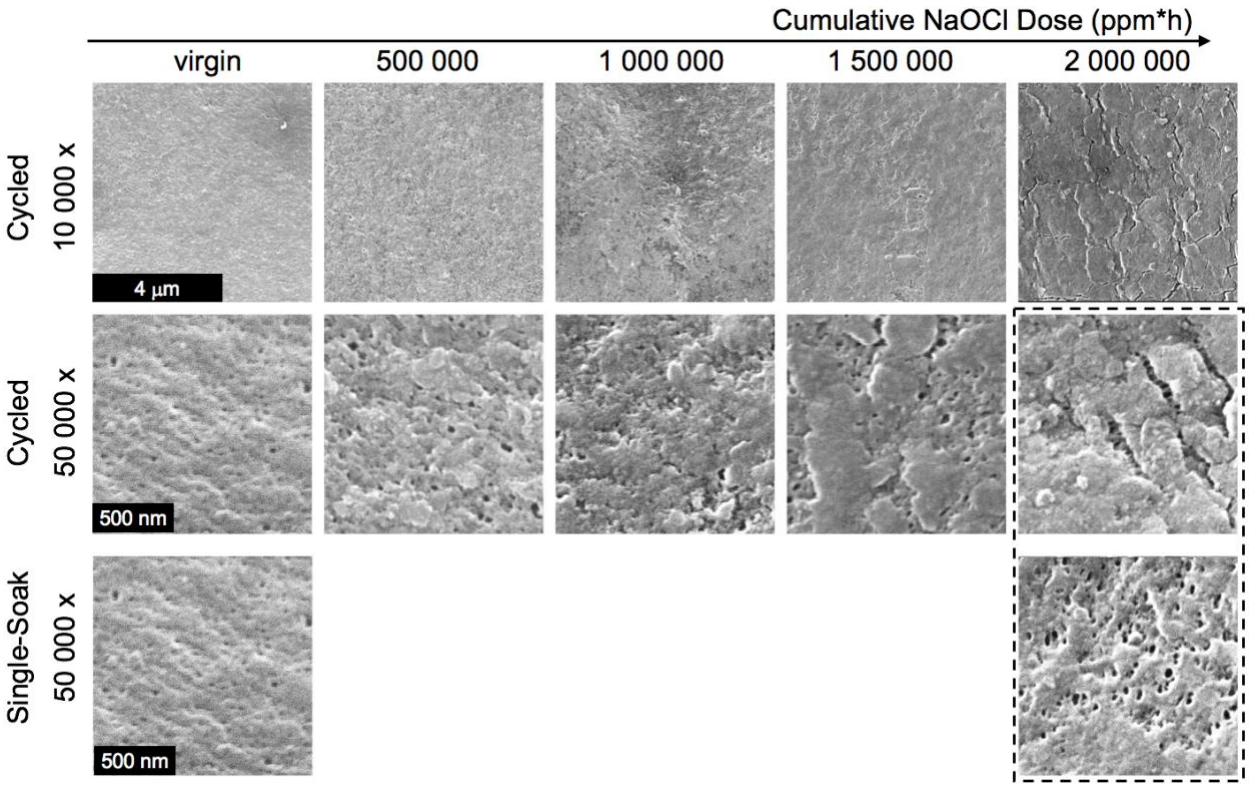

Figure 31. Representative SEM images for single-soak and cycled (scheme A) membranes with increasing cumulative NaOCl dose. The dashed box highlights the difference between single-soaked and cycled membranes at the highest dose. Both 10 000x and 50 000x images are included to give context for detailed surface evolution.

The discussion which follows provides qualitative data to support the discussions introduced in the prior sections. A comprehensive quantitative analysis of SEM images was outside the scope of the present work.

For single-soaked membranes, the apparent pore size was greater for aged membranes compared to virgin membranes, as illustrated in Figure 31, bottom row. A pore size increase caused by single-soaking of PVDF membranes has been observed by others (Abdullah and Bérubé, 2013). The increase in pore size was attributed to the removal of

hydrophilic additive (HA) by NaOCl, causing a rearrangement of PVDF molecules and pore enlargement (Chapter 2).

For cycled membranes, changes in surface characteristics were more complex than those observed for single-soaked membranes (Figure 31, top two rows). No apparent difference was observed among the operational schemes (A, B and C), which is consistent with the clean water resistance results, which were also similar among the three schemes. With increasing NaOCl dose, the irreversible foulants appeared to gradually accumulate on the membrane surface. Some pores, which are visible in openings between deposits of irreversible foulants, appear to be enlarging with NaOCl dose. It is unknown whether the openings in the irreversible foulant layer were formed when the membranes were dried for imaging, or were present during operation. Regardless, these images are consistent with our proposed ageing mechanism: although pore enlargement occurs with age, the accumulation of irreversible foulants on cycled membranes causes the decrease in resistance observed for single-soak membranes to be offset. Wang *et al.* presented SEM images of virgin and intensively cleaned membranes, following cycled ageing (Wang et al., 2010). Although not discussed, pore size and porosity decrease was evident from the SEM images presented by Wang *et al*.

For full-scale aged membranes, SEM images have not been reported. SEM was not performed for the membranes discussed in Chapter 4 due to the smaller relative pore size of full-scale aged membranes considered for the study, which could not be resolved using

the SEM available. However, we expect that irreversible foulant accumulation would also be evident for full-scale aged membranes.

5.4 Conclusions & Full-Scale Ageing Implications

By monitoring performance factors and physical/chemical characteristics of bench-scale aged membranes, we have advanced our understanding of ageing at bench- and full-scale. The overall findings of the present work are summarized in Table 7 and discussed below.

Table 7. Summary of changes in performance factors and physical/chemical characteristics for two bench-scale ageing protocols, and their proposed relation to full-scale membrane ageing.

Factor or Characteristic	Single-Soak Bench-Scale	Cycled Bench-Scale	Full-Scale	Outcome
clean membrane resistance	↓↓	↓	↑[1,2,3]	cycled bench-scale captures only part of full-scale irreversible fouling
operational resistance	--	↑	↑*	operational resistance increase indicates it may be a useful full-scale indicator
fouling rate	↑	↑	↑[1]	both ageing techniques mimic full-scale fouling rate increase
HA content	↓↓	↓↓	↓↓[1]	both ageing techniques mimic full-scale HA removal
hydrophobicity	↑↑	↑	↑*	related to HA content, either ageing technique would reflect full-scale hydrophobicity

Based on [1]Chapter 3, [2](Fenu et al., 2012), [3](He et al., 2014), *Expected trend from present work.
-- indicates that this information is unavailable.

Our first objective was to understand the discrepancies between bench-scale ageing and full-scale ageing. The clean membrane resistance was observed to decrease in both bench-scale experiments, though it increases at full-scale. We expect that this is due to the higher prevalence of irreversible fouling at full-scale. The operational resistance increased for cycled bench-scale experiments, and would be expected to increase at full-scale, though such full-scale data were unavailable. The increase in fouling rate for single-soak, cycled,

and full-scale can be attributed to removal of HA, which causes hydrophobicity to increase. We expect that the hydrophobicity increase was greater for single-soaked than cycled bench-scale ageing because irreversible foulants were not present on single-soaked membranes. Although porosity was not quantified in the present work, SEM imaging suggests that pore size and porosity increased for single-soaked membranes. Although pore size appeared to increase for cycled membranes, porosity appeared to be lower due to the accumulation of irreversible foulants. We expect that the porosity of full-scale aged membranes would reflect their greater clean membrane resistance, with irreversible foulant impacts causing significant reduction in porosity. Overall, cycled bench-scale ageing is a better surrogate for full-scale ageing than is single-soaked ageing, but neither can fully mimic the degree of fouling expected at full-scale. Either cycled or single-soaked ageing is an appropriate surrogate for full-scale ageing where chemical composition (e.g. HA degradation) is of concern, as the extent of HA removal was similar among bench-scale conditions and when compared to full-scale.

Our second objective was to use bench-scale ageing to understand how physical/chemical characteristics change and impact membrane performance. We determined that resistance change is likely due to combined mechanisms of pore enlargement (dominant in single-soak) and irreversible foulant accumulation (dominant in full-scale). Cycled operation captures both effects, whereas single-soak operation only captures the pore enlargement. We also established that declining HA likely causes increased hydrophobicity, which increases membrane fouling rate for both cycled and single-soak bench-scale operation; this is consistent with results reported in the literature for full-scale aged membranes.

Infrequent but longer cleaning cycles may cause slower deterioration of some ageing metrics (operational resistance, fouling rate). This suggests that plants should consider rigorous chemical cleaning of membranes only when necessary, rather than according to a predetermined schedule. However, the cycle schedules for schemes A, B and C were highly accelerated, so this cleaning approach should be studied at full-scale before being adopted.

Chapter 6 - Conclusions & Engineering Significance

6.1 Summary of Major Findings

Detailed conclusions from the full-scale and bench-scale ageing projects were presented in Section 4.6 and Section 5.4, respectively. Major conclusions are summarized here.

6.1.1 Major Findings of Full-Scale Membrane Ageing Project

The primary objective of the full-scale ageing project was to determine which performance factors change over many years of field-ageing. There were no significant changes observed for 1000A membranes or 1000B membranes with less than 5 years of full-scale operation. However, for 1000B membranes with over 5 years of full-scale operation, we observed changes in performance: an increase in fouling rate and clean membrane resistance, and a degradation of mechanical properties. Changes in membrane chemical characteristics were also observed for 1000B membranes with over 5 years of full-scale operation, manifested as a decrease in both the surface and bulk hydrophilic additive (HA) content. Although no changes were observed for 1000A membranes, an accelerated NaOCl soak of these membranes suggests that this was because they are too young to show an effect.

A comparison of membrane performance and characteristics suggested the cause of increased fouling rate for full-scale aged 1000B membranes. We observed that the fouling rate was the highest for 1000B membranes with lower HA content on the membrane surface. This indicates that more hydrophobic membranes have a higher affinity for organic foulants as the surface HA content decreases.

Membrane resistance could provide a useful benchmark to both WTPs and membrane manufacturers seeking to easily track membrane ageing at full-scale. This could enable improved optimization of full-scale operating conditions, or better prediction of the expected product life. Further, the increased propensity for fouling of aged membranes, compared with new ones, indicates that cleaning protocols could be tailored towards the membranes' age. For example, plants could consider applying shorter or lower concentration cleaning cycles for newer membranes, and longer cycles once clean membrane resistance deviates from that of new membranes. Such a change in protocol for newer membranes would have the advantages of decreasing downtime, decreasing chemical consumption, and slowing membrane ageing.

Finally, although C*t was not used as a metric of membrane age, we observed that for a treatment plant applying an atypically high dose of NaOCl, the effective age of the membranes appeared to be greater than the actual age. Thus, as indicated by the results of lab-studies, avoiding excessive cumulative NaOCl exposure is advised.

6.1.1 Major Findings of Bench-Scale Membrane Ageing Project

The primary objective of the bench-scale ageing project was to better understand the discrepancies between bench-scale ageing (i.e. single-soak and cycled operation) and full-scale ageing. Overall, cycled bench-scale ageing is a better surrogate for full-scale than single-soaked ageing, but neither can mimic the full extent of irreversible fouling in full-scale operation. This shortcoming is due to the limitations of achievable cumulative foulant

mass loading at bench-scale. Either cycled or single-soaked ageing is an appropriate surrogate for full-scale ageing where chemical composition (e.g. HA degradation) is of interest.

The second objective was to use bench-scale ageing to understand how physical/chemical characteristics change and impact membrane performance. We determined that clean membrane resistance change is likely due to combined mechanisms of pore enlargement (dominant in single-soak) and irreversible foulant accumulation (dominant in full-scale). Cycled operation captures both effects, whereas single-soak operation only captures the pore enlargement. We also established that declining HA likely causes increased hydrophobicity, which increases membrane fouling rate for both cycled and single-soak bench-scale aged membranes. The improved understanding of ageing mechanisms from bench-scale was crucial to our explanation of ageing at full-scale.

6.2 Knowledge Gaps & Future Work

Because the present research was the first to thoroughly characterise full-scale aged membranes, several research avenues were identified for future work.

In full-scale ageing, a clear question is whether, after sufficient time, the 1000A membranes will show similar ageing behaviour to the 1000B membranes. The *ad hoc* NaOCl soak test of 1000A membranes suggests that their HA content can be degraded, but full-scale aged membranes with such degradation were not available. Harvesting from the WTPs with

1000A membranes in the present work should be continued or resumed in several years to capture their ageing behaviour.

In future monitoring of full-scale ageing, inclusion of raw water characteristics & cleaning protocols could be useful in understanding irreversible fouling. If the specific raw water components responsible for irreversible fouling are identified, bench-scale experiments may have more success in emulating the irreversible foulant loading of full-scale ageing.

Beyond improving the bench-scale ageing emulation of irreversible foulant loading, differences between cycled bench-scale and full-scale operation should be considered in more detail. These differences could include factors such as membrane packing density, concentration factors, hydrodynamics, and cleaning protocols.

Another research avenue that emerged from the full-scale ageing project is the observation that membrane surface HA appeared to degrade more rapidly than bulk HA. Insufficient data were available to fully support this observation, but further study could help to better elucidate membrane degradation mechanisms, allowing for improved membrane design, for example by copolymerizing HA with PVDF.

The membrane susceptibility to breach was identified as a performance factor in Chapter 2, yet it was assessed only indirectly, via mechanical testing, in Chapter 4. If WTP data on breach repair frequency were available for analysis, they could yield an improved understanding of this important performance factor. Furthermore, analysis linking breach

frequency to mechanical properties could be truly valuable in forecasting membrane breach rates.

The SEM images in the bench-scale ageing study suggested that irreversible foulants play an important role in ageing of cycled membranes. In the present study, SEM imaging was only used qualitatively, but a quantitative analysis of images (e.g. using software-aided mapping to calculate pore size and number) could help to take this understanding further. Furthermore, SEM imaging of full-scale aged membranes could provide information to better explain why the clean membrane resistance increases with age.

Finally, a metric based on achievable operational resistance (or permeability, a related measure) could be a useful diagnostic for full-scale facilities. However, this observation has not yet been reconciled in full-scale membrane ageing studies. The feasibility of diagnostic measures for practical membrane resistance is an area ripe for exploration.

References

Abdullah, S.Z., 2013. Membrane weathering during chemical cleaning. University of British Columbia.

Abdullah, S.Z., Bérubé, P.R., 2018. Filtration and cleaning performances of PVDF membranes aged with exposure to sodium hypochlorite. Sep. Purif. Technol. 195, 253–259.

Abdullah, S.Z., Bérubé, P.R., 2013. Assessing the effects of sodium hypochlorite exposure on the characteristics of PVDF based membranes. Water Res. 47, 5392–5399. doi:10.1016/j.watres.2013.06.018

Abdullah, S.Z., Bérubé, P.R., Horne, D.J., 2014. SEM imaging of membranes: Importance of sample preparation and imaging parameters. J. Memb. Sci. 463, 113–125. doi:10.1016/j.memsci.2014.03.048

Ameduri, B., Ladavière, C., Delolme, F., Boutevin, B., 2004. First MALDI-TOF mass spectrometry of vinylidene fluoride telomers endowed with low defect chaining. Macromolecules 37, 7602–7609. doi:10.1021/ma0496394

Antony, A., Leslie, G., 2011. Degradation of polymeric membranes in water and wastewater treatment, in: Advanced Membrane Science and Technology for Sustainable Energy and Environmental Applications. Elsevier Inc, pp. 718–745.

APHA, 2005. Standard methods for the examination of water and wastewater, 21st ed. American Public Health Association.

Arkhangelsky, E., Goren, U., Gitis, V., 2008. Retention of organic matter by cellulose acetate membranes cleaned with hypochlorite. Desalination 223, 97–105. doi:10.1016/j.desal.2007.04.070

Arkhangelsky, E., Kuzmenko, D., Gitis, V., 2007a. Impact of chemical cleaning on properties and functioning of polyethersulfone membranes. J. Memb. Sci. 305, 176–184. doi:10.1016/j.memsci.2007.08.007

Arkhangelsky, E., Kuzmenko, D., Gitis, N. V., Vinogradov, M., Kuiry, S., Gitis, V., 2007b. Hypochlorite cleaning causes degradation of polymer membranes. Tribol. Lett. 28, 109–116. doi:10.1007/s11249-007-9253-6

ASTM, 2014. Standard test method for tensile properties of single textile fibers D3822/D3822M. doi:10.1520/D3822

Bégoin, L., Rabiller-Baudry, M., Chaufer, B., Hautbois, M.-C., Doneva, T., 2006. Ageing of PES industrial spiral-wound membranes in acid whey ultrafiltration. Desalination 192, 25–39. doi:10.1016/j.desal.2005.10.009

Causserand, C., Rouaix, S., Lafaille, J.-P., Aimar, P., 2008. Ageing of polysulfone membranes in contact with bleach solution: Role of radical oxidation and of some dissolved metal ions. Chem. Eng. Process. 47, 48–56. doi:10.1016/j.cep.2007.08.013

Causserand, C., Rouaix, S., Lafaille, J.-P., Aimar, P., 2006. Degradation of polysulfone membranes due to contact with bleaching solution. Desalination 199, 70–72. doi:10.1016/j.desal.2006.03.144

Crittenden, J.C., Trussel, R.R., Hand, D.W., Howe, K.J., Tchobanoglous, G., 2005. Water Treatment: Principles and Design, 2nd ed.

da Costa, P.R., Alkmin, A.R., Amaral, M.C.S., de França Neta, L.S., Cerqueira, A.C., Santiago, V.M.J., 2015. Ageing effect on chlorinated polyethylene membrane of an MBR caused by chemical cleaning procedures. Desalin. Water Treat. 53, 1460–1470.

doi:10.1080/19443994.2014.943063

Delattre, J., Rabaud, B., Brehant, A., Glucina, K., Sollogoub, C., Thominette, F., 2012. Ageing of hollow fiber membranes in polyvinylidene fluoride (PVDF) used in water treatment. Procedia Eng. 44, 764–767. doi:10.1016/j.proeng.2012.08.562

Do, V.T., Tang, C.Y., Reinhard, M., Leckie, J.O., 2012a. Effects of chlorine exposure conditions on physiochemical properties and performance of a polyamide membrane-mechanisms and implications. Environ. Sci. Technol. 46, 13184–92. doi:10.1021/es302867f

Do, V.T., Tang, C.Y., Reinhard, M., Leckie, J.O., 2012b. Effects of hypochlorous acid exposure on the rejection of salt, polyethylene glycols, boron and arsenic(V) by nanofiltration and reverse osmosis membranes. Water Res. 46, 5217–5223. doi:10.1016/j.watres.2012.06.044

Do, V.T., Tang, C.Y., Reinhard, M., Leckie, J.O., 2012c. Degradation of polyamide nanofiltration and reverse osmosis membranes by hypochlorite. Environ. Sci. Technol. 46, 852–9. doi:10.1021/es203090y

EPA, 1982. Handbook for sampling and sample preservation of water and wastewater. Environmental Protection Agency, Cincinnati.

Fenu, A., De Wilde, W., Gaertner, M., Weemaes, M., de Gueldre, G., Van De Steene, B., 2012. Elaborating the membrane life concept in a full scale hollow-fibers MBR. J. Memb. Sci. 421–422, 349–354. doi:10.1016/j.memsci.2012.08.001

Flemming, H.C., Neu, T.R., Wozniak, D.J., 2007. The EPS matrix: The “house of biofilm cells.” J. Bacteriol. 189, 7945–7947. doi:10.1128/JB.00858-07

Gaudichet-Maurin, E., Thominette, F., 2006. Ageing of polysulfone ultrafiltration membranes in

contact with bleach solutions. J. Memb. Sci. 282, 198–204. doi:10.1016/j.memsci.2006.05.023

Giglia, S., Bohonak, D., Greenhalgh, P., Leahy, A., 2015. Measurement of pore size distribution and prediction of membrane filter virus retention using liquid–liquid porometry. J. Memb. Sci. 476, 399–409. doi:10.1016/j.memsci.2014.11.053

Gijsbertsen-Abrahamse, A.J., Cornelissen, E.R., Hofman, J.A.M.H., 2006. Fiber failure frequency and causes of hollow fiber integrity loss. Desalination 194, 251–258. doi:10.1016/j.desal.2005.11.010

Gregorio, R., 2006. Determination of the α, β, and γ crystalline phases of poly(vinylidene fluoride) films prepared at different conditions. J. Appl. Polym. Sci. 100, 3272–3279. doi:10.1002/app.23137

GVWD, 2016. Greater Vancouver Water District 2016 Quality Control Annual Report: Volume 1. Vancouver.

Hajibabania, S., Antony, A., Leslie, G., Le-Clech, P., 2012. Relative impact of fouling and cleaning on PVDF membrane hydraulic performances. Sep. Purif. Technol. 90, 204–212. doi:10.1016/j.seppur.2012.03.001

Hanafi, Y., Szymczyk, A., Rabiller-Baudry, M., Baddari, K., 2014. Degradation of poly (ether sulfone)/polyvinylpyrrolidone membranes by sodium hypochlorite: Insight from advanced electrokinetic characterizations. Environ. Sci. Technol. 48, 13419–13426.

Hashim, N.A., Liu, Y., Li, K., 2011. Stability of PVDF hollow fibre membranes in sodium hydroxide aqueous solution. Chem. Eng. Sci. 66, 1565–1575. doi:10.1016/j.ces.2010.12.019

He, Y., Sharma, J., Bogati, R., Liao, B.Q., Goodwin, C., Marshall, K., 2014. Impacts of ageing and

chemical cleaning on the properties and performance of ultrafiltration membranes in potable water treatment. Sep. Sci. Technol. 49, 1317–1325. doi:10.1080/01496395.2014.882359

Huber, S.A., Balz, A., Abert, M., Pronk, W., 2011. Characterisation of aquatic humic and non-humic matter with size-exclusion chromatography--organic carbon detection--organic nitrogen detection (LC-OCD-OND). Water Res. 45, 879–85. doi:10.1016/j.watres.2010.09.023

Jucker, C., Clark, M.M., 1994. Adsorption of aquatic humic substances on hydrophobic ultrafiltration membranes. J. Memb. Sci. 97, 37–52.

Jung, B., Yoon, J.K., Kim, B., Rhee, H.-W., 2004. Effect of molecular weight of polymeric additives on formation, permeation properties and hypochlorite treatment of asymmetric polyacrylonitrile membranes. J. Memb. Sci. 243, 45–57. doi:10.1016/j.memsci.2004.06.011

Keucken, A., Wang, Y., Tng, K.H., Leslie, G., Persson, K., Kohler, S.J., Spanjer, T., 2016. Evaluation of novel hollow fiber membranes for NOM removal by advanced membrane autopsy. Water Sci. Technol. Water Supply 16, 628–640. doi:10.2166/ws.2015.170

Kimura, K., Tanaka, K., Watanabe, Y., 2014. Microfiltration of different surface waters with/without coagulation: Clear correlations between membrane fouling and hydrophilic biopolymers. Water Res. 49, 434–443. doi:10.1016/j.watres.2013.10.030

Kwon, Y.-N., Leckie, J.O., 2006. Hypochlorite degradation of crosslinked polyamide membranes I. Changes in chemical/morphological properties. J. Memb. Sci. 283, 21–26. doi:10.1016/j.memsci.2006.06.008

Le-Clech, P., 2014. Predictive Tools for Membrane Ageing. IWA Publishing, London.

Levitsky, I., Duek, A., Arkhangelsky, E., Pinchev, D., Kadoshian, T., Shetrit, H., Naim, R., Gitis, V., 2011. Understanding the oxidative cleaning of UF membranes. J. Memb. Sci. 377, 206–213. doi:10.1016/j.memsci.2011.04.046

Levitsky, I., Duek, A., Naim, R., Arkhangelsky, E., Gitis, V., 2012. Cleaning UF membranes with simple and formulated solutions. Chem. Eng. Sci. 69, 679–683. doi:10.1016/j.ces.2011.10.060

Liang, Y.-M., Lin, X.-D., Zhang, Z.-L., Lu, J., Zhang, L., Liu, W., 2015. Integrity of PVC membranes after sequential cleaning with hypochlorite and citric acid. Desalin. Water Treat. 53, 2897–2094. doi:10.1080/19443994.2013.869663

Liang, Y., Lu, J., Qin, X., Yang, X., Chen, B., Zhang, Z., Liu, W., 2013. Effluent particle size and permeability of polyvinylchloride membranes after sodium hypochlorite exposure. J. Environ. Eng. 139, 712–718. doi:10.1061/(ASCE)EE.1943-7870.0000677.

Lobo, H., Bonilla, J. (Eds.), 2003. Handbook of Plastics Analysis. CRC Press.

Lu, J., Zhang, Z., Ye, T., Qin, X., Huang, Y., Yang, X., Luo, W., Chen, B., Liu, W., Liang, Y., 2011. Ageing of polyvinylchloride membranes in ultrafiltration of drinking water by chemical cleaning. IEEE 3834–3837. doi:10.1109/ICMT.2011.6001734

Montaudo, G., Samperi, F., Montaudo, M.S., 2006. Characterization of synthetic polymers by MALDI-MS. Prog. Polym. Sci. 31, 277–357. doi:10.1016/j.progpolymsci.2005.12.001

Pabby, A.K., 2009. Handbook of membrane separations: chemical, pharmaceutical, food and biotechnology applications.

Pearce, G., 2017. Membrane filtration market trends based on a comprehensive reference list survey, in: 8th IWA Membrane Technology Conference & Exhibition for Water and

Wastewater Treatment and Reuse. Singapore, p. 7.

Peinador, R.I., Calvo, J.I., ToVinh, K., Thom, V., Prádanos, P., Hernández, A., 2011. Liquid–liquid displacement porosimetry for the characterization of virus retentive membranes. J. Memb. Sci. 372, 366–372. doi:10.1016/j.memsci.2011.02.022

Peldszus, S., Hallé, C., Peiris, R.H., Hamouda, M., Jin, X., Legge, R.L., Budman, H., Moresoli, C., Huck, P.M., 2011. Reversible and irreversible low-pressure membrane foulants in drinking water treatment: Identification by principal component analysis of fluorescence EEM and mitigation by biofiltration pretreatment. Water Res. 45, 5161–5170. doi:10.1016/j.watres.2011.07.022

Pellegrin, B., Mezzari, F., Hana, Y., Szymczyk, A., Remigy, J.-C., Causserand, C., Hanafi, Y., Szymczyk, A., Remigy, J.-C., Causserand, C., 2015a. Filtration performance and pore size distribution of hypochlorite aged PES/PVP ultrafiltration membranes. J. Memb. Sci. 474, 175–186. doi:10.1016/j.memsci.2014.09.028

Pellegrin, B., Mezzari, F., Hanafi, Y., Szymczyk, A., Remigy, J.-C., Causserand, C., 2015b. Filtration performance and pore size distribution of hypochlorite aged PES/PVP ultrafiltration membranes. J. Memb. Sci. 474, 175–186. doi:10.1016/j.memsci.2014.09.028

Pellegrin, B., Prulho, R., Rivaton, A., Thérias, S., Gardette, J.L., Gaudichet-Maurin, E., Causserand, C., 2013. Multi-scale analysis of hypochlorite induced PES/PVP ultrafiltration membranes degradation. J. Memb. Sci. 447, 287–296. doi:10.1016/j.memsci.2013.07.026

Porcelli, N., Judd, S., 2010. Chemical cleaning of potable water membranes: A review. Sep. Purif. Technol. 71, 137–143. doi:10.1016/j.seppur.2009.12.007

Pressdee, J.R., Veerapaneni, S., Shorney-Darby, H.L., Clement, J.A., Van der Hoek, P.J., 2006.

Integration of Membrane Filtration Into Water Treatment Systems.

Prulho, R., Rivaton, a., Therias, S., Gardette, J.L., 2012. Ageing mechanism of polyethersulfone/polyvinylpyrrolidone membranes in contact with bleach water. Procedia Eng. 44, 1031–1034. doi:10.1016/j.proeng.2012.08.666

Prulho, R., Therias, S., Rivaton, A., Gardette, J.-L., 2013. Ageing of polyethersulfone/polyvinylpyrrolidone blends in contact with bleach water. Polym. Degrad. Stab. 98, 1164–1172. doi:10.1016/j.polymdegradstab.2013.03.011

Puspitasari, V., Granville, A., Le-Clech, P., Chen, V., 2010. Cleaning and ageing effect of sodium hypochlorite on polyvinylidene fluoride (PVDF) membrane. Sep. Purif. Technol. 72, 301–308. doi:10.1016/j.seppur.2010.03.001

Qin, J.-J., Cao, Y.-M., Li, Y., 2005a. Effect of hypochlorite concentration on properties of posttreated outer-skin ultrafiltration membranes spun from cellulose acetate/poly(vinyl pyrrolidone) blends. J. Appl. Polym. Sci. 97, 227–231. doi:10.1002/app.21756

Qin, J.-J., Cao, Y.-M., Li, Y.-Q., Li, Y., Oo, M.-H., Lee, H., 2004. Hollow fiber ultrafiltration membranes made from blends of PAN and PVP. Sep. Purif. Technol. 36, 149–155. doi:10.1016/S1383-5866(03)00210-7

Qin, J.-J., Li, Y., Lee, L.-S., Lee, H., 2003. Cellulose acetate hollow fiber ultrafiltration membranes made from CA/PVP 360 K/NMP/water. J. Memb. Sci. 218, 173–183. doi:10.1016/S0376-7388(03)00170-4

Qin, J.-J., Oo, M.H., Li, Y., 2005b. Development of high flux polyethersulfone hollow fiber ultrafiltration membranes from a low critical solution temperature dope via hypochlorite treatment. J. Memb. Sci. 247, 137–142. doi:10.1016/j.memsci.2004.09.018

Qin, J.-J., Wong, F.S., 2002. Hypochlorite treatment of hydrophilic hollow fiber ultrafiltration membranes for high fluxes. Desalination 146, 307–309. doi:10.1016/S0011-9164(02)00497-6

Rabuni, M.F., Sulaiman, N.M.N., Aroua, M.K., Yern Chee, C., Hashim, N.A., 2015. Impact of in situ physical and chemical cleaning on PVDF membrane properties and performances. Chem. Eng. Sci. 122, 426–435. doi:10.1016/j.ces.2014.09.053

Regula, C., Carretier, E., Wyart, Y., Gésan-Guiziou, G., Vincent, A., Boudot, D., Moulin, P., 2014. Chemical cleaning/disinfection and ageing of organic UF membranes: A review. Water Res. 56, 325–365. doi:10.1016/j.watres.2014.02.050

Ross, G.J., Watts, J.F., Hill, M.P., Morrissey, P., 2000. Surface modification of poly (vinylidene fluoride) by alkaline treatment 1. The degradation mechanism. Polymer (Guildf). 41, 1685–1696.

Rouaix, S., Causserand, C., Aimar, P., 2006. Experimental study of the effects of hypochlorite on polysulfone membrane properties. J. Memb. Sci. 277, 137–147. doi:10.1016/j.memsci.2005.10.040

Simon, A., McDonald, J.A., Khan, S.J., Price, W.E., Nghiem, L.D., 2013. Effects of caustic cleaning on pore size of nanofiltration membranes and their rejection of trace organic chemicals. J. Memb. Sci. 447, 153–162. doi:10.1016/j.memsci.2013.07.013

Teella, A., Zydney, A.L., Zhou, H., Olsen, C., Robinson, C., 2014. Effects of chemical sanitization using NaOH on the properties of polysulfone and polyethersulfone ultrafiltration membranes. doi:10.1002/btpr.2008

Thominette, F., Farnault, O., Gaudichet-maurin, E., 2006. Ageing of polyethersulfone

ultrafiltration membranes in hypochlorite treatment 200, 7–8. doi:10.1016/j.desal.2006.03...221

Tian, J.Y., Ernst, M., Cui, F., Jekel, M., 2013. Correlations of relevant membrane foulants with UF membrane fouling in different waters. Water Res. 47, 1218–1228. doi:10.1016/j.watres.2012.11.043

Tng, K.H., Antony, A., Wang, Y., Leslie, G.L., 2015. Membrane ageing during water treatment: Mechanisms, monitoring, and control, in: Basile, A., Cassano, A., Rastogi, N. (Eds.), Advances in Membrane Technologies for Water Treatment. Elsevier Inc, pp. 349–378. doi:10.1016/B978-1-78242-121-4.00011-3

Van Der Bruggen, B., Vandecasteele, C., Van Gestel, T., Doyen, W., Leysen, R., 2003. A review of pressure-driven membrane processes in wastewater treatment and drinking water production. Environ. Prog. 22, 46–56.

Van Der Kooij, D., 1992. Assimilable organic carbon as an indicator of bacterial regrowth. J. AWWA 84, 57–65.

Vanysacker, L., Bernshtein, R., Vankelecom, I.F.J., 2014. Effect of chemical cleaning and membrane aging on membrane biofouling using model organisms with increasing complexity. J. Memb. Sci. 457, 19–28. doi:10.1016/j.memsci.2014.01.015

Wang, P., Wang, Z., Wu, Z., Zhou, Q., Yang, D., 2010. Effect of hypochlorite cleaning on the physiochemical characteristics of polyvinylidene fluoride membranes. Chem. Eng. J. 162, 1050–1056. doi:10.1016/j.cej.2010.07.019

Wolff, S.H., Zydney, A.L., 2004. Effect of bleach on the transport characteristics of polysulfone hemodialyzers. J. Memb. Sci. 243, 389–399. doi:10.1016/j.memsci.2004.06.044

Yadav, K., Morison, K., Staiger, M.P., 2009. Effects of hypochlorite treatment on the surface morphology and mechanical properties of polyethersulfone ultrafiltration membranes. Polym. Degrad. Stab. 94, 1955–1961. doi:10.1016/j.polymdegradstab.2009.07.027

Yadav, K., Morison, K.R., 2010. Effects of hypochlorite exposure on flux through polyethersulphone ultrafiltration membranes. Food Bioprod. Process. 88, 419–424. doi:10.1016/j.fbp.2010.09.005

Yuan, W.E.I., Zydney, A.L., 2000. Humic acid fouling during ultrafiltration. Environ. Sci. Technol. 34, 5043–5050.

Zondervan, E., Zwijnenburg, A., Roffel, B., 2007. Statistical analysis of data from accelerated ageing tests of PES UF membranes. J. Memb. Sci. 300, 111–116. doi:10.1016/j.memsci.2007.05.015

Appendix 1 - Literature Review Supplementary Material

Connections made in membrane ageing literature were categorized using the following symbols:

Performance Factors
- α - Breach Frequency
- β - Cleaning Rate
- γ - Resistance
- δ - Fouling Rate
- ε - Infrastructure Deterioration

Chemical & Physical Membrane Characteristics
- 1 - Foulant Accumulation
- 2 - Polymer Surface Chemical Composition (or Hydrophobicity)
- 3 - Polymer Phase (α, β, γ, etc)
- 4 - Pore Geometry (r, L)
- 5 - Porosity
- 6 - Polymer Molecular Weight
- 7 - Polymer Bulk Composition

Analytical Methods
- A - Cleaning Rate
- B - ATR FTIR
- C - Fouling Rate
- D - Contact Angle
- E - AFM
- F - Mass Spectrometry
- G - XPS
- H - Elasticity
- I - Breaking Force
- J -TGA
- K - SEM
- L - Challenge Tests
- M - GPC
- N - XRD
- O - Clean Membrane Resistance
- P - NMR
- Q - Integrity Testing
- R - Bulk FTIR
- S - Porometry
- T - Zeta Potential
- U - Yield Strength
- V - Maximum Elongation

Table 8. Summary of membrane ageing studies for polymeric membranes used in water treatment. Links discussed in each paper are indicated using symbols corresponding to performance factors (Greek letters), chemical/physical characteristics (numbers), and analytical methods (letters). Where a link is drawn to a "?" a given performance factor or technique was discussed or employed; however, the authors did not attribute the observations to membrane characteristics. Journal articles highlighted in grey have been added to the compilation since the review paper was published.

Reference	Membrane Type	Experimental Approach	Performance Factors Discussed & Characteristic Explanations	Implications of Techniques re Changing Characteristics (PVDF only)
Abdullah and Bérubé, 2013, WaterRes (Abdullah and Bérubé, 2013)	PVDF + HA	NaOCl soak, var C & t, pH 10	γ-4,5	B-2,7 D-2 K-4,5 L-4,5 O-4,5 P-7 U-5
Abdullah, 2018, SepPurTech Abdullah, 2014, Dissertation (Abdullah, 2013)	PVDF + HA	NaOCl soak, var C & t, pH 10, clean water, filt activated sludge, clean	δ-2,7 β-?	C-2,7 A-? O-?
Arkhangelsky et al., 2007, JMembSci (Arkhangelsky et al., 2007a)	polyethersulfone UF flat sheet	foul with BSA / clean w NaOCl soak, repeat, pH 7.2	γ-2,4,5,6,7 δ-2 α-7	

Arkhangelsky et al., 2007, TriLett (Arkhangelsky et al., 2007b)	asymmetric PES, CA, PVDF flat sheet UF	BSA foul, soak in NaOCl, var t, pH 7.2	α-2,4,5,6,7	PVDF results not reported
Arkhangelsky et al., 2008, Desalination (Arkhangelsky et al., 2008)	CA flat sheet UF	permeate with WWTP 2° effluent, NaOCl soak	γ-2 δ-2	
Bégoin et al., 2006, Desalination (Bégoin et al., 2006)	PES spiral wound UF	Virgin ageing in various solutions; 8000 hours of standard filtration	not discussed	
Causserand et al., 2006, Desalination (Causserand et al., 2006)	PES/PVP blend HF UF	soak in HOCl pH 5,7,8&10, var t, other cleaning chemicals	γ-? α-6	
Causserand et al., 2008, ChemEngProc (Causserand et al., 2008)	PES/PVP blend HF UF	filter raw water / HOCl pH 5,7,8,10&12, other cleaning chemicals	γ-1	
Causserand et al., 2015, WaterRes	PES/PVP HF UF	static vs dynamic soak in NaOCl, var t	γ-4,5,7	
da Costa et al., 2015, DesalWatTr (da Costa et al., 2015)	Polyethylene UF	Repeated acid and NaOCl cleaning of virgin membrane, fix C, CWF	γ-2,4,5	
Delattre et al., 2012, ProcEng (Delattre et al., 2012)	PVDF and PVP/PVDF UF	Soak in NaOCl, fix C & t, ph 6, 7.5, 11.5	not discussed	I-?
Do et al., 2012, EnvironSciTech (p852) (Do et al., 2012c)	PA-based NF	Soak in NaOCl, var C & t, pH 5, CWF, salt rejection	γ-2	
Do et al., 2012, EnvironSciTech (p13184) (Do et al., 2012a)	PA-based NF	Soak in NaOCl var conc & pH	γ-2,5,6	
Do et al., 2012, WaterRes (Do et al., 2012b)	PA-based NF	Soak in NaOCl, var C & t	γ-2	
Fenu et al., 2012, JmembSci (Fenu et al., 2012)	Unknown (probably Zeeweed)	Operate in MBR	not discussed	
(Gao et al., 2016) JMembSci	PVDF HF UF, MOTIMO	Soak in NaOCl, 2000 ppm, var t	γ-2,4	B-2,6,7 D-7 J-6 K-2,4,5 O-2,4
(Gao et al., 2017) JMembSci	PVDF 100 kDa, SEPRO	Soak in NaOCl, 2000 ppm, var t	γ-2,4,5 δ-2	B-2 C-2 D-? K-? O-2,4,5 T-2
Gaudichet-Maurin and Thominette, 2006, JmembSci (Gaudichet-Maurin and Thominette, 2006)	PSF fibre, PEG, PVP UF	soak PSF fibre and film in hypo	α-6	
Gijsbertsen-Abrahamse et al., 2006, Desalination (Gijsbertsen-Abrahamse et al., 2006)	Various UF/MF membrane	monitor operational membrane plants	α-7	
Hashim et al., 2011, ChemEngSci (Hashim et al., 2011)	PVDF HF (Kynar, Solef 1015, Solef 6010)	NaOH soak, var C & t	α-3,6	B-2,3 H-3 I-3,7 N-3 V-3 W-3,6

Hajibabania et al., 2012, SepPurTech (Hajibabania et al., 2012)	Lab made PVDF HF (hydrophilic) UF	cycle NaOCl & artificial feed	γ-1,2,4,5,7 δ-2	B-2,7 C-2 D-1,2,4 I-3 L-2,4 O-2,4,5,7 S-4 V-3 J-6
Hanafi et al., 2014, EnvironSciTech (Hanafi et al., 2014)	PES/PVP UF/NF	NaOCl soak, var C &t , fix pH	α-5,7	
He et al., 2014, SepSciTech (He et al., 2014)	Zenon PVDF HF	Virgin membrane, various, fix C, vary t; 3-year operated membranes	γ-1 α-4	B-2 I-4 O-1
Jung et al., 2004, JmembSci (Jung et al., 2004)	PAN/PVP var MW UF	NaOCl soak to remove NaOCl	γ-4,5,6,7	
Keuken et al., 2016 WatSciTech	Sulfonated PES	operate in WTP, 1 year	not discussed	
Le-Clech, 2014, WRA (Le-Clech, 2014)	PVDF hollow fibre, flat sheet, various	NaOCl & other cleaning agent soak	not discussed	B-2 O-? S-4 J-6,7 V-? I-? H-?
Levitsky et al., 2011, JMembSci, (Levitsky et al., 2011)	PVDF and PES UF	pre-foul, NaOCl soak/vibrate, var t, pH 10	γ-2 δ-1	D-2 E-7 L-2 O-2
Levitsky et al., 2012, ChemEngSci (Levitsky et al., 2012)	PVDF and PES UF	pre-foul, NaOCl soak, other chemicals	δ-2	D-2
Liang, 2013, JEnvEng (Liang et al., 2013)	PVC HF	pre-foul, NaOCl soak, var C & t	γ-4	
Liang et al, 2015, DesalWatTreat (Liang et al., 2015)	PVC HF UF	pre-foul, NaOCl soak, Citric	γ-1,2,4	
Lu et al., 2011, IEEE (Lu et al., 2011)	PVC UF	Virgin membrane, NaOCl soak, var C & t; Fouling followed by ageing	γ-4	
Pellegrin et al., 2013, JMS (Pellegrin et al., 2013)	Commercial UF HF PES/PVP	NaOCl soak, Fix C, var t & pH	γ-4,5,7	
Pellegrin et al., 2015, JMS (Pellegrin et al., 2015a)	Commercial UF HF PES/PVP	NaOCl soak, Fix C & pH, var t, dextran filtration	γ-4,5	
Prulho et al., 2012, ProcEng (Prulho et al., 2012)	PES/PVP HF UF	NaOCl soak, fix C, var pH	not discussed	
Prulho et al., 2013, PolyDegStab (Prulho et al., 2013)	PES/PVP HF UF	NaOCl soak, Fix C, Var pH	not discussed	
Puspitasari et al., 2010, SepPurTech (Puspitasari et al., 2010)	flat sheet PVDF UF	pre-foul & NaOCl clean (4 cycles); soak NaOCl 0-18 weeks	γ-2,4,5	B-2 D-2 G-2 S-2,4 O-2
Qin et al., 2002, Desalination (Qin and Wong, 2002)	PSf/PVP UF	soak NaOCl 4000 ppm, up to 48 h	γ-4,5,7	

Qin et al., 2003, JMembSci (Qin et al., 2003)	Lab made CA/PVP UF HF	soak NaOCl, var t, fix C & pH	γ-4,5,7 δ-2	
Qin et al., 2004, SepPurTech (Qin et al., 2004)	Lab made PAN/PVP UF HF	soak NaOCl, var c, fix t & pH	γ-4,5,7 δ-2	
Qin et al., 2005, JAppPolySci (Qin et al., 2005a)	CA/PVP UF HF	soak NaOCl	γ-4,5,7 δ-2	
Qin et al., 2005, JMembSci (Qin et al., 2005b)	PES/PVP UF UF	soak NaOCl, fix C, t & pH	γ-4,5,7	
(Ravereau, 2016) JMembSci	PVDF hollow fibre (with & without additives)	soak in NaOCl, var pH	γ-?	B-2 P-7
Rouaix et al., 2006, JMembSci (Rouaix et al., 2006)	PSf/PVP HF and FS UF	soak in NaOCl, fix C, var t and pH	α-6	
Thominette et al., 2006, Desalination (Thominette et al., 2006)	PES UF	soak NaOCl, pH 8 for var t	not discussed	
Vanysacker et al., 2014, JMembSci (Vanysacker et al., 2014)	PVDF/PE/PES MF	soak in NaOCl and Citric Acid, Fix C & t, CEF and fouling	γ-? δ-?	C-? K-4,5 O-?
Wang et al., 2010, ChemEngJ (Wang et al., 2010)	PVDF flat sheet MF	MBR fouling, NaOCl cleaning cycles, Var C & t, CWF	γ-1 δ-?	B-2 C-? D-1,2 H-? I-? O-1 V-?
(Wang et al., 2018) AppSurfSci	PVDF	soak in NaOCl, var C, var t	γ-2,6 δ-2	D-2 E-6 I-7 O-2,6 V-7
Wolff and Zydney, 2004, JMembSci (Wolff and Zydney, 2004)	PSf/PVP HF UF	Fix C & t	γ-2,4,5	
(Wu, 2017) JEnvSci	PVDF (NIPS and TIPS)	soak in NaOCl, 5000 ppm, var t	γ-4,5	B-7 D-2 E-2 K-2 O-4,5
Yadav et al., 2009, PolyDegStab (Yadav et al., 2009)	PES UF	soak in NaOCl, fix C, var t & pH, whey protein separation	α-6	
Yadav and Morison, 2010, FoodBioprod (Yadav and Morison, 2010)	PES UF	soak NaOCl, var pH	γ-4,6 δ-?	
(Zhang 2017) SepPurTech	PES	soak NaOCl, fix C & pH, var t	γ-2,4 δ-2,4	
(Zhang 2017) WaterRes	PES and PVDF (both 30 kDa HF UF, MOTIMO)	soak NaOCl, fix C & pH, var t	γ-2,4,5 δ-2	B-? C-2,4,5 D-2 G-7 J-7 O-2 T-?
(Zhou 2017) EnvSciTech	PES/PVP	soak NaOCl, fix C, var pH, var t	γ-2,4 δ-2,4	
Zondervan et al., 2007, JMembSci (Zondervan et al., 2007)	PES UF	vary foulant, NaOCl concentration, back-pulse length/strength, mechanical stress	not discussed	

Table 9. Summary of information from Table 8. The number in each cell indicates the number of publications that make a particular link.

	1	2	3	4	5	6	7	?	
α		4	1	2	2	5	4		α
β								1	β
γ	4	10		17	14	4	9	1	γ
δ	1	5					1	1	δ
ε									ε
A								1	A
B		7	1				2		B
C		2					1	2	C
D	2	6		1					D
E							1		E
F									F
G		1							G
H			1					2	H
I			2	1			1	3	I
J						2	1		J
K				2	2				K
L		2		2	1				L
M									M
N			1						N
O	2	3		2	2		1	3	O
P							1		P
Q									Q
R									R
S		1		3					S
T									T
U					1				U
V			2					2	V
W			1			1			W
	1	2	3	4	5	6	7	?	

Appendix 2 - Storage Considerations for Natural Water

The following Appendix presents an independent project that was carried out prior to the dissertation work. These data were used to inform storage of water samples in the research projects presented in Chapters 4 and 5.

A2.1 Abstract

When storing and transporting water samples, the character of the natural organic matter should be preserved. This is particularly important when considering water treatment, as various components of raw water will affect treatment processes differently. For example, the biopolymer fraction of natural organic matter (NOM) contributes to membrane fouling. However, the impact of storage and transport conditions on the biopolymer content of water samples has not yet been characterized. In the present study, water samples with significant biopolymer fractions of NOM were stored at two temperatures: 4 °C and 20 °C. The recommendations from this work are twofold: 1) storage, transport or analysis of source water samples can proceed at 20 °C, provided that these procedures do not take longer than 2 days, though refrigeration is recommended where possible; 2) samples can be refrigerated prior to analysis for up to one month without repercussions for their biopolymer content.

A2.2 Introduction

Natural organic matter (NOM) is an important factor in water treatment processes. However, NOM is a mixture of many constituents, so the role of particular NOM fractions is important in predicting treatability of water. Membranes, for example, are increasingly being used in water treatment processes. Natural organic matter (NOM) has frequently been cited as a cause of membrane fouling (Jucker and Clark, 1994; Yuan and Zydney, 2000). Biopolymers have been established as a key indicator of fouling potential for low-pressure membranes (Kimura et al., 2014; Peldszus et al., 2011; Tian et al., 2013). In conventional treatment biopolymers will influence the efficacy of coagulation and flocculation processes. The NOM composition can also affect the biological stability of water, which impacts the microbial quality of water over time (Van Der Kooij, 1992).

In order to determine the applicability of treatment methods for a given water source researchers and consultants must profile the raw water's characteristics. This can involve raw water samples' shipment for analysis, storage in a research facility, or queueing for analysis. For example, SEC of NOM involves retention times of over an hour (Huber et al., 2011), so samples may be waiting at ambient lab temperature for prolonged periods. Thus, it is important to ensure that the characteristics of the water are retained from sample collection through to analysis.

Biopolymers are usually classified based on a molecular weight of over 10 kDa (Huber et al., 2011), and constitute the first fraction to elute during size exclusion chromatography (SEC). Low relative ultraviolet detection (UVD) response from the biopolymer peak of a chromatogram indicates that they are mainly unsaturated structures. Polysaccharides and

proteins are known to dominate the biopolymer composition in NOM (Flemming et al., 2007).

Although biopolymer content is a particularly important metric for water treatability, guidelines regarding sample handling for biopolymer analysis do not exist. Established methods are available for general handling of water samples (APHA, 2005; EPA, 1982) however, there is no indication that the character of the NOM (relative abundance of different constituents) has been considered in these protocols.

The objective of the present study was to establish storage guidelines which maintain the NOM characteristics of the raw water, as determined using size exclusion chromatography. The aim was to characterise two contrasting natural water sources, as a basis for understanding biopolymer storage behaviour. These were 1) water from an algae-impacted natural pond (Jericho Pond in Vancouver), and 2) secondary effluent from a wastewater treatment system (UBC Pilot Plant). These sources are expected to have contrasting degradation behaviour and biopolymer content; effluent organic matter (EfOM) is influenced by raw wastewater characteristics and microbial products generated during treatment, whereas pond water is influenced by terrestrial NOM and algae products. A synthetic water containing Suwanee River NOM (SRNOM) was also characterized. In contrast to the pond water and effluent, SRNOM is not expected to contain any biopolymers.

A2.3 Methods

Water samples were collected from Jericho Pond and the UBC activated sludge system effluent in late July. Both were diluted to achieve a concentration of approximately 5 ppm dissolved organic carbon (DOC). Suwanee River NOM (International Humic Substances

Society) water was prepared with Milli-Q water to 5 ppm DOC and run with each batch as a standard to ensure reproducibility.

All water samples were filtered (0.45 μm, cellulose) to remove particulates, and placed in clean, oven-dried, amber glass bottles for storage. Sample volume in each bottle was 1 L, with 1 L of headspace. Bottles were stored in dark, temperature-controlled facilities at 4 °C or 20 °C for 36 days. Each storage protocol was performed in duplicate. Note that the range of data in the presented in results corresponds to the maximum and minimum values obtained via two replicates.

Aliquots for analysis were collected from all bottles at the following time points: 0 h, 24 h, 48 h, 7 d, 14 d, and 36 d. The water sample aliquots were characterized using SEC with DOC and UV detection (SEC-DOC/UV). For SEC analysis, the method developed by Huber *et al.* (2011) was used. In brief, buffer (2.26 g $Na_2HPO_4 \cdot 7H_2O$, 2.5 g KH_2PO_4 per L Milli-Q water) was prepared and filtered (0.45 μm, cellulose). An HPLC (Waters 600 controller, Waters 717plus autosampler) with a size exclusion column (TOSCH Bioscience TSKgel HW-50S), UV detector (Waters 486), and DOC analyzer (Sievers 900 Turbo) with inorganic carbon removal were used. SEC injections were 1 mL with a buffer flow rate of 1 mL/minute and 100 minutes between injections.

Time-domain chromatograms collected by both UV and DOC detectors were transformed to log(molecular weight), i.e. log(MW), using PEG (600 to 6000 Da) and PSS (15 to 41 kDa) standards for mass calibration. The transformed chromatograms were separated into a biopolymer fraction and a lower MW DOC fraction for analysis of the fate of biopolymers. Based on PEG and PSS calibration, the biopolymer peak represented molecular weights of 20 kDa and higher. ProFit was used using event-based Gaussian peak fitting to de-

convolute the lower molecular weight peaks into four fractions, related to the sub-fractions (e.g. humics, fulvics, building blocks) identified by Huber *et al.* (2011).

A2.4 Results & Discussion

Preliminary chromatogram analysis revealed that the only fraction with a significant change during storage was biopolymers (Figure 32). For this reason, in the following discussion, only the biopolymer fraction is considered in isolation.

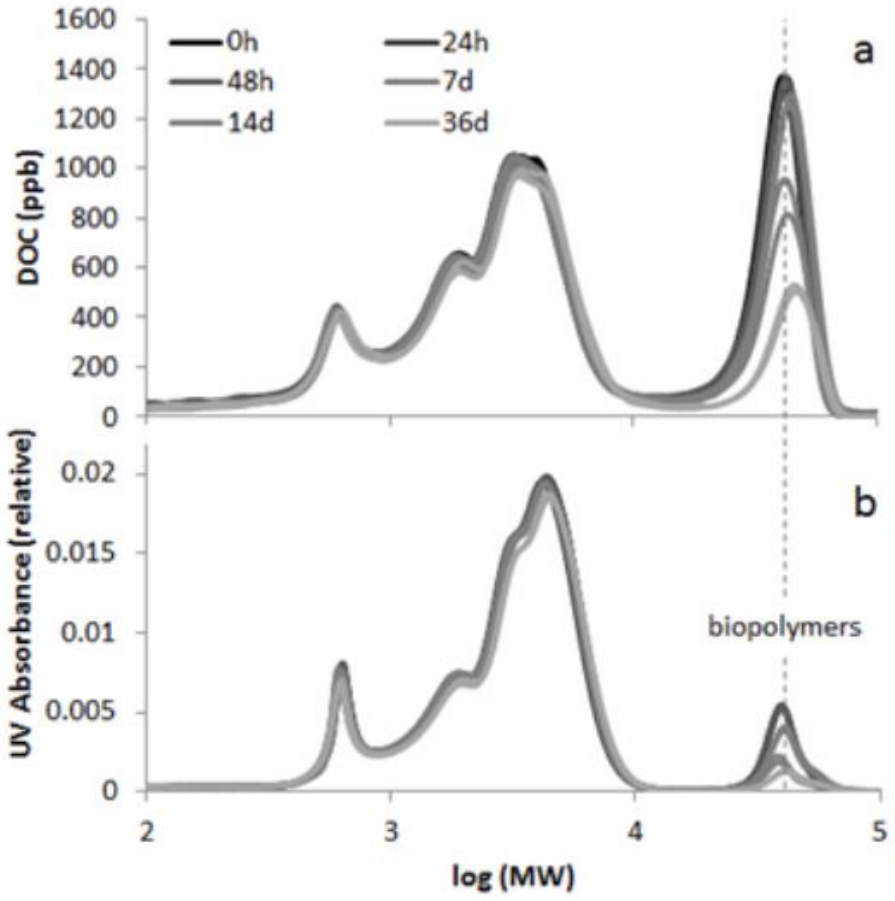

Figure 32. Typical SEC chromatograms for samples stored at 20 ℃.
a - organic carbon detector; b - UV detector.

The total DOC, and the biopolymer fraction are plotted in Figure 33 (a, b), normalized relative to the DOC concentration at sample collection. Within 7 days at 20 °C, the reduction in total DOC becomes significant for both waters considered. Furthermore, most

of the reduction in total organic content can be attributed to a decrease in the biopolymer fraction. The chromatograms suggest that the biopolymers are entirely mineralized, rather than broken down to smaller products, as the concentration of low molecular weight material remains constant. However, it is possible that some break-down products simply replace other low molecular weight material that is mineralized during storage. Within 36 days at 4 °C, the reduction in total organic content is not significant for either water considered. Similarly, there is no significant reduction in the biopolymer fraction at 4 °C.

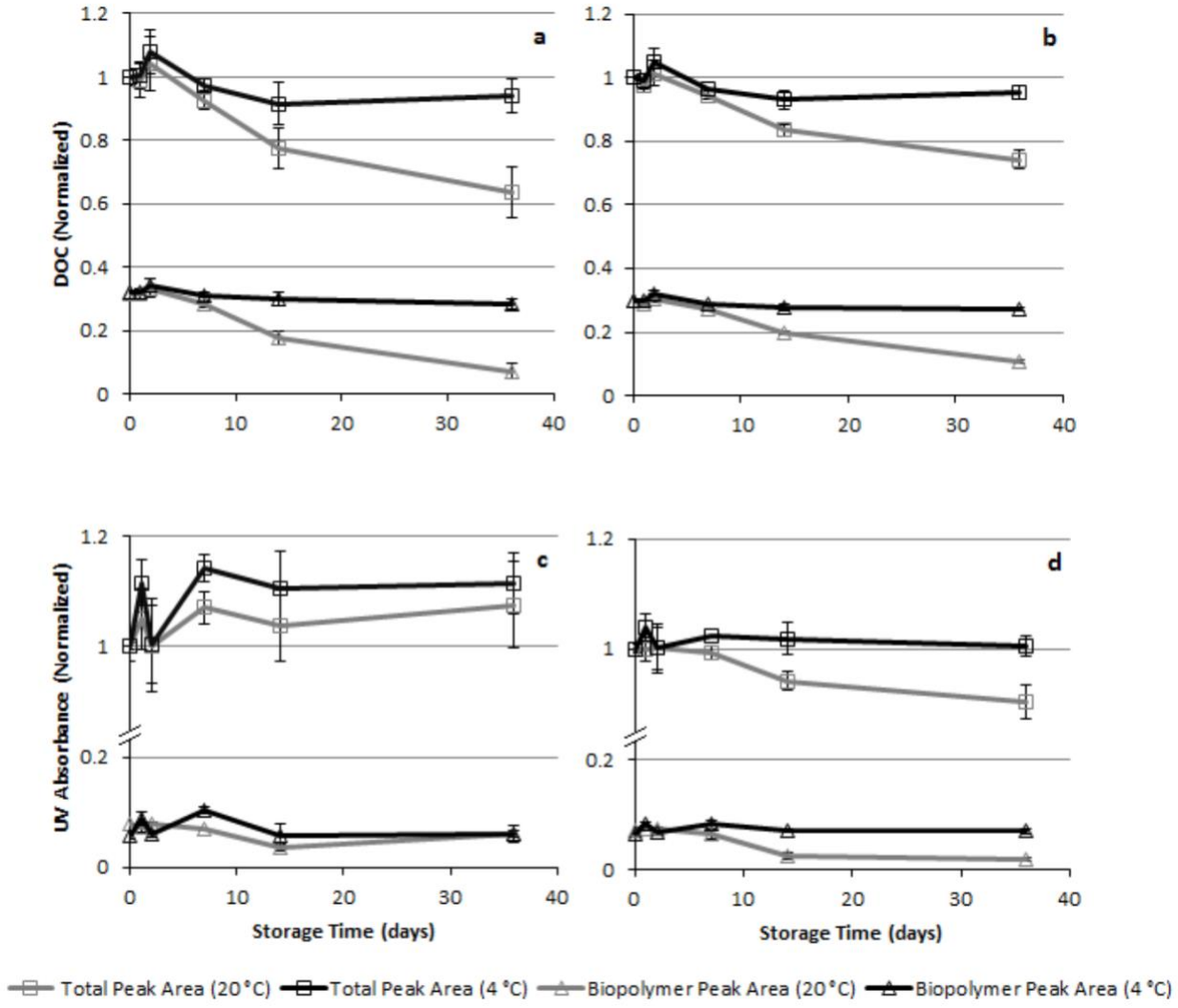

Figure 33. Changes in characteristics of water over time. Error bars correspond to maximum and minimum peak area. All peak areas are normalized relative to the total peak area for that sample/detector combination at time = 0 hours. (a, b - peaks integrated from organic carbon detector; c, d - peaks integrated from UV detector; a, c - pond water; b, d - effluent)

In contrast to the results obtained using the organic carbon detector, those obtained using UV absorbance suggest that the biopolymers are not degrading substantially at 20 °C for pond water. Thus, UV analysis is not an acceptable way to determine whether the biopolymer concentration - and therefore the DOC concentration - is changing with time. This is consistent with the biodegradation literature (Flemming et al., 2007). For effluent stored at 20 °C, a small reduction in UV absorbance was observed after 14 and 36 days (6% and 10%, respectively), most of which could be attributed to a significant decrease in the biopolymer fraction UV absorbance. No significant change in UV absorbance was observed for either water considered when stored at 4 °C.

Because the small change in UV absorbance of the Jericho Pond water stored at 20 °C is also reflected as variation in the biopolymer peak, it appears that the low molecular weight material is not degrading and being replaced by biopolymer breakdown products. The rationale is that biopolymer breakdown products would be much less UV-active than aromatic low molecular weight NOM components. Such a stark decrease in the low molecular weight UV absorbance is not observed.

No significant change in the characteristics of SRNOM was observed for any of the storage conditions considered and, as expected, no biopolymer peak was detected.

A2.5 Recommendations

When storing and transporting natural water, care should be taken to maintain the character of the natural organic matter present. This is of particular importance when studying treatability of raw water, as various components of source water will make different demands of treatment processes.

Based on two contrasting water sources - an algae-impacted pond, and wastewater treatment plant effluent - it was observed that room temperature (20 °C) for up to 2 days has negligible impact on the biopolymer content and general composition of source water. However, within a week at 20 °C, significant biopolymer degradation was observed for both model waters. Refrigeration (4 °C) minimized degradation of biopolymers, as well as degradation of overall DOC in both water samples. In addition, the UV absorbance profile for refrigerated samples was more stable than for water stored at 20 °C.

The recommendations from this work are twofold. Storage, transport or analysis of source water samples can proceed at 20 °C, provided that these procedures do not take longer than 2 days, though refrigeration is recommended where possible. Secondly, samples can be refrigerated prior to analysis for up to one month without repercussions for their biopolymer content. It is recommended that all samples should be stored in amber glass containers, which have been fired to remove any initial DOC contamination.

Appendix 3 - Full-Scale Ageing Project Methods (Extended)

This section is intended as a reference for future researchers studying membrane ageing.

A3.1 Sampling of Membranes at Full-Scale

In Chapter 4, membranes were collected from partner plants after recovery cleaning. The protocol provided to partners was as follows:

When to Sample

- Harvest fibres immediately following a chlorine recovery clean to ensure consistent sampling.
- If immediate harvesting is impossible (e.g. due to insufficient personnel), allow train to sit in treated water prior to sampling. Please avoid operating the train, as the resultant fouling will interfere with the ageing data.

Where to Sample

- Sample from **ten** ("1000" modules) or **six** ("500" modules) locations in a given module.
- Ideally, should sample as close to the centreline as possible, avoiding extreme ends.
- Collect fibres which have not been compromised or breached.

Example:

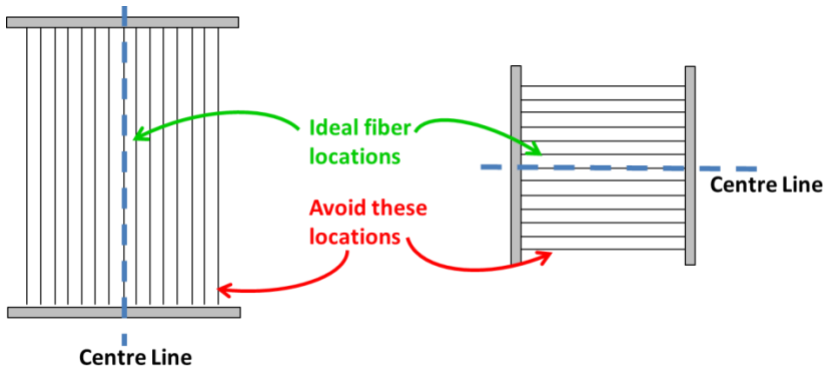

Figure 34. Ideal sampling locations from a monitored module.

How to Sample

- Perform a routine chlorine recovery clean on module(s) selected for sampling.
- Moisten lint-free towels with distilled water (clean water if DW unavailable) & place onto a clean tray.
- For "1000" modules, remove shroud from module (as per protocol provided by GE).
- Cut fibres to harvest at one end, carefully pull away from module, cut at other end.
    - for "1000" modules, cut **ten** full-length fibres (selected as above)
    - for "500" modules, cut **six** fibres (selected as above)
- Rinse fibres with distilled water (clean water if DW unavailable).
- Place fibres onto moist towels on tray, fold into towels and place in Ziploc bag.
- Indicate fibre identity & date on Ziploc bag, by labeling with Sharpie for example:
    1. plant location
    2. date
    3. train ID (T1, T2…); cassette ID (C1, C2…); module ID (e.g. serial number)
- Fill cuts from harvested fibers' residual holes with Loctite 3924 glue (as per protocol provided by GE).
- For "1000" modules, replace shroud (as per protocol provided by GE).
- Place Ziploc bag(s) into envelope provided, and courier, 1-2 days to UBC.

Example:

A3.2 Membrane Storage

Throughout the project, membranes were collected from 10 water treatment plants. Once received, the following steps were taken to store membranes:

- Remove kimwipe and rinse membranes thoroughly with distilled water
- Cut holes in Ziploc bag to allow soak in communal disinfectant bath
- Store Ziplocs in order collected by stringing top corners onto a cord inside the bath
- Store in fridge with other membranes, soaked in a ~2 to 5 ppm chlorine solution (updated bimonthly)

A3.3 Membrane Potting

Membranes were potted as miniature benchtop modules for performance testing. For each membrane sample, **two** modules were constructed.

- Cut 3-7 fibres (membrane-dependent) to 2 cm longer than required
- Cut potting tubing; 10 cm for 500's 3 cm for 1000's (¼" O.D. for 1000s; ¼" I.D. for 500's)
- Insert 'open' ends into long tubing and seal
- Test all individual fibres for flow using air into 'open' end; this ensures full surface area is active in filtration.
- Insert 'closed' end into tubing and seal module with 17 to 20 cm exposed (depending on fibre type). If not enough fibre, make a smaller module & note the size.
- Test module for leaks at 55kPa (8 psi)

A3.4 Assessment of Performance Factors for Full-Scale Aged Membranes

The following explains the logistics of performance testing for full-scale aged membranes.

Day 1

- Build membrane modules (see A3.3).
- Allow epoxy to harden overnight, keeping modules moist.

Day 2

- Fill each of the 5 buckets with 10 L of tap water to de-gas and temperature-adjust overnight
- Prepare NaOH and HCl solutions for pH adjustment
- Check membrane modules for leaks at 55 kPa (8 psi)
- Install membrane modules into 12 ports
- Run membranes a bit (use program but play with plugs to get feed vs hypo flow)
    - Run membranes forward for ~10-15 minutes with tap water
    - Run membranes in reverse for ~5 mins (via hypo tanks) with tap water
    - Run membranes forward for ~5 minutes (via hypo tanks, switching pumps, switch back at the end) with tap water
- Drain reactors
- Pour 500 ppm, pH 10 NaOCl into reactors for overnight soak

Day 3

- Permeate membranes forward for 15 minutes with hypo (in reactors overnight), adjusting flow rate to 2.5 mL/min average flow (10 mL/min per setup).

- Backwash membranes for 5 minutes (from BW tanks)
- Replace NaOCl in reactors with distilled water
- Note the **temperature** of water in tanks
- Permeate membranes for 30 minutes with distilled water, measuring flow by mass in graduated cylinders.
- Prepare fouling solution in foulant tanks and begin performance testing (schematic in Figure 35, timer programming in Table 10 and Table 11).
- Mix NaOCl into water backwash tanks after 2 hydraulic cleans.
- Replace the NaOCl backwash solution with tap water following final NaOCl clean, rinsing lines.
- Record mass flow rate for 12 systems during clean water flux tests (first and final), by mass collected, as well as periodically during the performance test experiment.
- Record mass flow rate of backwash solution periodically. This can be a handy way to change the backwash tank solution during a backwash.
- Save 2 L of the NaOCl solution for the overnight soak (prior to the other clean water flux tests).
- Following all cycled performance testing, drain all tanks & fill feed/backwash with tap water.
- Fill 3 membrane tanks with reserved NaOCl solution to soak overnight

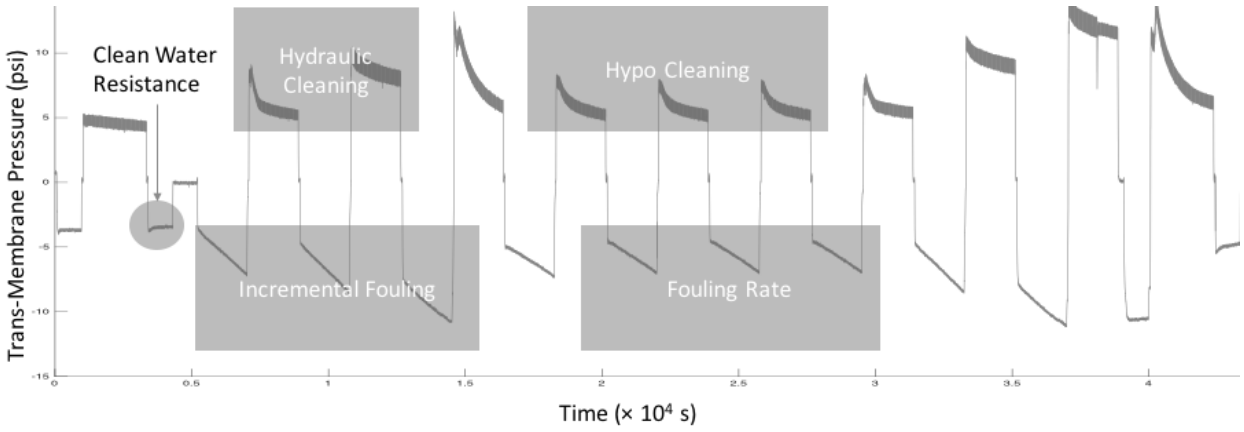

Figure 35. Illustration of cycle types used for full-scale membrane performance testing. The incremental fouling had very low reproducibility, so the fouling and cleaning data from NaOCl cleaning cycles were analyzed.

Table 10. Timer allocation for performance setup used to test both full-scale and bench-scale aged membranes.

Timer	**ON**	**OFF**
T1 (on/off)	valve V1 open (ctrl by L1)	valve V1 closed (autonomous)
T2 (on/off)	valve V2 open (ctrl by L2 = L1)	valve V2 closed (autonomous)
T3 (on/off)	valve V3 open	valve V3 closed
T4 (on/off)	pump 4 on	pump 4 off
T5 (on/off)	pump 5 on	pump 5 off

Table 11. Timer programming for performance testing of full-scale aged membranes.

Time Point:	**Timer ID:**					**Initiates Action:**	**Step Duration (default):**
	T1	**T2**	**T3**	**T4**	**T5**		
1	on	off	off	off	off	fill reactor with feed	0.5 minutes
2	on	off	off	on	off	permeate through membranes	40 minutes
3	off	off	off	off	on	backwash with water	10 minutes
4	off	off	on	off	off	drain foulant	0.5 minutes
5	off	on	off	off	off	fill reactor with hypo	0.5 minutes
6	off	off	off	off	off	soak with hypo	10/20/40 min
7	off	off	on	off	off	drain hypo	0.5 minutes
8 = 1	on	off	off	off	off	fill reactor with feed	0.5 minutes

Day 4

- Permeate membranes forward for 15 minutes with hypo (in reactors overnight)
- Backwash membranes for 5 minutes (from BW tanks)

- Replace NaOCl in reactors with distilled water
- Note **temperature** of water in tanks
- Permeate membranes for 30 minutes with distilled water, measuring flow by mass in graduated cylinders.

A3.5 Performance Data Analysis

The following shows typical MATLAB-processed output from 12 test modules during "Day 3" of performance testing. Note both incremental fouling (hydraulic cleaning) and repeatable fouling (NaOCl cleaning) are included. Only cycles with NaOCl cleaning were presented in the dissertation because hydraulic cleaning cycles were not sufficiently reproducible.

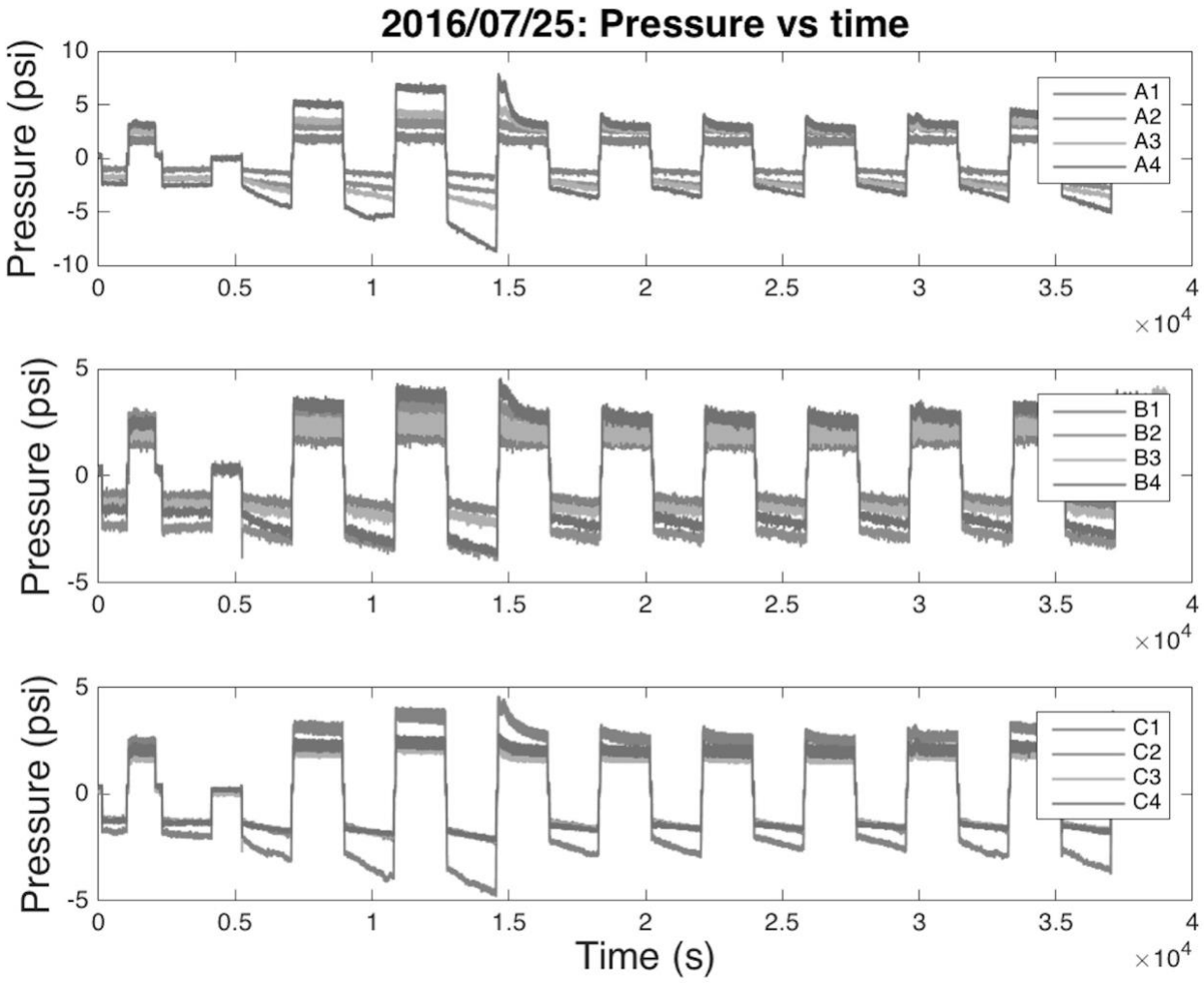

Figure 36. Example MATLAB output plots for performance testing of full-scale aged membranes.

A3.6 ATR-FTIR Analysis

The following shows typical ATR-FTIR spectra for 1000A and 1000B membranes.

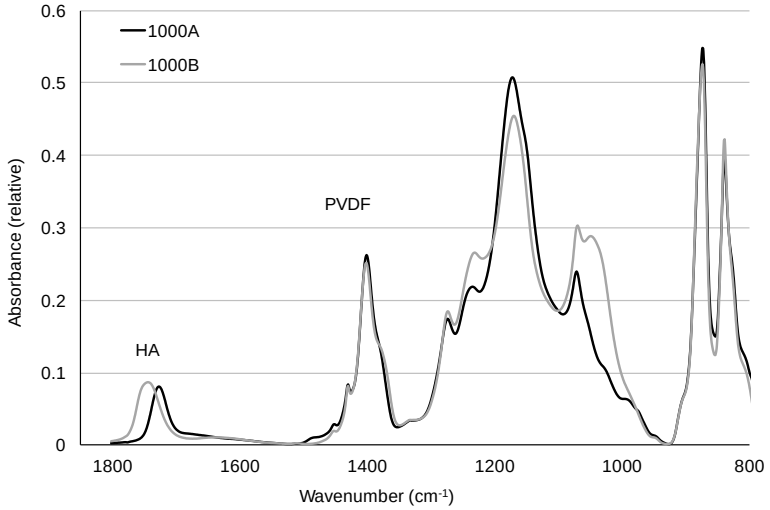

Figure 37. Example ATR-FTIR spectra for representative, full-scale aged 1000A and 1000B membranes. Note the shared PVDF peak, but slightly different additive peaks, resulting from different carbonyl stretching modes for the A and B additives.

A3.6.1 ATR-FTIR Sample Preparation

- Set oven to 50 °C (do so well in advance to ensure set-point is correct)
- Cut clean membrane fibre coupons out of test modules.
- Place fibres into clean, labeled 15 mL centrifuge tubes, reserving caps

A3.6.2 ATR-FTIR Instrumental Protocol

- Collect 1.5 L of N_2 (lq) from Chemistry Store
    - store is in Chemistry C-wing; dispensing station is in D-wing
- Instrument is located in Room 4351 of the Life Sciences Centre
    - contact the hub manager in advance & sign in at reception for access

- Pour N_2 (lq) into designated port using the funnel provided, lifting the funnel as you pour to allow the liquid to flow freely. Stop pouring when the port begins to overflow.
- Install ATR accessory to Thermo-Nicolet Nexus 670 FT-IR Raman spectrometer
    - Use black accordion-style cuffs to restrict airflow around the beam
    - Attach a dry air hose to one of the instrument ports to purge the instrument
- Clean the ATR accessory diamond window and pressure-tip thoroughly using a methanol-soaked kimwipe
- Open Omnic software and input experimental setup as follows:
    - Collect: 32 scans, 2 cm^{-1} res, absorbance mode, bkgd every 300 minutes
    - Bench: Main, MCT-A, KBr, IR, ATR, diamond, 4000-650 cm^{-1}, gain 1, OV 1.26, aperture 23
    - Diagnostic: reset bench & align
    - You may need to adjust the aperture on the "Bench" tab if the detector is saturated.
- Close experimental setup and collect a background spectrum (allow instrument to purge and cool for ~30 minutes first).
- Save the background spectrum.
- Re-open experimental setup, selecting the collected background spectrum from file.
- To run a blank, secure the pressure tip onto the diamond window but DO NOT tighten the tip.
- To run a sample:
    - lay membrane fibre front-to-back along centre of window

    - carefully lower pressure tip onto sample and lock arm in place
    - tighten pressure tip using black knob; it is designed not to overtighten
    - run spectrum
    - loosen pressure tip using black knob
    - lift arm off sample; membrane should be flattened in the centre
- Blanks should be run every few, depending on consistency. Background should be re-run if blanks become inconsistent.

A3.6.3 ATR-FTIR Data Processing

In Omnic Software:

- Auto-correct baseline between 780 cm^{-1} and 1810 cm^{-1} (see Figure 37 for example of a spectrum baseline-corrected to this range).
- Subtract an adjacent blank if the spectrum shows evidence of blank migration.
- Save spectra as CSV files for export to Microsoft Excel.

In Excel:

- integrate HA and PVDF peaks over the regions shown in Figure 37
- further baseline-correction was not applied, as corrected peak areas correlated almost exactly with uncorrected peak areas.
- report HA:PVDF peak ratio to quantify relative HA content.

A3.7 NMR Analysis

The following shows typical ^{1}H-NMR spectra for 1000A and 1000B membranes.

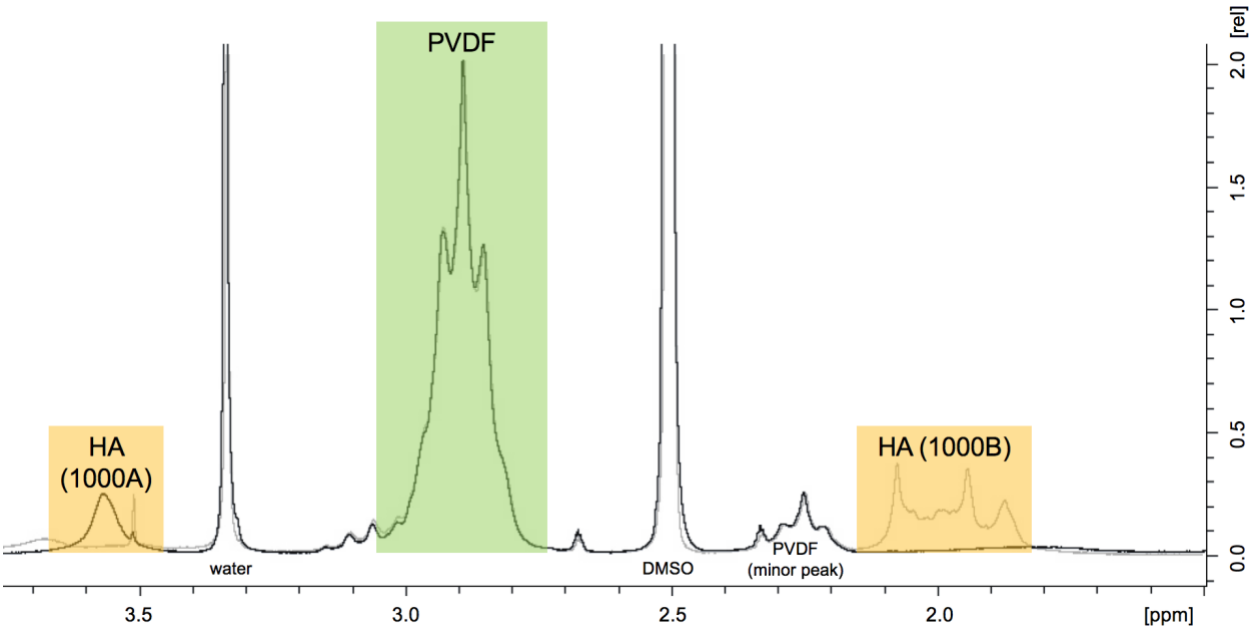

Figure 38 Example ^{1}H-NMR spectra for 1000A and 1000B membranes, 400 MHz, DMSO-d_6. Composition was normalized to the area of the major PVDF peak.

A3.7.1 NMR Sample Preparation

- Dry fibres as described in Appendix 3.6.1
- Membrane: 1.2 cm of 500 = 4 mg
    - 2.2 cm of 1000A = 4 mg
    - 3 cm of 1000B = 4 mg
- Solvent: Deuterated DMSO, 0.7 mL
- Add membrane and solvent to 7”, 400 MHz NMR tube
- Invert several times so that membrane is submerged
- Place tube in beaker of warm (40-50 °C) water - not too hot as it could damage tube
- Sonicate beaker/tube 15 minutes, shaking and inverting tube occasionally
- Inspect visually to ensure that the membrane has dissolved.

- Wipe tube down with Kim-Wipe & isopropanol prior to NMR analysis

A3.7.2 NMR Instrumental Operation

Samples were run on a 400 MHz Bruker NMR Spectrometer (UBC Pharmaceutical Sciences). The contacts in this endeavour were Sonia Lin (NMR coordinator) and David Grierson (PI in charge of NMR).

^{1}H Spectra were performed using default instrumental settings with 128 scans (default is 16) to improve signal-to-noise ratio.

A3.7.3 NMR Data Processing

^{1}H NMR spectra were processed using "Topspin" software with a free academic license. ^{19}F Spectra were also collected but the results were not reported. The software protocol is as follows:

- Calibrate to DMSO pentet at 2.50 (enter 'cal' and pick peak)
- Perform 0-order and 1-order phase correction so major peaks are symmetrical. (water and DMSO)
- Remove automatic integrals (in process>integrate)
- Integrate peaks of interest (Table 12)
- Do NOT correct for bias or slope of integral (leave defaults, fix later if needed)
- Calibrate to triplet at 2.25 ppm = 1 (actually 2 PVDF protons, split into triplet by F)
- pick peaks for all integrated peaks (ignore satellite peaks from DMSO)

Table 12. Typical 1H-NMR spectrum peak assignments (e.g. sample hA2, 1000B).

Peak Location	Type	Assignment	Integral
3.34	s	water	2.11
2.89	p	PVDF	1.00
2.67	p	DMSO satellite	0.0122
2.5	p	DMSO	0.76
2.24	t	PVDF' + DMSO sat	0.097
1.95	m	HA	0.242

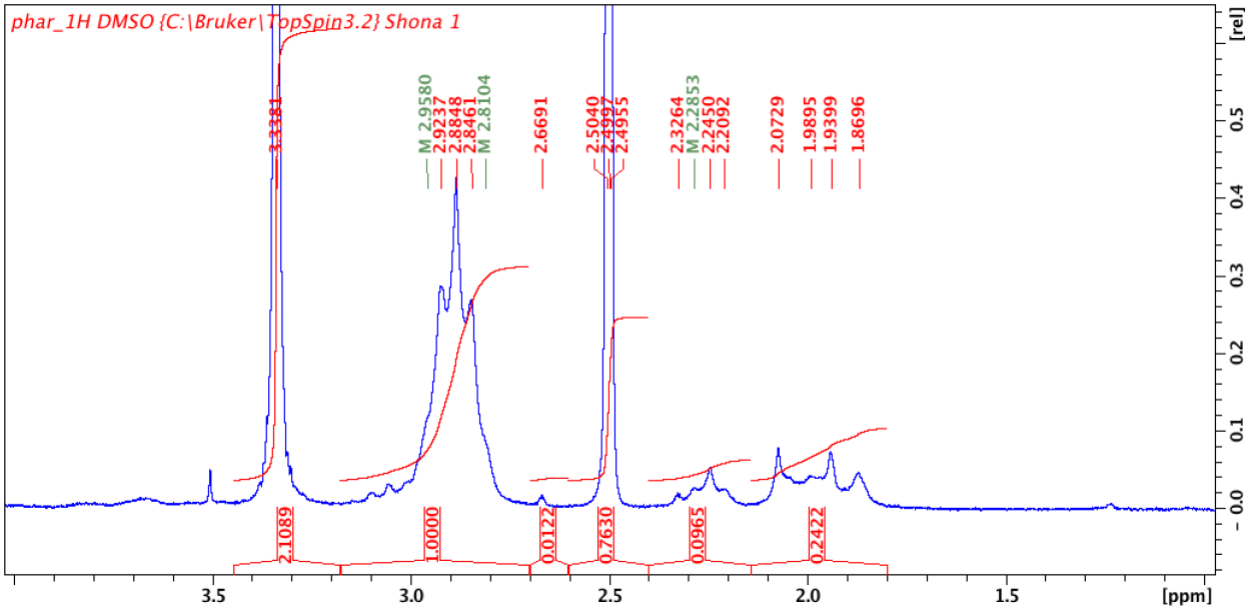

Figure 39. Typical 1H-NMR Spectrum during processing in Topspin (e.g. sample hA2, 1000B).

A3.8 Tensile Testing

The following shows typical stress-strain curves from tensile testing of membranes.

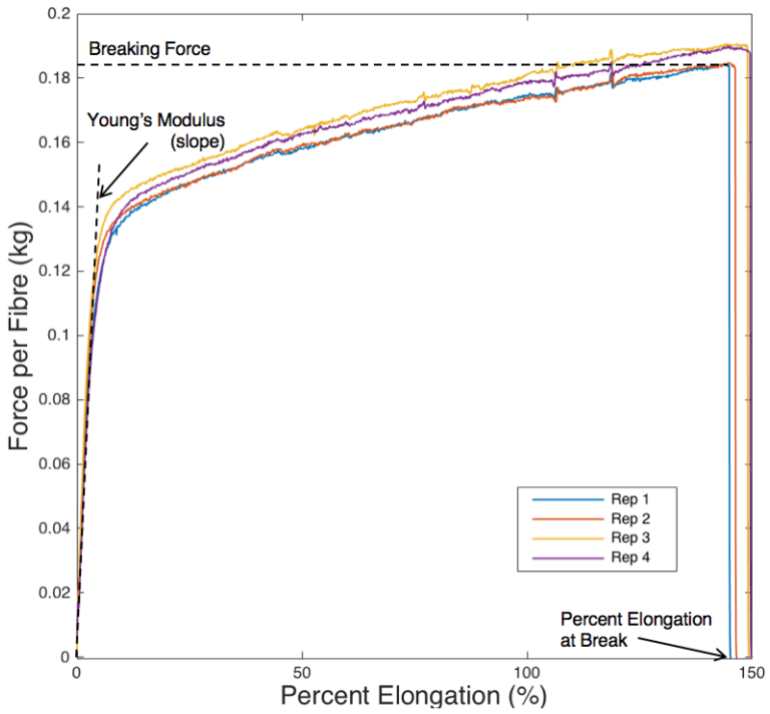

Figure 40. Interpretation of sample stress-strain curves. Breaking force is proportional to maximum stress; Young's modulus surrogate was interpolated from the initial slope; percent elongation at break is proportional to ultimate strain.

A3.8.1 Tensile Sample Preparation

- Print out sheets of sample holders templates as shown in Figure 41. Letter-size paper can fit about 7 rows.

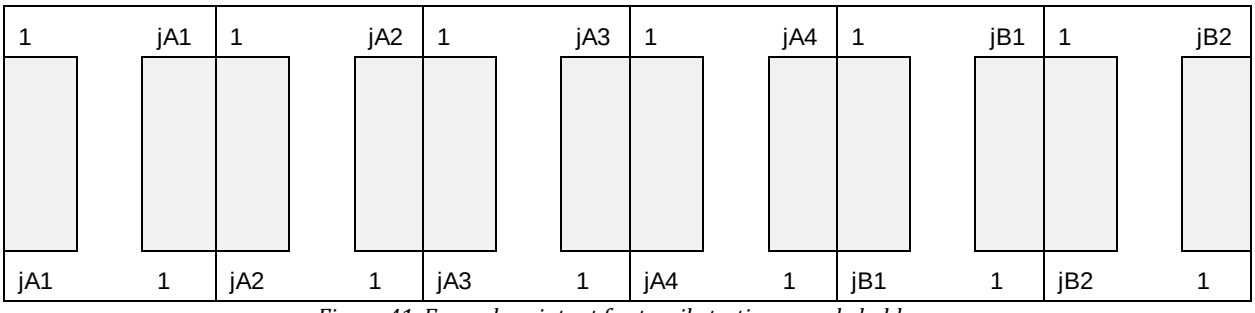

Figure 41. Example printout for tensile testing sample holders.

- Cut sheets into vertical strips between sample holders
- Trim away grey sections

- Pre-fold sample holder strips along midline, as illustrated in Figure 42.
- Tape dried membrane fibres into holders, as depicted.

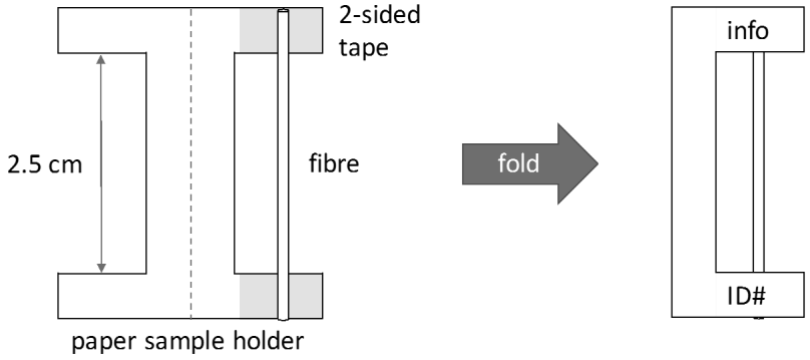

Figure 42. Sample holder preparation for tensile testing.

A3.8.2 Tensile Instrumental Protocol

- KES-G1 multi-purpose tensile tester is located in the Ampel building (Prof. Frank Ko's lab). Arrange to use it in advance.
- Set instrument sensitivity to 1x10.
- Set initial X-length to 2.54 cm.
- Use pressure transducer "B", (i.e. 5 kg)
- Use either 0.2 mm/s (>100% elongation expected), or 1.0 mm/s (100% elongation expected).
- Perform a test-run without a membrane in place to calibrate elongation speed.
- Clasp sample into load cell and trim away part of the holder backbone, as illustrated in Figure 43.
- Begin recording data in LabVIEW software application.
- Press "SINGLE" to start tensile test.
- Press "STOP" once fibre breaks.

- Stop recording in software.
- Press “RES” to return the sample holder to its initial position.

Figure 43. Tensile testing sample configuration: before, during, and after a test.

A3.8.3 Tensile Data Import & Processing

The following MATLAB code was used to import tensile data:

```
%% Import data from text file.
% Script for importing data from lvm files  in a specified folder:
%    /Users/shonajrobinson/Documents/Tensile Data/**sample ID**-1.lvm
%    /Users/shonajrobinson/Documents/Tensile Data/**sample ID**-2.lvm
%    /Users/shonajrobinson/Documents/Tensile Data/**sample ID**-3.lvm
%    /Users/shonajrobinson/Documents/Tensile Data/**sample ID**-4.lvm
%% Create a string for the requested filenames
prompt='What is the sample name? (e.g. aA1)  ';
samplename=input(prompt);
s1='/Users/shonajrobinson/Documents/Tensile Data/';
s2=samplename;
s3='-1.lvm';
filename = strcat(s1,s2,s3);

%% Identifies tab delimiter and starts in row 25
delimiter = '\t';
startRow = 24;

%% Format string for each line of text:
%   column2: text (%s)
% For more information, see the TEXTSCAN documentation.
formatSpec = '%*s%f%*s%[^\n\r]';

%% Open the text file.
fileID = fopen(filename,'r');

%% Read columns of data according to format string.
```

```
% This call is based on the structure of the file used to generate this
% code. If an error occurs for a different file, try regenerating the code
% from the Import Tool.
dataArray = textscan(fileID, formatSpec, 'Delimiter', delimiter, 'EmptyValue' ,NaN,'HeaderLines'
,startRow-1, 'ReturnOnError', false);

%% Close the text file.
fclose(fileID);

%% Post processing for unimportable data.
% No unimportable data rules were applied during the import, so no post
% processing code is included. To generate code which works for
% unimportable data, select unimportable cells in a file and regenerate the
% script.

%% Allocate imported array to column variable names
rep1 = dataArray{:, 1};

%% Repeat for Rep 2
s3='-2.lvm';
filename = strcat(s1,s2,s3);
delimiter = '\t';
startRow = 24;
formatSpec = '%*s%f%*s%[^\n\r]';
fileID = fopen(filename,'r');
dataArray = textscan(fileID, formatSpec, 'Delimiter', delimiter, 'EmptyValue' ,NaN,'HeaderLines'
,startRow-1, 'ReturnOnError', false);
fclose(fileID);
rep2 = dataArray{:, 1};
%% Repeat for Rep 3
s3='-3.lvm';
filename = strcat(s1,s2,s3);
delimiter = '\t';
startRow = 24;
formatSpec = '%*s%f%*s%[^\n\r]';
fileID = fopen(filename,'r');
dataArray = textscan(fileID, formatSpec, 'Delimiter', delimiter, 'EmptyValue' ,NaN,'HeaderLines'
,startRow-1, 'ReturnOnError', false);
fclose(fileID);
rep3 = dataArray{:, 1};
%% Repeat for Rep 4
s3='-4.lvm';
filename = strcat(s1,s2,s3);
delimiter = '\t';
startRow = 24;
formatSpec = '%*s%f%*s%[^\n\r]';
fileID = fopen(filename,'r');
dataArray = textscan(fileID, formatSpec, 'Delimiter', delimiter, 'EmptyValue' ,NaN,'HeaderLines'
,startRow-1, 'ReturnOnError', false);
fclose(fileID);
rep4 = dataArray{:, 1};

%% make  4 correctly named vectors
eval([strcat(samplename,'_1') '=rep1;']);
eval([strcat(samplename,'_2') '=rep2;']);
eval([strcat(samplename,'_3') '=rep3;']);
eval([strcat(samplename,'_4') '=rep4;']);
%% Clear temporary variables
clearvars prompt filename delimiter startRow formatSpec fileID dataArray ans s1 s2 s3;
```

The following MATLAB code was used to process imported tensile data:

```
% %% keep the original data in order to check the output against something
% rep1=cC2_1;
% rep2=cC2_2;
% rep3=cC2_3;
% rep4=cC2_4;

%% baseline-correct sample 1 and dump the prior data
%this is pretty brute force; assumes break is fast
 drop = find(diff(rep1) < -.3, 1, 'first');    %finds when the fibre broke, need to correct for a
general variable name
 baseline = mean(rep1(drop+10:drop+60));       %finds the average value 10 to 60 cells after the drop
 rep1 = rep1 - baseline;                      %baseline corrects the data
 rep1 = rep1(1:drop+5);                      %gets rid of cells more than 5 data after the break

 %% identify where the curve begins and dump the prior data
%this is a bit brute force; it would be better to extrapolate the curve down
 %[~,min_ind] = min(rep1);             %finds min value and location
 %rep1 = rep1(min_ind:drop+5);

  %% identify where the curve begins and dump the prior data
%this is a bit brute force; it would be better to extrapolate the curve down
 b=find(rep1>0.25,1,'first');
 c=find(rep1>0.50,1,'first');
 a=2*b-c;
 rep1 = rep1(a:drop+5);

%% do the same thing for the other 3 samples
 drop = find(diff(rep2) < -.3, 1, 'first');
 baseline = mean(rep2(drop+10:drop+60));
 rep2 = rep2 - baseline;
 rep2 = rep2(1:drop+5);
 %[~,min_ind] = min(rep2);
 %rep2 = rep2(min_ind:drop+5);
 b=find(rep2>0.25,1,'first');
 c=find(rep2>0.50,1,'first');
 a=2*b-c;
 rep2 = rep2(a:drop+5);

 drop = find(diff(rep3) < -.3, 1, 'first');
 baseline = mean(rep3(drop+10:drop+60));
 rep3 = rep3 - baseline;
 rep3 = rep3(1:drop+5);
 %[~,min_ind] = min(rep3);
 %rep3 = rep3(min_ind:drop+5);
 b=find(rep3>0.25,1,'first');
 c=find(rep3>0.50,1,'first');
 a=2*b-c;
 rep3 = rep3(a:drop+5);

 drop = find(diff(rep4) < -.3, 1, 'first');
 baseline = mean(rep4(drop+10:drop+60));
 rep4 = rep4 - baseline;
 rep4 = rep4(1:drop+5);
 %[~,min_ind] = min(rep4);
 %rep4 = rep4(min_ind:drop+5);
 b=find(rep4>0.25,1,'first');
 c=find(rep4>0.50,1,'first');
 a=2*b-c;
 rep4 = rep4(a:drop+5);

 clearvars drop min_ind baseline

%% input the sensitivity (y) and speed (x) for all 4 samples
prompt='What are the sensitivity and speed for the samples? (e.g. [1*10;0.2] OR 2-by-4 mat)  ';
calib_vals=input(prompt);
if size(calib_vals)==[2,1]
    calib_vals=[calib_vals,calib_vals,calib_vals,calib_vals];
else calib_vals=calib_vals;
end
clearvars prompt

%% scale the y-values from V to kg for all 4 matrices
```

```
rep1=rep1/calib_vals(1,1);
rep2=rep2/calib_vals(1,2);
rep3=rep3/calib_vals(1,3);
rep4=rep4/calib_vals(1,4);

%% adjust x-increments to equal 0.016% strain (i.e. 0.2mm/s / 50 Hz / 25 mm = 0.016%)
if calib_vals(2,1)==0.2
    rep1=rep1;
elseif calib_vals(2,1)==1
    explode=[];
    while length(rep1) > 1
    inc=0.2*(rep1(2,1)-rep1(1,1));                                  %gives the incremental for 5-point
extrapolation
    explode=[explode;rep1(1,1);rep1(1,1)+inc;rep1(1,1)+2*inc;rep1(1,1)+3*inc;rep1(1,1)+4*inc];
    rep1=rep1(2:length(rep1));
    end
    rep1=explode;
clearvars explode
else display 'The speed for rep_1 was neither 0.2 or 1 mm/s. Re-code or fix manually!'
end

if calib_vals(2,2)==0.2
    rep2=rep2;
elseif calib_vals(2,2)==1
    explode=[];
    while length(rep2) > 1
    inc=0.2*(rep2(2,1)-rep2(1,1));
    explode=[explode;rep2(1,1);rep2(1,1)+inc;rep2(1,1)+2*inc;rep2(1,1)+3*inc;rep2(1,1)+4*inc];
    rep2=rep2(2:length(rep2));
    end
    rep2=explode;
clearvars explode
else display 'The speed for rep_2 was neither 0.2 or 1 mm/s. Re-code or fix manually!'
end

if calib_vals(2,3)==0.2
    rep3=rep3;
elseif calib_vals(2,3)==1
    explode=[];
    while length(rep3) > 1
    inc=0.2*(rep3(2,1)-rep3(1,1));
    explode=[explode;rep3(1,1);rep3(1,1)+inc;rep3(1,1)+2*inc;rep3(1,1)+3*inc;rep3(1,1)+4*inc];
    rep3=rep3(2:length(rep3));
    end
    rep3=explode;
clearvars explode
else display 'The speed for rep_3 was neither 0.2 or 1 mm/s. Re-code or fix manually!'
end

if calib_vals(2,4)==0.2
    rep4=rep4;
elseif calib_vals(2,4)==1
    explode=[];
    while length(rep4) > 1
    inc=0.2*(rep4(2,1)-rep4(1,1));
    explode=[explode;rep4(1,1);rep4(1,1)+inc;rep4(1,1)+2*inc;rep4(1,1)+3*inc;rep4(1,1)+4*inc];
    rep4=rep4(2:length(rep4));
    end
    rep4=explode;
clearvars explode inc
else display 'The speed for rep_4 was neither 0.2 or 1 mm/s. Re-code or fix manually!'
end

%% concatenate all the data
cat_mat = rep1;        %cat_mat and cat_vec are the matrix and vector to concatenate
cat_vec = rep2;

l_mat = size(cat_mat,1);                        %figure out whether matrix or new vector is longer
l_vec = size(cat_vec,1);
l_max = max(l_mat,l_vec);

l_mat_fix = (l_max)-(l_mat);                     %create NaN cells to append to matrix if shorter
l_mat_app = NaN(l_mat_fix,size(cat_mat,2));
cat_mat = vertcat(cat_mat,l_mat_app);

l_vec_fix = (l_max)-(l_vec);                     %create NaN cells to append to vector if shorter
```

```
l_vec_app = NaN(l_vec_fix,1);
cat_vec = vertcat(cat_vec,l_vec_app);

cat_mat=horzcat(cat_mat,cat_vec);               %concatenates matrix and vector
%% Do it again for rep 3
cat_vec = rep3;

l_mat = size(cat_mat,1);                       %figure out whether matrix or new vector is longer
l_vec = size(cat_vec,1);
l_max = max(l_mat,l_vec);

l_mat_fix = (l_max)-(l_mat);                    %create NaN cells to append to matrix if shorter
l_mat_app = NaN(l_mat_fix,size(cat_mat,2));
cat_mat = vertcat(cat_mat,l_mat_app);

l_vec_fix = (l_max)-(l_vec);                    %create NaN cells to append to vector if shorter
l_vec_app = NaN(l_vec_fix,1);
cat_vec = vertcat(cat_vec,l_vec_app);

cat_mat=horzcat(cat_mat,cat_vec);               %concatenates matrix and vector
%% Do it again for rep 4
cat_vec = rep4;

l_mat = size(cat_mat,1);                       %figure out whether matrix or new vector is longer
l_vec = size(cat_vec,1);
l_max = max(l_mat,l_vec);

l_mat_fix = (l_max)-(l_mat);                    %create NaN cells to append to matrix if shorter
l_mat_app = NaN(l_mat_fix,size(cat_mat,2));
cat_mat = vertcat(cat_mat,l_mat_app);

l_vec_fix = (l_max)-(l_vec);                    %create NaN cells to append to vector if shorter
l_vec_app = NaN(l_vec_fix,1);
cat_vec = vertcat(cat_vec,l_vec_app);

cat_mat=horzcat(cat_mat,cat_vec);               %concatenates matrix and vector
%% Set x axis
percent_elong = (0.016:0.016:length(cat_mat)*.016)';
%% put the x axis onto the big old matrix
copy_mat=horzcat(percent_elong,cat_mat);               %concatenates matrix and vector
%% rename the matrix with the sample name & get rid of temp vars
eval([strcat(samplename,'_matrix') '=cat_mat;']);
clearvars l_mat l_vec l_max l_mat_fix l_mat_app l_vec_fix l_vec_app cat_vec cat_mat rep_1 rep_2 rep_3
rep_4 calib_vals

%% Plot 'force (kg)' versus 'percent elongation'
figure;
plot(percent_elong,eval(strcat(samplename,'_matrix')),'LineWidth',1);
xlabel('Percent Elongation (%)','FontSize',16);
ylabel('Force per Fibre (kg)','FontSize',16);
titletext=strcat(samplename,': Stress-Strain Curve');
title(titletext,'FontSize',16);
legend('Rep 1','Rep 2','Rep 3','Rep 4');

%%

%% Save the plot as a .fig, in the MATLAB figures folder
savefig(strcat('/Users/shonajrobinson/Documents/MATLAB/tensile/figures/',samplename,'.fig'));
clearvars titletext

%% Save the compiled matrix to a new data file
% the * is a wildcard, so the coding was easier than matching samplename
save(strcat('/Users/shonajrobinson/Documents/MATLAB/tensile/',samplename),'percent_elong','*_matrix','s
amplename');
```

A3.9 Ageing of Membranes in the Lab

For cycled bench-scale testing of membranes, the following programs were uses for Setups A, B, and C (Table 13, Table 14, and

Table 15). Timer descriptions were given in Table 10. Note that filling begins 5 s before draining ends, which allows the membrane tanks to be flushed slightly, as well as helping to reduce plugging of the drain valve.

Table 13. Timer programming for cycled operational scheme A.

Timer ID:					**Initiates Action:**	**Step Duration:**	**Start**	**End**
T1	**T2**	**T3**	**T4**	**T5**			(s)	(s)
on	off	off	off	off	fill reactor with feed 1.0	0.5 minutes -5	0	30
on	off	off	on	off	permeate feed	30 minutes	30	1830
off	off	off	off	on	backwash with water	10 minutes	1830	2430
off	off	on	off	off	drain feed	0.5 minutes	2430	2460
off	on	off	off	off	fill reactor with hypo	0.5 minutes -5	2455	2490
off	off	off	off	off	soak with hypo	40 min	2490	4890
off	off	on	off	off	drain all reactors	0.5 minutes	4890	4920
on	off	on	off	off	fill with feed during drain	5 s	4915	4920
on	off	off	off	off	fill reactor with feed 1.0	0.5 minutes -5	0	30

Table 14. Timer programming for cycled operational scheme B.

Timer ID:					**Initiates Action:**	**Step Duration:**	**Start**	**End**
T1	**T2**	**T3**	**T4**	**T5**			(s)	(s)
on	off	off	off	off	fill reactor with feed 1.0	0.5 minutes -5	0	30
on	off	off	on	off	permeate feed	30 minutes	30	1830
off	off	off	off	on	backwash with water	10 minutes	1830	2430
off	off	on	off	off	drain feed	0.5 minutes	2430	2460
on	off	off	off	off	fill with feed 2.0	0.5 minutes -5	2455	2490
on	off	off	on	off	permeate feed	30 minutes	2490	4290
off	off	off	off	on	backwash with water	10 minutes	4290	4890
off	off	on	off	off	drain feed	0.5 minutes	4890	4920
off	on	off	off	off	fill reactor with hypo	0.5 minutes -5	4915	4950
off	off	off	off	off	soak with hypo	81 min	4950	9810
off	off	on	off	off	drain all reactors	0.5 minutes	9810	9840
on	off	on	off	off	fill with feed during drain	5 s	9835	9840
on	off	off	off	off	fill reactor with feed 1.0	0.5 minutes -5	0	30

Table 15. Timer programming for cycled operational scheme C.

Timer ID:					Initiates Action:	Step Duration:	Start	End
T1	T2	T3	T4	T5			(s)	(s)
on	off	off	off	off	fill reactor with feed 1.0	0.5 minutes -5	0	30
on	off	off	on	off	permeate feed	30 minutes	30	1830
off	off	off	off	on	backwash with water	10 minutes	1830	2430
off	off	on	off	off	drain feed	0.5 minutes	2430	2460
on	off	off	off	off	fill with feed 2.0	0.5 minutes -5	2455	2490
on	off	off	on	off	permeate feed	30 minutes	2490	4290
off	off	off	off	on	backwash with water	10 minutes	4290	4890
off	off	on	off	off	drain feed	0.5 minutes	4890	4920
on	off	off	off	off	fill with feed 3.0	0.5 minutes -5	4915	4950
on	off	off	on	off	permeate feed	30 minutes	4950	6750
off	off	off	off	on	backwash with water	10 minutes	6750	7350
off	off	on	off	off	drain feed	0.5 minutes	7350	7380
off	on	off	off	off	fill reactor with hypo	0.5 minutes -5	7375	7410
off	off	off	off	off	soak with hypo	122 min	7410	14730
off	off	on	off	off	drain all reactors	0.5 minutes	14730	14760
on	off	on	off	off	fill with feed during drain	5 s	14755	14760
on	off	off	off	off	fill reactor with feed 1.0	0.5 minutes -5	0	30

A3.10 Contact Angle

Contact angle raw data are presented below (measured angle on both sides of each drop):

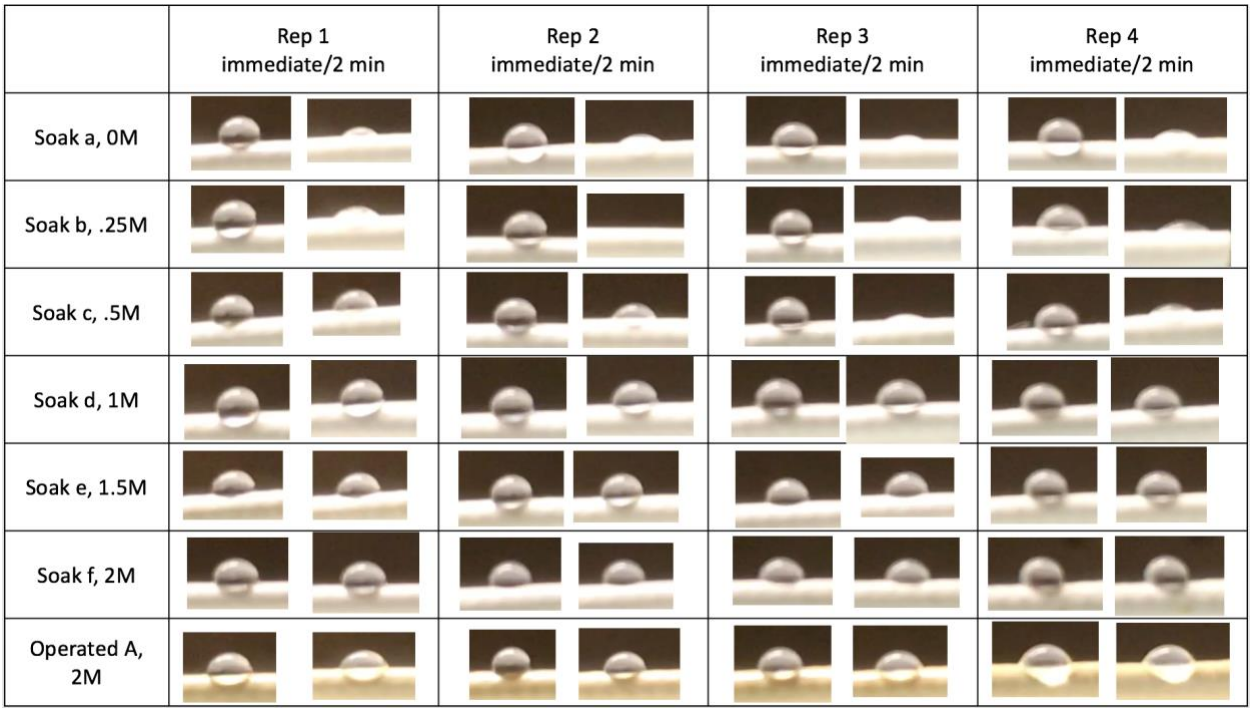

Figure 44. Array of all membrane contact angle images analyzed.

A3.10.1 Contact Angle Sample Preparation

- Dry membranes as per 3.6.1

A3.10.2 Contact Angle Protocol

- set up dry fibres on the edge of a flat surface
- set up a camera in clamp-stand level with membrane fibres
- start recording video
- drop 20 uL of water onto each fibre sample
- continue filming for 2 minutes after drop #4

A3.11 Scanning Electron Microscopy

SEM original images are provided below. Representative areas of these images were selected for inclusion in the body of the dissertation.

Ageing Protocol & Dose	10 000 x	50 000 x
Virgin	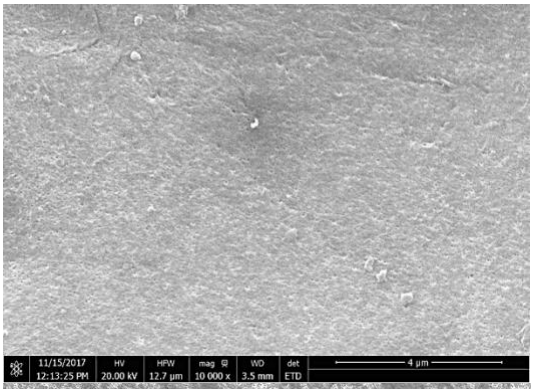	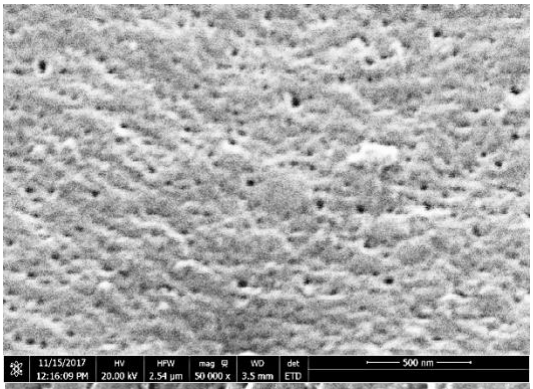
Single-Soak, 2M	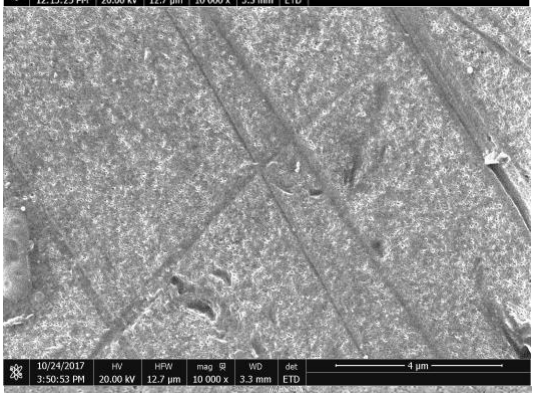	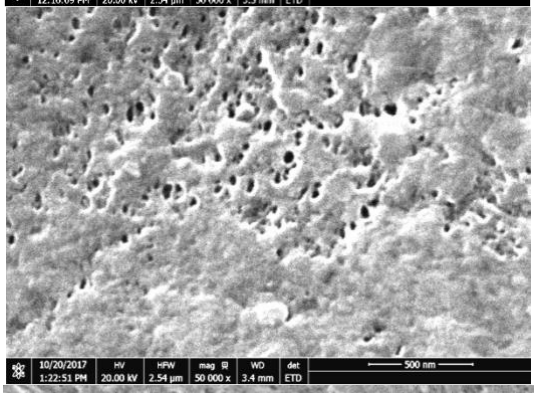
Cycled, 500k		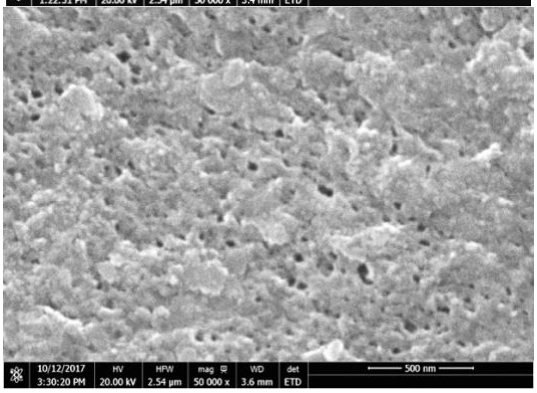

Cycled, 1M

Cycled, 1.5M

Cycled, 2M

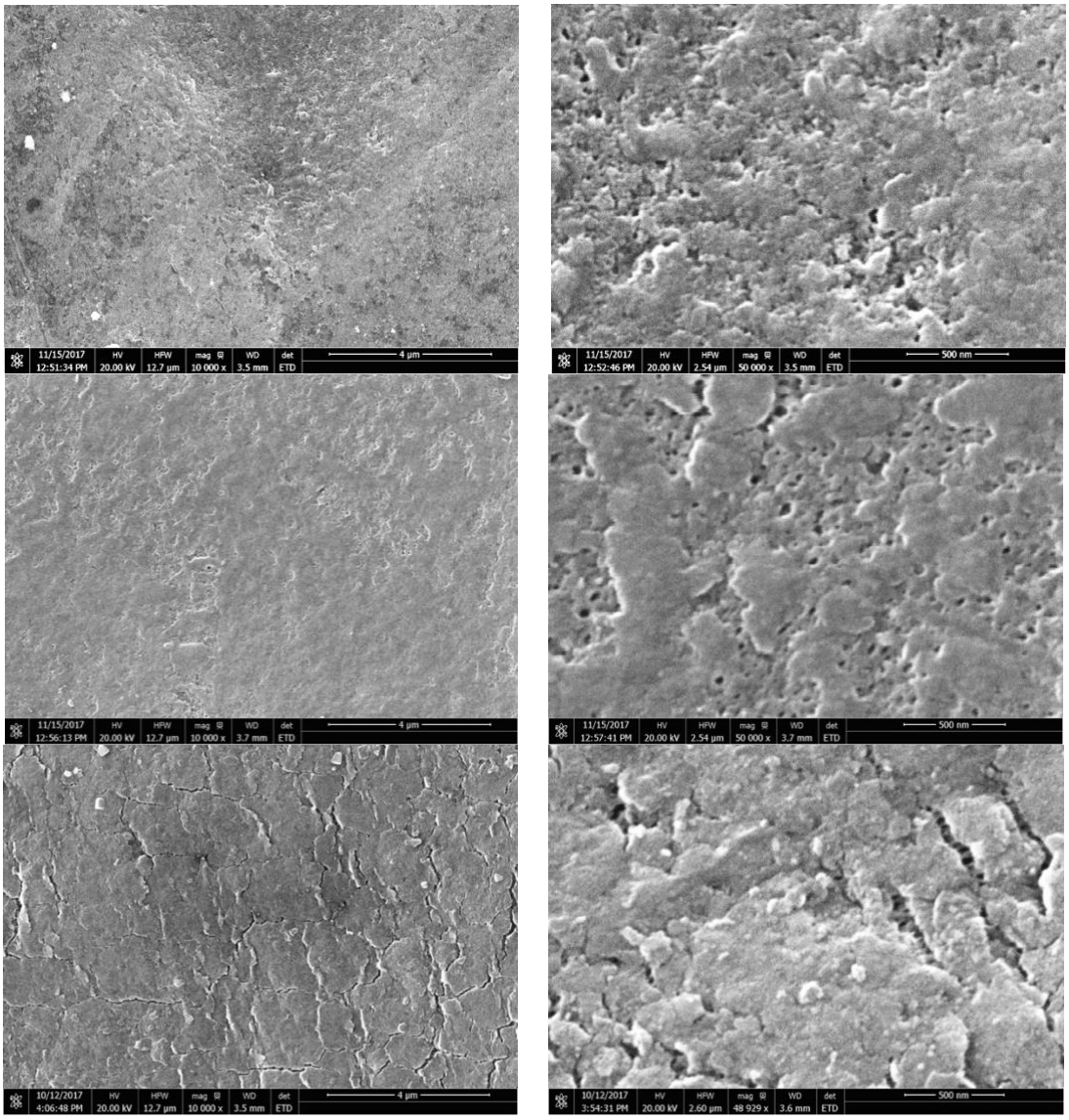

Figure 45. Full view of SEM images used in qualitative analysis.

A3.11.1 SEM Sample Preparation

- Dry membranes as per 3.6.1
- Attach small membrane lengths to SEM stubs in a flat orientation
- Coat membranes using sputter coater, protocol provided
- Be careful not to touch membranes with skin as oils can harm the SEM

A3.11.2 SEM Instrumental Protocol

- SEM imaging was performed using instrument-specific instructions.

- Images should be collected directly on top of membrane samples for consistency
- Images were collected at 10 000 x and 50 000 x in the present work.

A3.11.3 SEM Data Processing

Data processing was not performed. For qualitative analysis, brightness and contrast were adjusted.

Appendix 4 - Membrane Ageing in Full-Scale WTPs

A4.1 Statistical Analyses for Trends in Membrane Performance Factors

As discussed in Chapter 4, statistical analysis was performed on the measured performance factors. The trends and relevant p-values are summarized in this section.

Table 16. Summary of statistical analysis for the correlation of clean membrane resistance and fouling rate with full-scale membrane age. p-values in bold indicate trends that were considered statistically significant.

	Clean Membrane Resistance		**Membrane Fouling Rate**	
Membrane Type	p-Value	Slope ± Std Err ($*10^{-12}m^{-1}$/year)	p-Value	Slope ± Std Err ($*10^{-12}$ $min^{-1}m^{-1}$/year)
1000A (all data)	0.81	0.005±0.020	0.11	-0.007±0.004
1000B (pre-5-years)	0.75	0.032±0.096	0.17	-0.014±0.009
1000B (post-5-years)	**0.029**	0.738±0.309	**0.036**	0.039±0.017

Table 17. Summary of statistical analysis for the correlation of fouling rate with full-scale membrane age. P-values in bold indicate trends that were considered statistically significant.

	Ultimate Elongation		**Ultimate Tensile Strength**		**Young's Modulus**	
Membrane Type	p-Value	Slope ± Std Err (%/year)	p-Value	Slope ± Std Err (kg/year)	p-Value	Slope ± Std Err (kg/%/year)
1000A (all data)	0.97	0.000±0.013	0.97	0.000±0.001	0.98	0.000±0.001
1000B (pre-5-years)	0.52	-0.039±0.056	0.98	0.000±0.011	0.34	-0.004±0.004
1000B (post-5-years)	**0.010**	0.366±0.127	**0.017**	-0.011±0.004	**0.017**	-0.007±0.003

A4.2 Statistical Analyses for Trends in Membrane Characteristics

As discussed in Chapter 4, statistical analysis was performed on the measured characteristics. The trends and relevant P-values are summarized in this section.

Table 18. Summary of statistical analysis for the correlation of clean membrane resistance and fouling rate with full-scale membrane age.

	Membrane Surface HA (FTIR)		**Membrane Bulk HA (NMR)**	
Membrane Type	p-Value	Slope ± Std Err (/year, relative)	p-Value	Slope ± Std Err (/year, relative)
1000A (all data)	**0.0007**	-0.022±0.005	0.29	-0.013±0.012
1000B (pre-5-years)	0.71	0.008±0.022	0.90	0.005±0.038
1000B (post-5-years)	**0.007**	-0.135±0.044	**0.018**	-0.15±0.058

A4.3 Other Correlations of Interest

As discussed in Chapter 4, clean membrane resistance correlated well with all other metrics considered, as illustrated below.

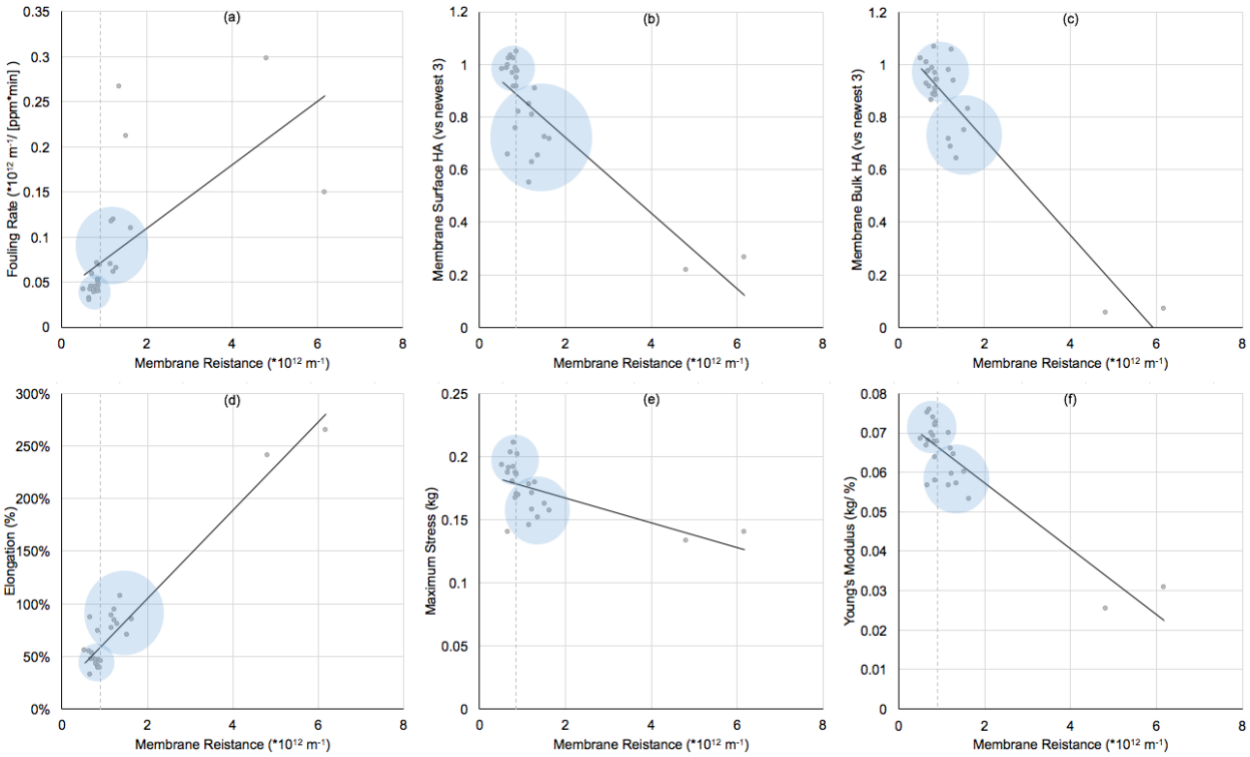

Figure 46. Correlations between clean membrane resistance and other measured parameters. Lines are plotted to illustrate overall trends, but do not imply causal relationships. The shaded circles represent clusters of membranes for which ageing is or isn't apparent.

Table 19. Slopes and significance of trends presented in Figure 46, including the atypical plant. Note that relationships are still statistically significant when the atypical plant is excluded (in table, not plotted)

		Including atypical plant		Excluding atypical plant	
	Slope Units	**p-Value**	**Slope ± Std Err**	**p-Value**	**Slope ± Std Err**
Fouling Rate	$(ppm*min)^{-1}$	$5.7*10^{-4}$	0.035 ± 0.009	$5.4*10^{-5}$	0.140 ± 0.028
Surface HA	$m*10^{-12}$	$2.3*10^{-7}$	-0.143 ± 0.020	$9.2*10^{-4}$	-0.317 ± 0.083
Bulk HA	$m*10^{-12}$	$1.6*10^{-11}$	-0.182 ± 0.015	$3.8*10^{-3}$	-0.214 ± 0.066
Ultimate Elongation	$\%*m*10^{-12}$	$2.6*10^{-14}$	0.419 ± 0.028	$4.0*10^{-4}$	0.489 ± 0.117
Maximum Stress	$kg*m*10^{-12}$	$1.1*10^{-3}$	-0.010 ± 0.003	$6.4*10^{-3}$	-0.034 ± 0.011
Young's Modulus	$(kg / \%)*m*10^{-12}$	$3.2*10^{-9}$	-0.008 ± 0.001	$2.2*10^{-3}$	-0.013 ± 0.004

The cleaning Rate and extent of cleaning both correlated with fouling rate, indicating that the reason for increased cleaning was increased fouling to begin with. Thus, discussion of cleaning behaviour did not enrich the discussion. These correlations are included in Figure 47 and Figure 48 for completeness.

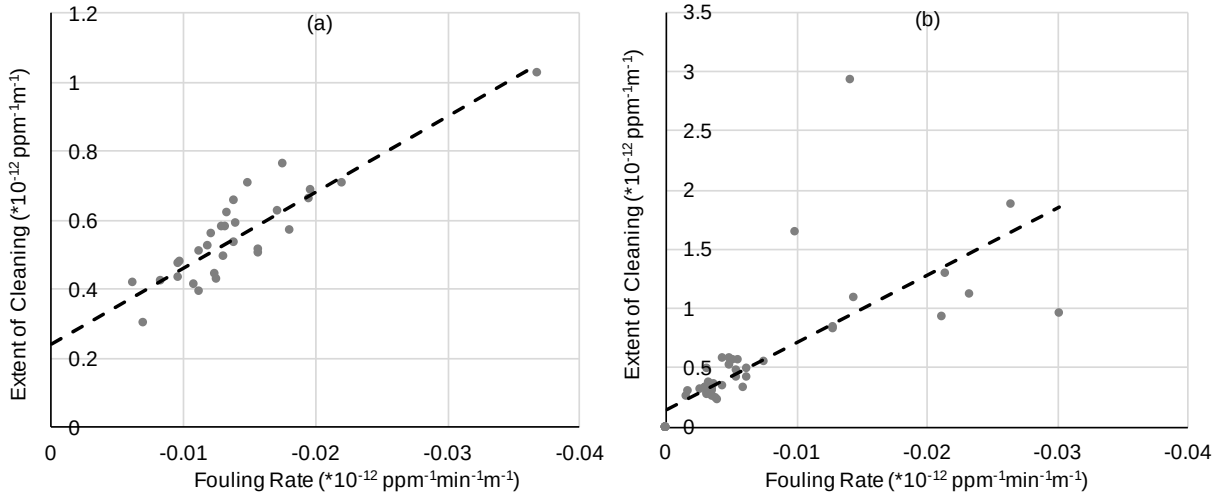

Figure 47 Extent of cleaning was correlated with fouling rate for both 1000A (a) and 1000B (b) membranes.

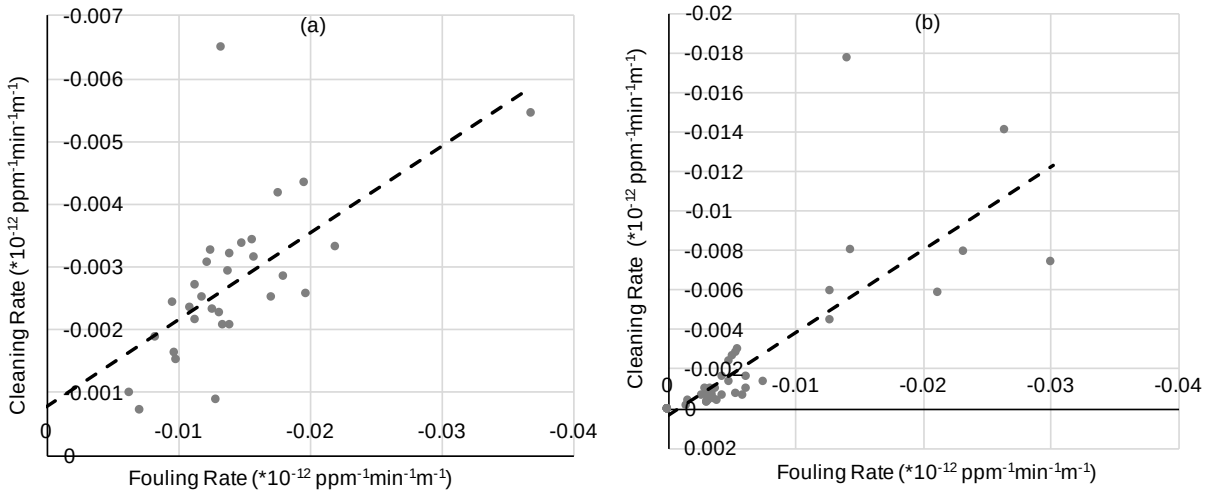

Figure 48 Cleaning rate was correlated with fouling rate for both 1000A (a) and 1000B (b) membranes.

A4.4 Placing Atypical Membranes at 13 Years

As discussed in Chapter 4, the effective age of the atypically operated membranes was greater than the actual age. Although the actual age (approximately 8 years) was modeled in the analysis presented, all trends showed improved p-values when the data was plotted at the effective age (approximately 13 years), as presented below.

Table 20. Summary of statistical analysis for the correlation of clean membrane resistance and fouling rate with full-scale membrane age.

	Clean Membrane Resistance		**Membrane Fouling Rate**	
1000B Membranes > 5 years	p-Value	Slope ± Std Err ($*10^{-12}m^{-1}$/year)	p-Value	Slope ± Std Err ($*10^{-12}$ $min^{-1}m^{-1}$/year)
X actual age (8 years)	0.029	0.738±0.309	0.036	0.039±0.017
X effective age (13 years)	$1.3*10^{-8}$	0.609±0.060	$4.8*10^{-3}$	0.022±0.007

Table 21. Summary of statistical analysis for the correlation of fouling rate with full-scale membrane age.

	Ultimate Elongation		**Ultimate Tensile Strength**		**Young's Modulus**	
1000B Membranes > 5 years	p-Value	Slope ± Std Err (%/year)	p-Value	Slope ± Std Err (kg/year)	p-Value	Slope ± Std Err (kg/%/year)
X actual age (8 years)	0.010	0.366±0.127	0.017	-0.011±0.004	0.017	-0.007±0.003
X effective age (13 years)	$5.1*10^{-9}$	0.266±0.025	$2.9*10^{-3}$	-0.006±0.002	$1.1*10^{-6}$	-0.005±0.001

Table 22. Summary of statistical analysis for the correlation of clean membrane resistance and fouling rate with full-scale membrane age.

	Membrane Surface HA (FTIR)		**Membrane Bulk HA (NMR)**	
1000B Membranes > 5 years	p-Value	Slope ± Std Err (/year, relative)	p-Value	Slope ± Std Err (/year, relative)
X actual age (8 years)	0.007	-0.135±0.044	0.018	-0.15±0.058
X effective age (13 years)	$3.3*10^{-6}$	-0.086±0.013	$7.9*10^{-8}$	-0.114±0.013

Appendix 5 - ZW500 Membranes

A third type of membrane, in addition to the 1000A and 1000B, was harvested. Two additional plants, Abbotsford and Kamloops, provided membranes for this analysis. Unfortunately only very new (<3 years) and old (>10 years) membranes were available, and only 2 WTPs harvested these membranes reliably. Furthermore, 500-type membranes are typically used to treat more challenging water, such as silty river water and concentrate from primary treatment trains. Therefore, the data from the full-scale aged ZW500 membranes is presented in this appendix.

		ZW500 Membranes
test module specifications	number of fibres	3
	fibre length	17 cm
	total surface area	30 cm^2
	target testing flux	50 $L/(m^2*h)$

membrane specifications	nominal pore diameter	0.04 µm
	fibre outer diameter	1.9 mm
	flow range	19-77 $L/(m^2*h)$
	pressure range	-55 to 55 kPa

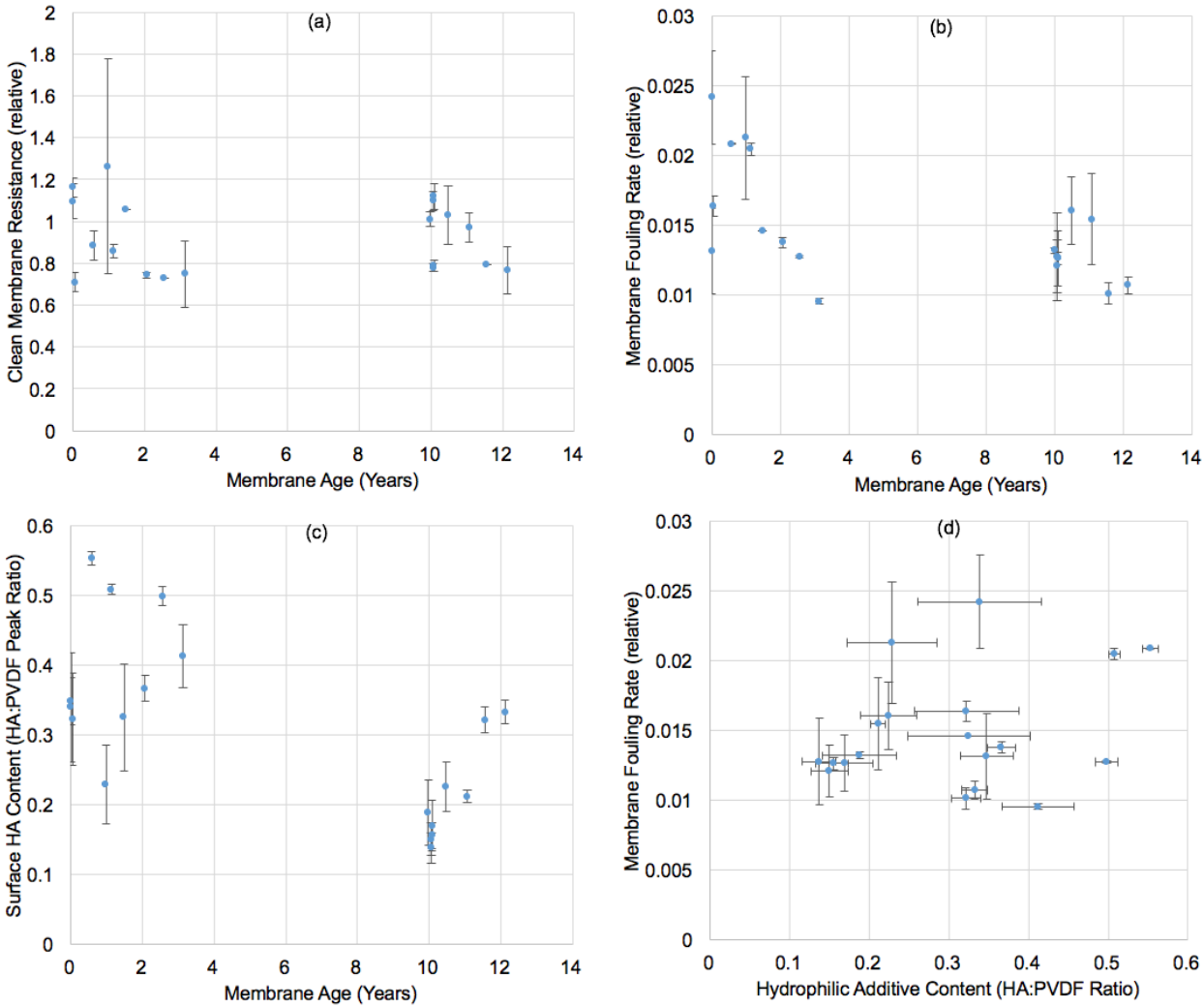

Figure 49. Change in ZW500 performance and characteristics for full-scale membranes. Panes a, b, c, and d correspond to plots Figure 15, Figure 16, Figure 18, and Figure 21 in the dissertation body, respectively.

Appendix 6 - Lab-Aged Membrane Supplementary Information

A6.1 Statistical Analysis

Statistical analysis of cycled membrane data was performed to compare schemes A, B and C. Although the total number of cycles was 600 for all three schemes, to compare fairly the operational resistance and fouling rate immediately after chemical cleans were compared. The three systems synchronize with respect to cleaning every 6 cycles, so the data from those synchronized time-points were compared.

As discussed in Chapter 5, statistical analysis was performed on the measured performance factors. The trends referenced in the text and relevant p-values are summarized in this section.

Table 23. Average operational resistance for three operational schemes over four experimental periods. The "±" indicates the standard error of the slope within each period. Units are normalized to initial operational resistance.

Operational Scheme		Period 1 0-150 cycles 0-0.5M ppm*h	Period 2 150-300 cycles 0-0.5M ppm*h	Period 3 300-450 cycles 0-0.5M ppm*h	Period 4 450-600 cycles 0-0.5M ppm*h
A	average	1.148±0.131	1.689±0.621	1.95±0.646	1.633±0.434
B	average	1.158±0.126	1.353±0.294	1.502±0.331	1.098±0.206
C	average	1.07±0.054	1.29±0.274	1.116±0.191	1.069±0.155

Table 24. p-Values for operational resistance differences among operational schemes; values are bolded if <0.05

Operational Scheme		Period 1 0-150 cycles 0-0.5M ppm*h	Period 2 150-300 cycles 0-0.5M ppm*h	Period 3 300-450 cycles 0-0.5M ppm*h	Period 4 450-600 cycles 0-0.5M ppm*h
A vs B	p-value	7.83E-01	**2.26E-02**	**4.67E-03**	**4.86E-06**
B vs C	p-value	**3.57E-03**	4.43E-01	**1.63E-05**	5.85E-01
A vs C	p-value	**1.10E-02**	**7.07E-03**	**1.75E-06**	**1.67E-06**

Table 25. Average fouling rate for three operational schemes over four experimental periods. The "±" indicates the standard error of the slope within each period. Units are normalized to initial fouling rate.

Operational Scheme		Period 1 0-150 cycles 0-0.5M ppm*h	Period 2 150-300 cycles 0-0.5M ppm*h	Period 3 300-450 cycles 0-0.5M ppm*h	Period 4 450-600 cycles 0-0.5M ppm*h
A	average	0.927±0.061	1.115±0.141	1.446±0.131	1.551±0.451
B	average	0.960±0.096	1.078±0.190	1.144±0.236	0.999±0.239
C	average	0.855±0.163	1.114±0.216	1.286±0.116	1.139±0.13

Table 26. p-Values for fouling rate differences among operational schemes; values are bolded if <0.05.

Operational Scheme		Period 1 0-150 cycles 0-0.5M ppm*h	Period 2 150-300 cycles 0-0.5M ppm*h	Period 3 300-450 cycles 0-0.5M ppm*h	Period 4 450-600 cycles 0-0.5M ppm*h
A vs B	p-value	1.72E-01	4.44E-01	**3.58E-06**	**6.53E-06**
B vs C	p-value	**1.01E-02**	5.39E-01	**1.26E-02**	**1.69E-02**
A vs C	p-value	5.05E-02	9.85E-01	**5.05E-05**	**1.99E-04**

A6.2 Discussion of DOC Rejection (DOC, SEC-UV Analysis)

Due to limited data availability, a comprehensive study of DOC rejection by aged membranes was not performed. However, total DOC was monitored throughout the bench-scale ageing experiment, and selected SEC chromatograms were collected for aged and virgin membranes. These results are presented as follows.

The removal of DOC during filtration was used to quantify the impact of ageing on contaminant rejection (Figure 50). For single-soaked membranes, DOC removal was quantified during the fouling period of performance testing. For cycled membranes, DOC removal was quantified approximately every 37 cycles, plus immediately after intensive cleans. These permeate collection periods were illustrated by brackets in Figure 14. To gain further insight into the removal of organic matter, SEC-UV analysis was also performed on selected samples (Figure 51). Together, these data were used to estimate a mass balance on the foulant constituents present (Figure 52).

Overall, the improved DOC rejection with membrane age supports the notion that membrane hydrophobicity increases with age, and is evidence of the cause of increasing fouling rate with membrane age. Also, immediately after the intensive cleans (Figure 50), rejection increased. This suggests that adsorptive sites became available immediately following intensive cleaning. However, the rejection returned to the trend value within several cycles.

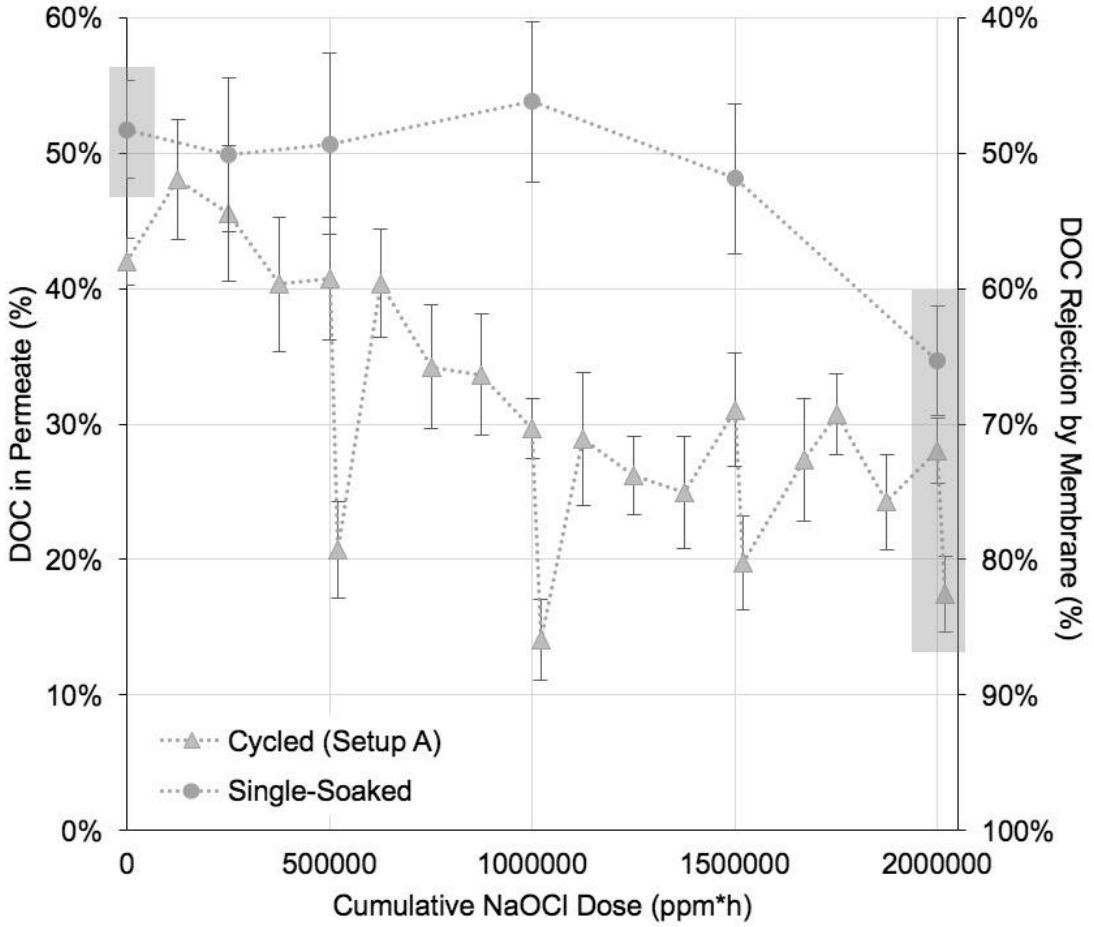

Figure 50. Permeate DOC content for single-soaked and cycled membranes with respect to cumulative NaOCl dose; DOC rejection is indicated on the alternate y-axis. Error bars represent standard error from four replicate aged membranes.

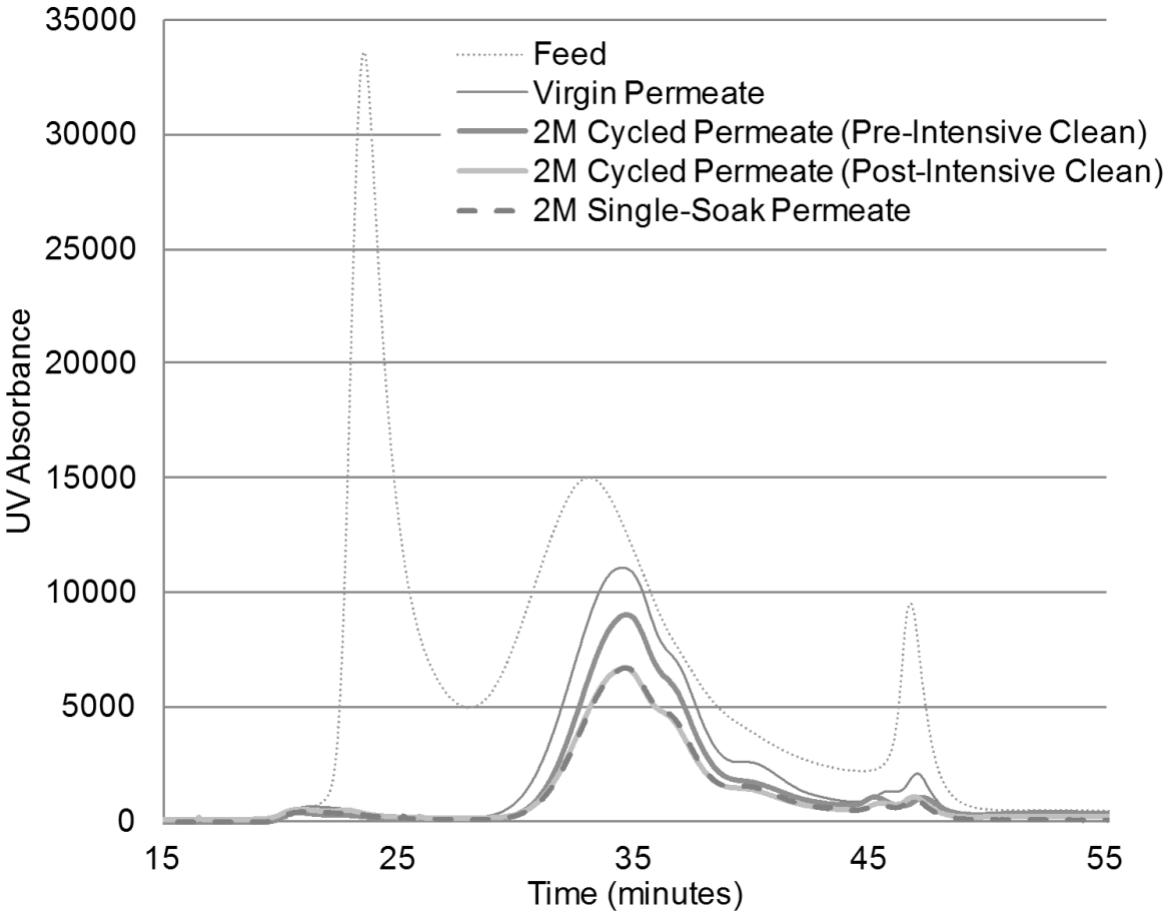

*Figure 51. SEC-UV chromatograms for feed solution and typical permeate samples; for the approach used, the peaks at 23 and 33 minutes correspond to BSA and humic acid, respectively. "2M" indicates the cumulative NaOCl dose was 2 000 000 ppm*h.*

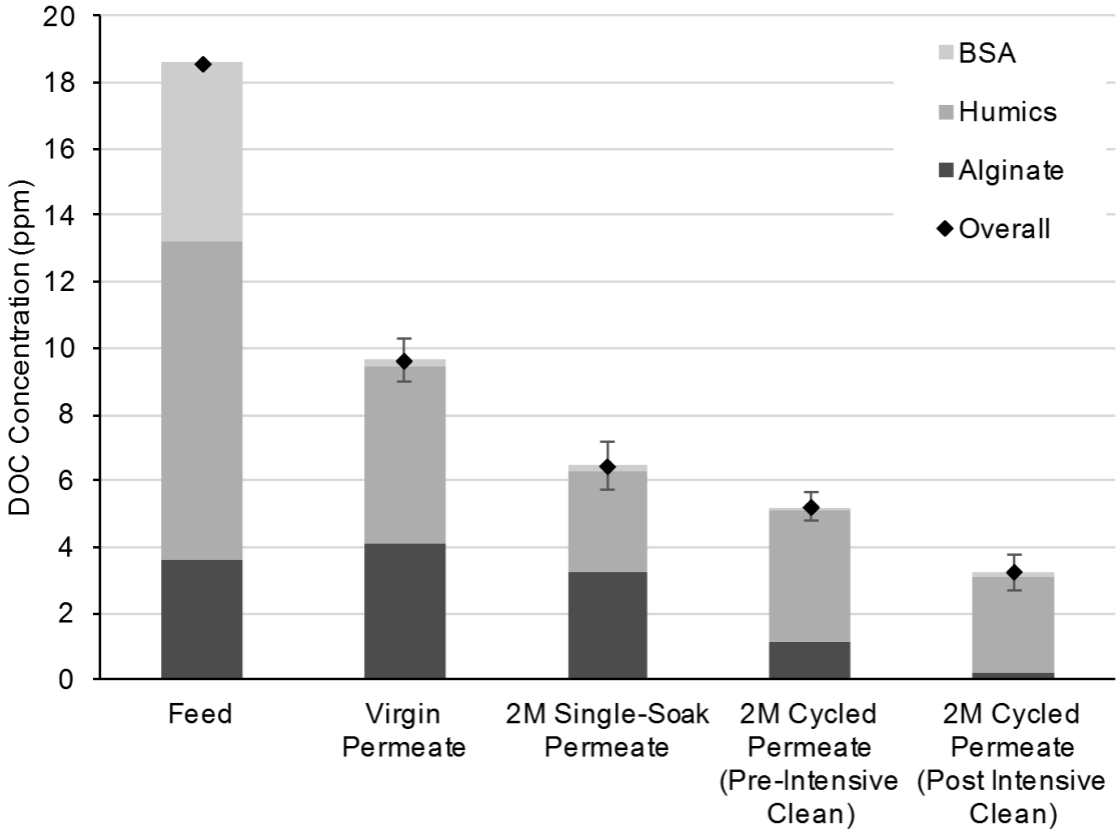

Figure 52. Feed and permeate composition for selected membrane ageing conditions. Feed DOC composition is based on carbon fraction from the three constituents. BSA and humics composition for permeate samples was determined based on SEC-UV, and alginate extrapolated from DOC mass balance. Error bars on overall DOC concentration represent standard error of four replicate aged membranes.